Alma Mater Studiorum – Università di Bologna

DOTTORATO DI RICERCA IN

BIOLOGIA CELLULARE, MOLECULARE E INDUSTRIALE:
BIOLOGIA FUNZIONALE DEI SISTEMI
CELLULARI E MOLECOLARI

Ciclo XXIV

Settore Scientifico Disciplinare: 05/E2
Settore Concorsuale di afferenza: BIO/11

TITOLO TESI

Trascriptome analysis and functional genomics of *Neisseria meningitidis* in human blood

Presentata da: **Elena Del Tordello**

Coordinatore Dottorato

Chiar.mo Prof.
Vincenzo Scarlato

Relatore

Chiar.mo Prof.
Vincenzo Scarlato

Dott.
Davide Serruto

Esame finale anno 2012

Il mio progetto di dottorato, presentato in questo lavoro di tesi, si è focalizzato principalmente sullo studio dei cambiamenti dell'espressione genica di *Neisseria meningitidis* durante l'incubazione in sangue intero umano, per capire come il batterio si adatta a crescere nel sangue, dato che questo rappresenta una fase fondamentale della patogenesi. La prima parte del progetto presentato è stata già pubblicata, mentre per la seconda parte, un articolo è in preparazione:

Del Tordello E, Bottini S, Muzzi A, Serruto D. *Identification of novel Neisseria meningitidis transcripts differentially expressed in human whole blood using high density tiling microarrays.*
In preparazione

Echenique-Rivera H, Muzzi A, **Del Tordello E**, Seib KL, Francois P, Rappuoli R, Pizza M, Serruto D. *Transcriptome analysis of Neisseria meningitidis in human whole blood and mutagenesis studies identify virulence factors involved in blood survival.* PLoS Pathog. May;7(5):e1002027. (2011)

Parallelamente all'analisi di trascrittomica e genomica funzionale, ho anche collaborato alla caratterizzazione immunologica e funzionale di antigeni del vaccino che Novartis Vaccine & Diagnostic in Siena sta sviluppando contro il sierogruppo B di *Neisseria meningitidis*. In particolare mi sono occupata della generazione di ceppi ricombinanti di meningococco, esprimenti diverse varianti dell'antigene fHbp, e della caratterizzazione genetica dei ceppi batterici ottenuti. I ceppi ricombinanti sono stati poi utilizzati in saggi di battericidia per valutare l'influenza della variabilità di sequenza sull'attività battericida indotta dall'antigene del vaccino. Il lavoro svolto è stato parte di una pubblicazione scientifica:

Brunelli B, **Del Tordello E**, Palumbo E, Biolchi A, Bambini S, Comanducci M, Muzzi A, Pizza M, Rappuoli R, Donnelly JJ, Giuliani MM, Serruto D. *Influence of sequence variability on bactericidal activity sera induced by Factor H binding protein variant 1.1.* Vaccine, Jan 29;29(5):1072-81. (2011)

Table of Contents

Abstract

Neisseria meningitidis (Nm) is the major cause of septicemia and meningococcal meningitis. During the course of infection, it must adapt to different host environments as a crucial factor for survival. Despite the severity of meningococcal sepsis, little is known about how Nm adapts to permit survival and growth in human blood.

A previous time-course transcriptome analysis, using an *ex vivo* model of human whole blood infection, showed that Nm alters the expression of nearly 30% of ORFs of the genome: major dynamic changes were observed in the expression of transcriptional regulators, transport and binding proteins, energy metabolism, and surface-exposed virulence factors. Starting from these data, mutagenesis studies of a subset of up-regulated genes were performed and the mutants were tested for the ability to survive in human whole blood; Nm mutant strains lacking the genes encoding NMB1483, NalP, Mip, NspA, Fur, TbpB, and LctP were sensitive to killing by human blood.

Then, the analysis was extended to the whole Nm transcriptome in human blood, using a customized 60-mer oligonucleotide tiling microarray. The application of specifically developed software combined with this new tiling array allowed the identification of different types of regulated transcripts: small intergenic RNAs, antisense RNAs, 5' and 3' untranslated regions and operons. The expression of these RNA molecules was confirmed by 5'-3'RACE protocol and specific RT-PCR.

Here we describe the complete transcriptome of Nm during incubation in human blood; we were able to identify new proteins important for survival in human blood and also to identify additional roles of previously known virulence factors in aiding survival in blood.

In addition the tiling array analysis demonstrated that Nm expresses a set of new transcripts, not previously identified, and suggests the presence of a circuit of regulatory RNA elements used by Nm to adapt to proliferate in human blood.

1. Introduction

1.1 *Neisseria meningitidis*, a strictly human pathogen

Neisseria meningitidis (Nm) is a Gram-negative B-proteobacterium. and member of the bacterial family of Neisseriaceae. It is a fastidious bacterium, dying within hours on inanimate surfaces, and is either an encapsulated or unencapsulated, aerobic diplococcus with a "kidney" or "coffee-bean" shape (Figure 1).

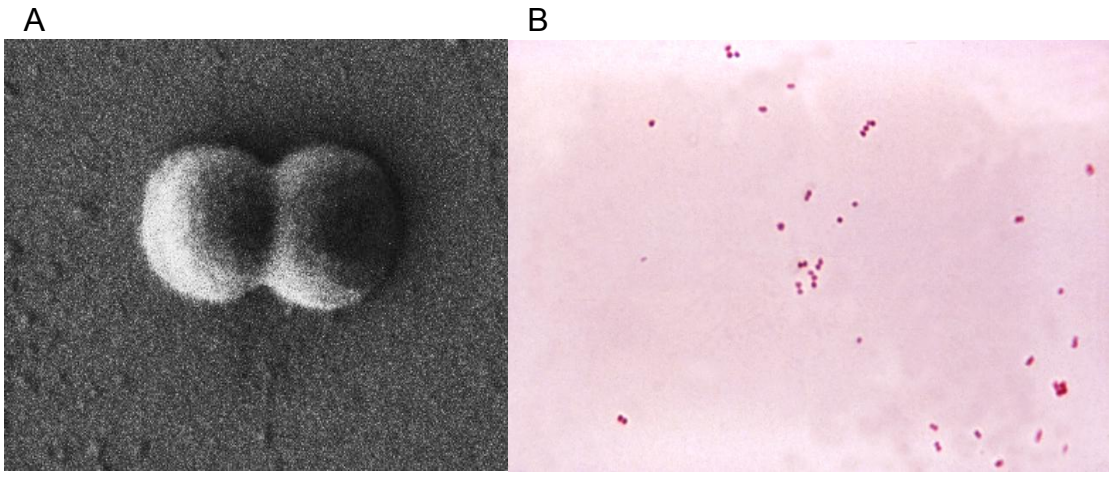

Figure 1. ***Neisseria meningitidis*** **diplococcus. A.** Scanning electron microscopy image of the gram negative bacterium *Neisseria meningitidis, showing* a diplococcus morphology. The size of the bacterium is about 1 micrometer (from http://www.stockholmmicro.se; owner Niklas Söderholm). **B.** *N. meningitidis* grown on an agar plate.
(from http://bioweb.uwlax.edu/bio203/s2008/bingen_sama)

Nm is a commensal and pathogen only of humans that are the unique reservoir for this bacterium. Virulence determinants include the polysaccharide capsule, outer membrane proteins including pili, the porins (PorA and B), the adhesion molecule Opc, iron sequestration mechanisms and endotoxin (lipooligosaccharide) [1]. N. meningitidis is now classified into 13 serogroups based on the immunogenicity and structure of the

polysaccharide capsule. At least 13 distinct meningococcal groups have been defined on the basis of their immunological reactivity and structure of the capsule's polysaccharide [2]. These serogroups are the following: A, B, C, E-29, H, I, K, L, W-135, X, Y, Z, and Z' (29E). Only six serogroups (A, B, C, W-135, X, Y) cause life-threatening disease. Further classification into serosubtype, serotype and immunotype is based on class 1 outer membrane proteins (PorA), class 2 or 3 (PorB) outer membrane proteins and lipopoly[oligo]saccharide structure, respectively [3], [1]. A genetic typing system based upon polymorphisms in multiple housekeeping genes (Multilocus Sequence Typing, MLST) is now the gold standard for molecular typing and has defined hyper-virulent meningococcal lineages [4].

Based on sequencing of eight genomes, the chromosome is between 2.0 and 2.1 megabases in size and contains about 2000 genes [73], [5], [6]. Each new strain sequenced has identified 40–50 new genes and the meningococcus shares about 90% homology at the nucleotide level with either *N. gonorrhoeae* or *N. lactamica*. Mobile genetic elements including IS elements and prophage sequences make up ~10% of the genome [5]. Other than the capsule locus, no core pathogenome has been identified suggesting that virulence may be clonal group dependent. Given that transformation is an efficient mechanism of genetic exchange and that meningococci have acquired DNA from commensal *Neisseria* spp. and other bacteria (e.g. *Haemophilus*) as well as phages, the gene pool for adaptation and evolution is quite large. Genome plasticity and phenotype diversity through gain and loss of DNA or, for example, through DNA repeats, is a characteristic of meningococcal evolution. This is in contrast to the relatively conserved genomes of for example *Bacillus anthracis*. The acquisition of the capsule locus by horizontal transfer possibly from *Pasteurella multocida* or *P. hemolytica* [6] appears to be a major event in the evolution of the pathogenicity of the meningococcus. Several repetitive sequence and polymorphic regions are present, usually in large heterogeneous arrays, suggesting active areas of genetic recombination. Another characteristic of the meningococcal genome is the presence of multiple genetic switches (e.g., slipped-strand misparing, IS element movement), contributing to the expression of pathogen-associated genes [7].

1.2 Meningococcal colonization and carriage

Colonization of the upper respiratory mucosal surfaces by N. meningitidis is the first step in establishment of a human carrier state and invasive meningococcal disease. Meningococcal transmission among humans occurs largely through respiratory droplets and secretions, but the inoculum size needed for transmission is unknown. Acquisition of N. meningitidis in the upper respiratory tract may be asymptomatic or may infrequently result in local inflammation, invasion of mucosal surfaces, access to the bloodstream and fulminant sepsis or focal infections such as meningitis [1]. Meningococcal disease usually occurs 1–14 days after acquisition of the pathogen [3]. Acquisition may also result in upper respiratory and pharyngeal meningococcal carriage. The duration of carriage can vary from days to months. From an evolutionary perspective, the interactions of meningococci and the human nasopharynx are key. Meningococcal carriage and transmission, not disease, determine the global variation and composition of the natural population of meningococci. The biological role of capsular polysaccharide in carriage/transmission is not well understood. Capsule-deficient strains may be transmitted efficiently, so the theory of resistance to dessication during transit or capsule antiadhesive properties promoting loss does not seem strong. Capsule is not required for efficient carriage. However, there is evidence of differences in propensity for carriage associated with the different capsular polysaccharides (serogroups), e.g. low carriage of serogroup C meningococci. The adaptive advantage of switching between the capsulate and non-capsulate state seems likely to provide a fitness advantage possibly for close adherence and initial steps in cell invasion. As noted, the redundancy of adhesins possessed by meningococci, e.g., pilus, Opa, NadA and their striking allelic variation, is impressive. The source of this variation is strongly influenced by lateral transfer of genetic information (recombination) and meningococci are naturally transformable. Nevertheless, most individuals are colonized with only one meningococcal strain (at least based on carriage studies) and this must place some constraints on the opportunity for genetic exchange between heterologous strains. Meningococcal adhesins are not known to be characteristic of other commensal Neisseria although this is not well studied. The relationship between meningococcal carriage rates and meningococcal disease and even the use of carriage prevalence as a proxy for predicting outbreaks of meningococcal disease has received considerable study. The important measure in terms of disease is the rate of acquisition of meningococci of

hypervirulent lineages, not overall meningococcal carriage [8]. The probability of meningococcal disease after the acquisition of N. meningitidis declines very sharply, such that invasive disease becomes unlikely 10–14 days after acquisition. Too little research has been done on the interactions of N. meningitidis with other upper respiratory tract commensals/pathogens. For example, carriage of pneumococci appears to be a risk factor for meningococcal carriage [9].

1.3 Invasive meningococcal disease

Meningococci that are transmitted by aerosol or contact with secretions colonize upper respiratory mucosal surfaces (e.g., the nasopharynx), may spread to adjacent mucosal surfaces (e.g., lower respiratory tract), and may invade epithelial surfaces and gain access to the bloodstream to produce systemic and focal infections (Figure 2).

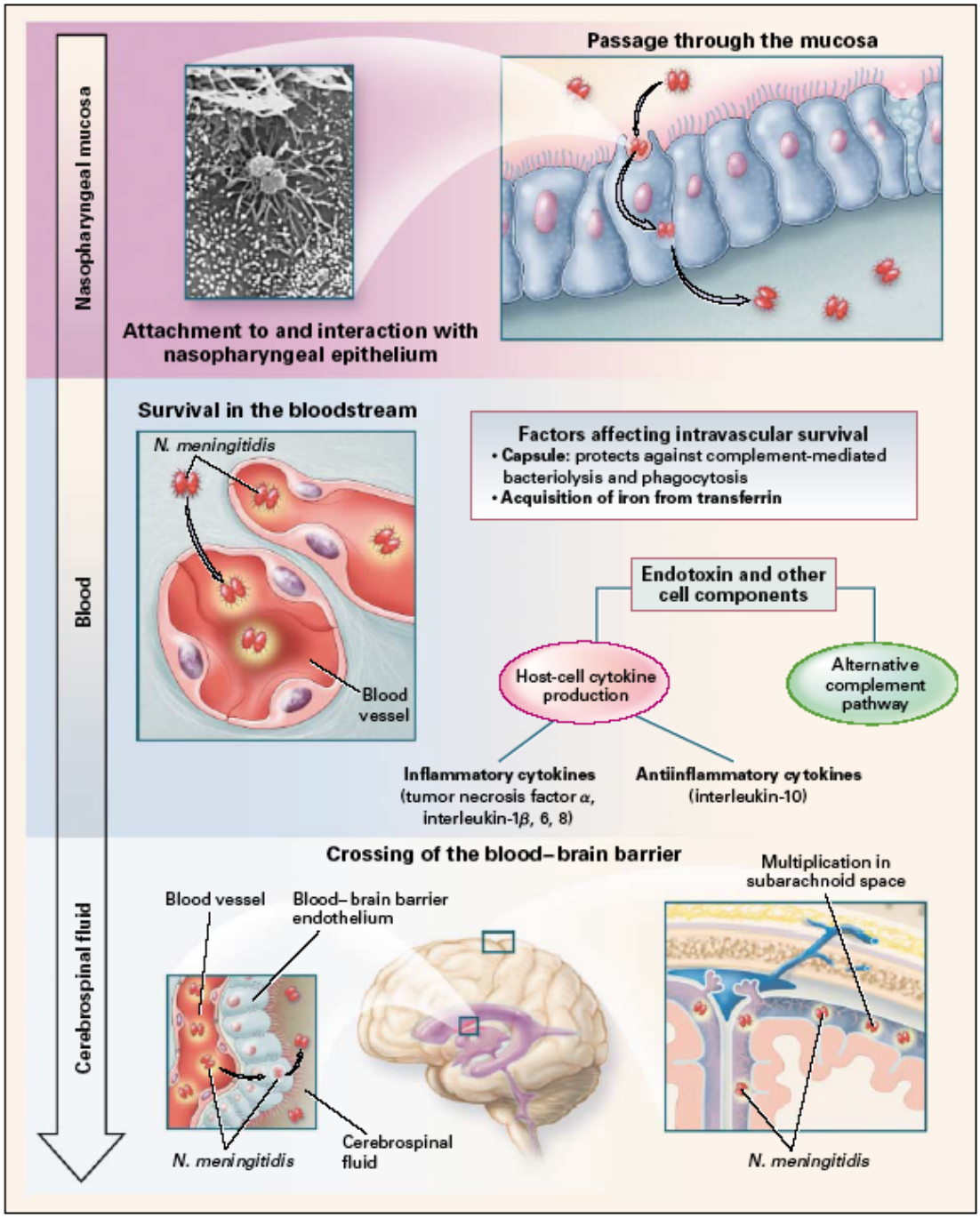

Figure 2. Colonization of *Neisseria meningitidis* in the nasopharynx and entry into the bloodstream and cerebrospinal fluid. *N. meningitidis* enters the nasopharynx and attaches to nonciliated epithelial cells, probably through the binding of the pili to the CD46 receptor (a membrane cofactor protein) and the subsequent binding of opacity-associated proteins, Opa and Opc, to the CD66e (carcinoembryonic antigen) and heparan sulfate proteoglycan receptors, respectively. The attached organisms are engulfed by the cells, enter phagocytic vacuoles, and may then pass through the cells. IgA1 protease (an outer-membrane protein) cleaves lysosome-associated membrane protein and may promote the survival of *N. meningitidis* in epithelial cells.

PorB (another outermembrane protein) crosses the cell membrane and arrests the maturation of the phagosome. In the bloodstream, the organisms release endotoxin in the form of blebs (vesicular outer-membrane structures) that contain 50 percent lipooligosaccharide and 50 percent outer-membrane proteins, phospholipids, and capsular polysaccharide. The endotoxin and probably other components stimulate cytokine production and the alternative complement pathway. *N. meningitidis* crosses the blood–brain barrier endothelium by entering the subarachnoid space, possibly through the choroid plexus of the lateral ventricles (from [3]).

Overcoming specific and nonspecific mucosal host defenses, crossing of the upper respiratory mucociliary blanket and attachment to human epithelial cells appears to be required for the colonization of the nasopharynx by meningococci. Twitching motility may allow meningococci to penetrate mucus and attach to epithelial cells. Meningococci can enter human nasopharyngeal epithelial cells by a process of parasite-induced endocytosis; bacteria may penetrate between epithelial or endothelial cells, transcytoses through them or are carried across the epithelial and endothelial barriers within cells (Trojan horse theory). Bacteria enter and accumulate in phagocytic vacuoles of nasopharyngeal epithelial cells, which may be released into interepithelial spaces below epithelial cell tight junctions. Alternatively, meningococci may invade upper respiratory epithelium damaged by smoking coinfections or other environmental factors. Entry of meningococci into the bloodstream is likely much more frequent than clinically recognized, but is usually transient. Once access to the bloodstream is obtained, meningococci may multiply rapidly to high levels. Meningococcal bacteremia can result in the seeding of the meninges, pericardium and large joints. Up to one third of patients with meningococcal disease present with meningitis or other closed space infections without signs of sepsis. Meningococci may also translocate across the blood-meningeal barrier, proliferate in the CNS and cause meningitis. How meningococci traverse the blood brain barrier and enter the cerebrospinal fluid (CSF) or reach other closed sites is unclear. Meningococci have been shown to invade endothelial cells both experimentally and in vivo. The chorioid plexus is also a potential site of entry of meningococci into the CSF. The inflammatory cytokines, TNF-α and IL-1, released in meningococcal bacteremia [10], may also enhance the permeability of the blood brain barrier and may allow meningococcal entry into the CSF. Meningitis and other closed space infections (e.g., arthritis, pericarditis) are the result of bacterial survival and multiplication at these sites.

The ability to cause invasive disease depends on environmental factors, meningococcal virulence factors and lack of a "protective immune response." Environmental factors that impair the integrity of the human nasopharyngeal mucosa such as tobacco [1], exposure to low humidity, dust and co-infections, expecially influenza and mycoplasma, [11]; increase the incidence of invasive meningococcal disease. There is epidemiologic, biological and pathological evidence for each of these events. Major meningococcal contributors to the invasive meningococcal disease include: capsular polysaccharide, other surface structures [pili, OMPs (e.g. PorA, PorB, Opa, Opc), lipooligosaccharide (LOS)] and genotype. Resistance to complement-mediated lysis and phagocytosis is determined by the expression of the capsule and lipooligosaccharide [12]. Meningococcal endotoxin released in blebs also plays a major role in the inflammatory events of meningococcemia and meningococcal meningitis [13]. LOS plays a role in the adherence of the meningococcus [13] and activation of the innate immune system. Severity of meningococcal sepsis has been correlated with circulating levels of meningococcal LOS [5]. Pili and other OMPs, facilitate the adherence of the meningococcus to endothelial surfaces. In coclusion, multiple meningococcal invasion virulence factors influence invasive disease and some are the focus of new vaccines [14].

1.4 Meningococcal disease: epidemiology

Invasive meningococcal disease results from the interplay of: (1) microbial factors influencing the virulence of the organism, (2) environmental conditions facilitating exposure and acquisition, and (3) host susceptibility factors favoring bacterial acquisition, colonization, invasion, and survival. In the pre-serum therapy and pre-antibiotic eras, 70–85% of meningococcal disease cases were fatal; today, the overall mortality rate in invasive meningococcal disease still remains high, at between 10 and 15% [15]. Meningococcal disease is also associated with marked morbidity including limb loss, hearing loss, cognitive dysfunction, visual impairment, educational difficulties, developmental delays, motor nerve deficits, seizure disorders, and behavioral problems [3]. Although rates of sporadic disease can reach ~5–10/100,000 population, a key characteristic of meningococcal disease are epidemic outbreaks. Seasonal epidemics

(usually due to serogroup A) occur yearly in sub-Saharan Africa and cyclical pandemics have occurred there every 8–10 years for the last 100 years. During seasonal epidemics and cyclical pandemics the incidence can climb to >1/1000 population for weeks before the frequency of disease declines in the immediate outbreak area. Serogroups B, C and Y are associated with sporadic disease, case clusters and outbreaks seen in the United States, Canada, New Zealand, South America, Europe and other parts of the world [3]. Serogroup W-135 is responsible for recent worldwide outbreaks associated with pilgrims returning from the Hajj [16]. The different characteristics of outbreaks are caused by hypervirulent lineages as defined by MLST. The worldwide W-135 outbreaks were caused by W-135 strains of the ST-37 clonal complex most often associated with serogroup C disease and outbreaks. The introduction of new virulent clones into a population can change the epidemiology and the clinical spectrum of meningococcal disease and the recent emergence of serogroup X meningococci in Niger [17] highlights the need for continued surveillance for new clonal complexes.

Meningococcal disease has the highest incidence in infants and children aged <4 years and adolescents [1]. Two-thirds of meningococcal disease in the first year of life in the US occurs in infants less than 6 months of age [18]. Worldwide, the rates of meningococcal disease are also highest for young children due to waning protective maternal antibody, but in epidemic outbreaks, older children and adolescents can have high rates of disease. Even though peak incidence occurs among infants and adolescents; one-third to one-half of sporadic cases are seen in adults older than 18 years. The early stages of disease can mimic viral infections such as influenza, but the disease course may be fulminant. Thus, it can be difficult to identify and treat the disease quickly. Rapid progression of the disease from bacteremia and/or meningitis to life-threatening septic shock syndrome or meningitis can occur within the first few hours after initial symptoms appear. Because of these parameters, prevention through vaccination is the best option for the control of this disease in a community. While significant progress is being made in understanding meningococcal pathogenesis and in new meningococcal vaccines and vaccine strategies, challenges remain. Dissecting the molecular basis of meningococcal pathogenesis also has important scientific lessons for understanding bacterial emergence, pathogenic genome structure, horizontal genetic exchange, and innate and adaptive immune responses [8].

1.5 The survival in blood as an important step of the pathogenesis

After breaching the mucosal barrier in the upper respiratory tract, invasive meningococci enter the circulation and start to proliferate. The growth velocity in the vasculature is a major determinant of the clinical presentation. A majority of patients reveal a comparatively low-grade meningococcemia, which subsequently seeds the subarachnoid space, where meningococci proliferate rapidly, leading to meningitis without shock symptoms. A minority of patients develop fulminant meningococcal septicemia, characterized by very rapid bacterial growth in the circulation [10], [1], [19] . The real bacterial loads in patients with fulminant meningococcemia have been quantified to be 105 to 108 bacteria/ml by determining the numbers of *N. meningitidis* DNA molecules, using robotized magnetic bead extraction of the bacterial DNA and real-time PCR [20], [21]. Survival and multiplication of meningococci in the bloodstream are directly dependent on the ability of the meningococcus to circumvent humoral and, to a lesser extent, phagocytic immune defenses. Multiplication of meningococci correlates with the systemic release of inflammatory cytokines (IL-1, IL-6, TNF-α), which are key elements in the pathogenesis of meningococcemia. In fact, the massive bacterial growth is reflected in high levels of endotoxin (lipopolysaccharide [LPS]), complement activation products, and cytokines in plasma [22], [23], [24]. Meningitis and its sequelae are due to the induction of local inflammatory cytokines and other mediators (e.g., nitric oxide), leukocyte infiltration across the blood brain barrier, breakdown of the blood brain barrier with edema, release of metaloproteases, induction of cellular apoptosis, coagulation of vessels and ischemia [22].

The ability of meningococcus to survive and grow in human whole blood is a crucial step of the bacterial pathogenesis and the establishment of an invasive disease. In fact, even in case of the development of meningitis, with a low grade of meningococcemia and no shock symptoms, the bacterium must survive and multiply in blood to reach the blood-brain barrier and enter in the subarachnoid space. To survive, Nm must adapt to the blood environment and to different interactions with host cells and factors; to do that, it has evolved molecular and cellular mechanism to protect itself from host immune system and to exploit the host to obtain nutrients. The knowledge of how Nm responds to adaptation in blood could be helpful to develop diagnostic and therapeutic strategies to control the devastating disease caused by this bacterium.

An infant rat model of invasive infection has been combined with a signature tagged

mutagenesis (STM) approach to identify genes essential for bacteremia [25]. However, since Nm is an exclusively human pathogen, existing animal models may not accurately simulate meningococcal disease. For this reason, human whole blood has been used as an *ex vivo* model of sepsis for studying the pathogenesis of Nm in terms of complement activation, cytokine production and immunity [86], [26], [27], [28].

1.6 Global changes in the gene expression profile of meningococcus in human whole blood

In order to evaluate the transcriptional response of Nm during growth in blood, in our research group we have analyzed the global changes in the transcriptional profile of a virulent Nm serogroup B strain in an *ex vivo* model of bacteremia, using incubation in human whole blood and a time-course oligo-microarray experiment [29]. The *ex vivo* human whole blood model enabled meningococcal responses to both host cellular and humoral bactericidal mechanisms to be analyzed and has shown potential to examine a number of parameters that are likely to be important in the cascade of events associated with acute systemic meningococcal infection [95] and to characterize Nm factors involved in the survival of the bacterium during infection [30], [31].

Freshly isolated whole venous blood collected from four healthy human volunteers (2 male and 2 female) was used. Nm MC58 bacteria (approximately $1x10^8$, grown in GC medium to early exponential phase) were mixed with blood from each donor in order to mimic disease. In order to evaluate the adaptation of Nm to human blood, samples were collected at six different time points: we then applied an *in vitro* transcription amplification/labeling step [32] to produce amplified-labeled cRNA that was then used in competitive hybridization experiments using a 60-mer Nm oligo-microarray. Transcriptional changes throughout the course of Nm incubation in human blood were defined by comparison of expression levels at various time points against time 0. The results showed that Nm alters the expression of nearly 30% of ORFs of the genome with 360 genes up-regulated and 277 genes down-regulated compared to the reference time 0. Interestingly, gene expression profiles clustered by K-means partitioning were modularly organized with respect to TIGRFAM functional classes [33] or KEGG metabolic pathways (Figure 3).

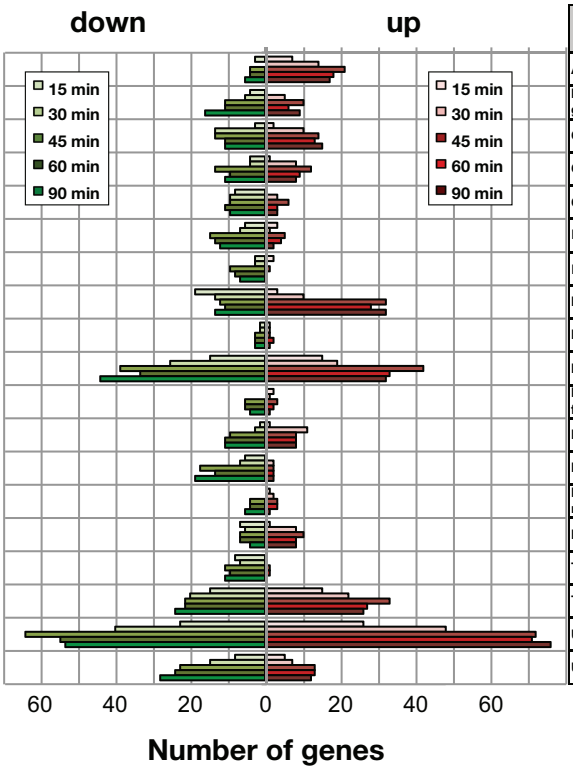

TIGR Mainrole	Total number of genes	Down regulated	Up regulated
Amino acid biosynthesis	76	6	24
Biosynthesis of cofactors, prosthetic groups, and carriers	80	15	10
Cell envelope	120	12	18
Cellular processes	111	10	14
Central intermediary metabolism	37	8	6
DNA metabolism	99	13	7
Disrupted reading frame	51	7	3
Energy metabolism	155	19	43
Fatty acid and phospholipid metabolism	30	3	2
Hypothetical proteins	318	41	52
Mobile and extrachromosomal element functions	63	4	6
Protein fate	68	8	14
Protein synthesis	121	17	2
Purines, pyrimidines, nucleosides, and nucleotides	41	4	3
Regulatory functions	53	10	10
Transcription	37	9	1
Transport and binding proteins	126	19	37
Unclassified	519	64	102
Unknown function	130	22	17

Figure 3. Time course distribution of up- and down- regulated genes within TIGRFAM main roles. The plot reflects the dynamics of Nm metabolic adaptation to blood, and the number of regulated genes within each TIGR family is shown for each time point. The total number of genes in each class and the number of up- and down-regulated genes are listed in the table (from [29]).

A wide range of hypothetical, unclassified ORFs and ORFs with unknown function was differentially regulated and the analysis of the unclassified ORFs regulated in blood may aid in their functional characterization. The major groups of differentially regulated genes are involved in energy metabolism, transport and binding, amino acid biosynthesis and regulatory functions (Figure 4).

Figure 4. *(see next page).*

Figure 4. Transcriptional profile of differentially regulated genes grouped by functional TIGRFAM family main roles. Detailed expression profiles of functionally related genes during the time course of Nm in human whole blood. Clusters were created using TMEV. **(A)** Regulatory functions **(B)** Transport and binding proteins **(C)** Energy metabolism **(D)** Amino acid biosynthesis. Each gene is represented by a single row and each time point by a single column; gene identification numbers (based on the MC58 annotation) and gene definitions are reported on the right. Gene expression is displayed in fold change represented by the color bar under the figure. The numerical gene expression values are shown for all the genes at the different time points (from [29]).

These groups are predominantly upregulated, suggesting a high degree of metabolic adaptation occurs in blood, enabling uptake of different substrates and induction of alternative metabolic pathways. In particular, we found that the gene encoding the regulator Fur, as well as all genes encoding iron uptake systems, were significantly up-regulated. Analysis of regulated genes encoding for surface-exposed proteins involved in Nm pathogenesis allowed us to better understand mechanisms used to circumvent host defenses. During blood infection, Nm activates genes encoding for the factor H binding proteins, fHbp and NspA, genes encoding for detoxifying enzymes such as SodC, Kat and AniA, as well as several less characterized surface-exposed proteins that might have a role in blood survival.

1.7 A broader view of transcriptional adaptation of bacteria to the environment

To survive and thrive in an often hostile environment, a bacterium has to monitor its surroundings and adjust its gene expression and physiology accordingly. This is especially important for pathogenic bacteria, which continuously interact with the host during an infection and need to tighly regulate virulence factors at gene expression level, in order to control the various steps of pathogenesis. Traditionally, this regulation have been

accredited to the activity of transcriptional factors, but studies in the past years have largely demonstrated the expression in bacteria of RNA regulatory molecules. Moreover, regulation mediated by RNAs and their associated proteins is more common than previously thought. Genome-wide analyses based on tiling arrays and high-throughput RNA-sequencing technologies have revealed the transcriptomes of several bacteria, including pathogenic bacteria [34]. Both techniques allow the unbiased visualization of all RNA molecules transcribed during specific conditions (for example, during stress, high osmolarity and low oxygen) without taking into account the positions of annotated ORFs. Therefore, the positions of all RNAs transcribed in a cell — namely, mRNAs (including operons), tRNAs, ribosomal RNAs, *cis*-acting antisense RNAs and *trans*-acting sRNAs — can be mapped with 1-nucleotide resolution. These studies have discovered unexpected numbers of small RNAs and other species of RNA regulators, that act to control the expression of genes encoding virulence factors at multiple levels and in a temporal manner, according to the stress [35], [36], [37], [38] and have shown that the transcriptional landscape of all organisms is much more complex than expected.

With this regard, it is conceivable that *Neisseria meningitis* can possess a circuit of regulatory RNAs involved in the regulation of different steps of pathogenesis. Indeed, three research groups independently demonstrated that the RNA chaperone Hfq, which is up regulated during incubation in human whole blood [29], is involved in stress response and virulence in Nm and is a pleiotropic regulator of protein expression, suggesting the presence in Nm of a large small RNA network, not yet defined [30], [39], [40].

1.8 Regulatory RNAs

RNAs are excellent regulatory molecules that can carry out a plethora of regulatory tasks [41]. For instance, RNAs can directly sense environmental cues, such as differences in temperature, pH and nutrient availability, through regulatory regions that lie upstream of the coding sequence on the same transcript, leading to an altered transcriptional read-through or translation initiation of that downstream coding sequence. Furthermore, bacteria can regulate transcript expression through *cis*-acting RNAs, which function in an antisense manner and control the expression of mRNAs encoded on the opposite DNA strand, or

trans-acting small non-coding RNAs (sRNAs), which function at a distance to alter the expression of target RNAs through an antisense mechanism. The fate of RNA transcripts can also be controlled by proteins, including RNases and RNA chaperones, which can degrade both *cis*- and *trans*-acting antisense regulatory RNAs and their target mRNAs or can facilitate the interaction of *trans*-acting sRNAs with the target mRNAs, respectively (Figure 5).

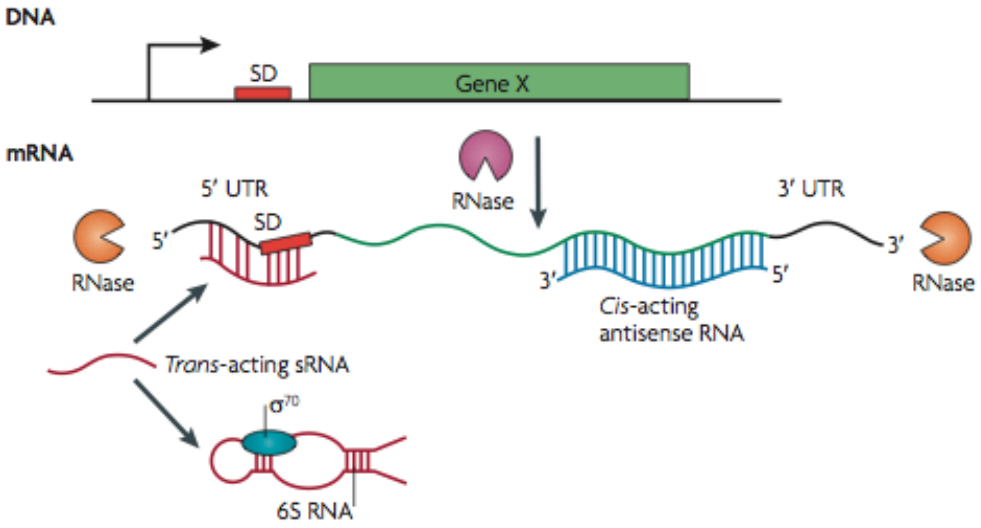

Figure 5. Control of mrNA activity and stability. The fate of an mRNA is controlled by several factors. 5′ untranslated regions (UTRs) lie upstream of the coding sequences and include thermosensors, pH sensors and riboswitches. 3′ UTRs lie at the other end of coding RNAs and, in many cases, determine transcription termination and stability. *Cis*-acting antisense RNAs are expressed from the opposite strand of the DNA. *Trans*-acting small non-coding RNAs (sRNAs) are expressed from a different location on the chromosome and most commonly bind to the Shine–Dalgarno (SD) sequence of a target mRNA in an antisense manner. *Trans*-acting sRNAs can also sequester target proteins; for example, 6S RNA sequesters the housekeeping RNA polymerase σ70 (also known as RpoD). The fate of transcripts can also be controlled by RNases, which function either exonucleolytically (orange), by targeting transcripts from the 5′ or 3′ end (such as RNase J1 and RNase J2, which are found in some Gram-positive bacteria) or endonucleolytically (purple), by targeting sequences in the middle of the transcript (from [42]).

Because pathogenic bacteria encounter diverse environmental conditions, they require rapid regulatory circuits to survive, making regulatory RNAs particularly suitable for controlling bacterial virulence. Together with regulatory proteins and two-component systems, regulatory RNAs integrate environmental stimuli into outputs that are important for pathogenicity. In fact, there is evidence that regulatory RNAs are more suitable than proteins for controlling gene expression. First, the energy cost of transcription (that is, generating regulatory and target RNAs) is much lower than that of translating regulatory proteins. Second, regulatory RNAs can control gene expression much faster than regulatory proteins; this is especially true for 5′ untranslated regions (UTRs), which directly dictate the expression of downstream mRNAs on sensing an environmental cue. Third, regulatory RNAs are generally much less stable than regulatory proteins, which allow their rapid clearance when they are no longer needed. Fourth, many regulatory RNAs act at post-transcriptional level and can therefore modify mRNAs that have already been expressed; they can thereby dictate and possibly overcome effects at the transcriptional level.

1.8.1 Trans-acting small RNAs

RNA molecules acting in *trans* on distant targets are commonly denoted as *trans*-acting sRNAs and are perhaps the best-studied form of regulatory RNA [43]. *Trans*-acting sRNAs, traditionally identified in intergenic regions, are encoded distally from their targets and share only limited complementarity with their target mRNAs.

These sRNAs regulate the translation and/or stability of target mRNAs and are, in many respects, functionally analogous to eukaryotic miRNAs. The majority of the regulation by the known trans-encoded sRNAs is negative [43]. Base pairing between the sRNA and its target mRNA usually leads to repression of protein levels through translational inhibition, mRNA degradation, or both (Figure 6). The bacterial sRNAs primarily bind to the 5’ UTR of mRNAs and most often occlude the ribosome binding site, inhibiting translation through base pairing far upstream of the AUG of the repressed gene ([44]; [45]). The sRNA-mRNA duplex is then frequently subject to degradation by RNase E. However, sRNAs can also activate expression of their target mRNAs through an anti-antisense mechanism

whereby base pairing of the sRNA disrupts an inhibitory secondary structure, which sequesters the ribosome binding site [46], [47], [48] (Figure 6).

Given that sRNAs are often degraded along with the mRNAs they regulate, in other words they are consumed in the process of regulation, the use of RNA regulators might be advantageous over regulatory proteins in achieving a fast and irreversible transition, which is often required during pathogenesis [49].

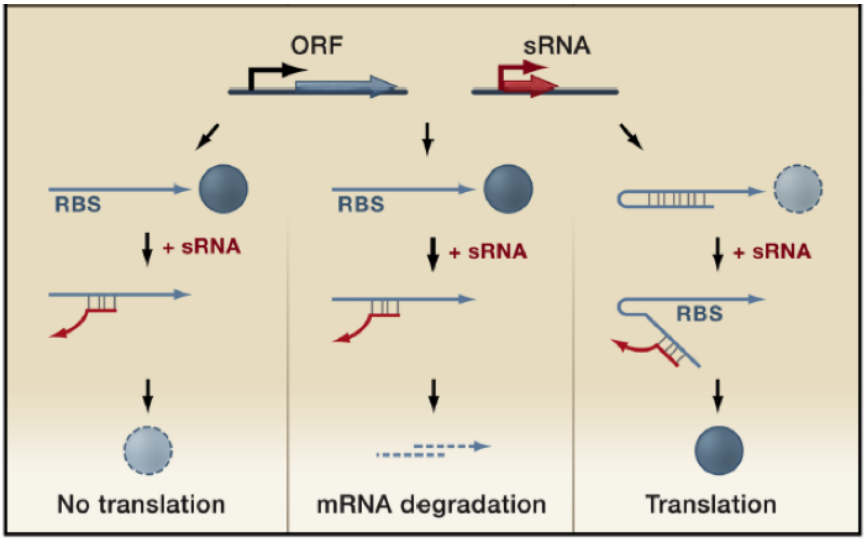

Figure 6. Regulatory functions of *trans*-acting small RNAs. Genome loci encoding *trans*-acting small RNAs (red) are located separate from the genes encoding their target RNAs (blue) and only have limited complementarity. These small RNAs can act negatively by base pairing with the 5' UTR and blocking ribosome binding (left panel) and/or targeting the sRNA-mRNA duplex for degradation by RNases (middle panel). *Trans*-acting sRNA can act positively by preventing the formation of an inhibitory structure, which sequesters the ribosome binding site (RBS) (right panel) (from [43]).

For trans-acting sRNAs, there is little correlation between the chromosomal location of the sRNA gene and the target mRNA gene. In fact, each trans-encoded sRNA typically base pairs with multiple mRNAs. The capacity for multiple base pairing interactions results from imperfect base-pairing with target mRNAs, rather than extended stretches of perfect complementarity, as for cis-encoded antisense sRNAs. The region of potential base pairing between trans-acting sRNAs and target mRNAs typically encompasses ~10–25 nucleotides, but in all cases where it has been examined only a core of the nucleotides

seem to be critical for regulation. In many cases, the RNA chaperone Hfq is required for trans-acting sRNA-mediated regulation, presumably to facilitate RNA-RNA interactions due to limited complementarity between the sRNA and target mRNA. Hfq-associated small RNAs are diverse in length (50-250 nucleotides); in several cases, Hfq binds in a AU-rich single strand region located upstream of the terminator and this binding may then expose the target binding domain of the sRNA to the potential mRNA partners [50]. Beyond facilitating base pairing, Hfq contributes to sRNA regulation through modulating sRNA levels. Once base paired with target mRNAs, many of the known sRNA-mRNA pairs are subject to degradation by RNaseE. Nevertheless, there are also cases of Hfq-independent sRNAs, for example, the recently characterized sRNA VrrA in *V. cholerae*, which modulates colonization of the host small intestine [51]. In general, longer stretches of base pairing, as is the case for the cis-encoded antisense sRNAs, usually do not require Hfq for function, and/or high concentrations of the sRNA may obviate a chaperone requirement.

Most of the trans-encoded sRNAs are synthesized under very specific growth conditions. In E. coli for example, these regulatory RNAs are induced by low iron (Fur-repressed RyhB), oxidative stress (OxyR-activated OxyS), outer membrane stress (σE-induced MicA and RybB) and elevated glycine (GcvA-induced GcvB) [52], [53], [54]. Most trans-acting sRNAs are involved in responding to rapidly changing environmental conditions, and there are cases of sRNAs with a role in virulence and pathogenesis, for example: Rli38 of *L. monocytogenes* [36], induced in human blood, RNAIII of *S. aureus* [55,56] and Qrr of *V. cholera* [57] involved in quorum-sensing and SprD of *S. aureus*, which negatively regulates the expression of the Sbi immune-evasion molecule [58].

The fact that a given base pairing sRNA often regulates multiple targets means that a single sRNA can globally modulate a particular physiological response, in much the same manner as a transcription factor, but at the post-transcriptional level [43].

1.8.2 Cis-encoded antisense RNAs

Cis acting antisense RNAs consist of two subtypes: bona fide antisense RNAs, which are present on the complementary strand to one or several ORFs, or overlapping UTRs, which

consist of a long 5' or 3' UTR of an mRNA that overlaps with the mRNA encoded by the other DNA strand (Figure 7).

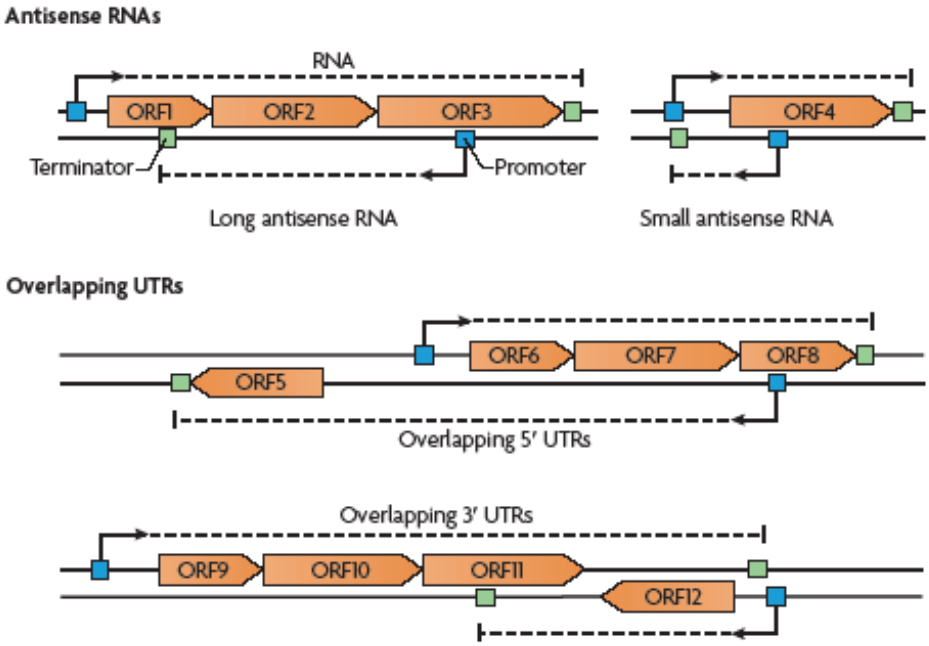

Figure 7. *Cis*-acting antisense RNAs. Schematic representation of the different types of antisense RNA molecules. These include bona fide antisense RNAs and overlapping 5′ and 3′ untranslated regions (UTRs). The antisense RNA may be either a long antisense RNA covering more than one ORF (in the example, the long antisense RNA overlaps ORF1, ORF2 and ORF3) or a small antisense RNA that overlaps the Shine–Dalgarno sequence (which lies between the promoter and the start codon) and affects mRNA stability and/or protein translation (for example, the antisense RNA overlapping ORF4). Overlapping 5′ UTRs are generated when the transcription of a certain gene (for example, ORF5) starts from a promoter located on the DNA strand opposite divergent genes (in this case, ORF6, ORF7 and ORF8). As a result, the ORF5 mRNA has a long 5′ UTR that overlaps the ORF6, ORF7 and ORF8 mRNA. Overlapping 3′ UTRs are generated when transcription of a certain gene ends in or after a gene located on the opposite DNA strand; for example, the transcription of the operon encoding ORF9, ORF10 and ORF11 ends after ORF12, so the long 3′ UTR completely overlaps the ORF12 mRNA (from [42]).

Until a few years ago, the understanding of cis-acting antisense RNAs was limited to studies in bacteriophages, plasmids and transposons. Recent technological advancements have shown that antisense transcription occurs in all species, including bacteria. Many

antisense transcripts have been found in Helicobacter pylori (46% of all ORFs were associated with at least one antisense transcription start site [38], *Listeria monocytogenes* [59] but also *Mycoplasma pneumoniae, Pseudomonas syringae* and *Bacillus subtilis* [60,61] [62]. It therefore seems that cis acting antisense RNAs are extremely abundant and the size of antisense transcripts can range from few bases to several kilobases, so one particular antisense RNA may overlap several genes (as reported for *L. monocytogenes* and *B. subtilis).*

Plasmid encoded antisense RNAs involved in the regulation of replication, are expressed constitutively. By contrast, chromosomally encoded antisense RNAs have been found to be expressed only under certain conditions, for example in stationary phase (e.g. GadY) [63] or under iron stress (e.g. IsrR) [64]. In *H. pylori*, seveval cis-acting antisense RNAs and their corresponding mRNA targets are induced by the same signal (in this case, acid stress). This is in contrast to most trans-acting sRNAs, which are typically controlled by a different regulator than their mRNA target.

Antisense RNAs could provide an advantage when the levels of a particular protein need to be repressed very tightly and expressed under very select circumstances, as in the case of transposase or toxin. Indeed, many of the characterized antisense RNA targets are subject to extensive regulation, where the antisense RNAs provide yet one more level of control [65]. In general, it is conceivable that only mRNA that is present at higher levels than its cis-acting antisense antagonist is translated, so translation of certain genes starts only when the mRNA concentration reaches a certain level [34].

In the majority of cases, antisense RNA action entails post-transcriptional inhibition of target RNA function but, in few cases, activating mechanisms have been found too. The currently known mechanisms employed by cis-encoded antisense RNAs are (Figure 8) [65]:

- Transcription interference: when transcription from one promoter is suppressed by a second promoter present in cis [66];
- Transcription attenuation: generally found on plasmids, when base pairing of the antisense RNA to the mRNA induce the formation of a terminator structure in the target mRNA;
- RNA cleavage: antisense RNA can also impact the stability of a target RNA by either promoting or blocking cleavage by endoribonucleases or exoribonucleases. In many bacteria, two major endoribonucleases have been linked to antisense RNA-induced target mRNA cleavage: RNase III that cleaves double-stranded RNA

and Rnase E, which cleaves single-stranded RNA. It is also possible that base pairing might block an RNaseE recongnition site, thus leading to increased stability of the target RNA. Moreover, the base pairing might impact the ability of an exonuclease to degrade a particular target RNA, in a way similar to the presence of stem-loops within a transcript.

- Translation block: many trans-encoded sRNAs base pair with the Shine-Dalgarno sequences of their target mRNAs thereby preventing ribosome binding and protein translation. Antisense RNAs for which the complementarity extends into the 5'UTR of the mRNA target may act by a similar mechanism.

In addition, some antisense RNAs are reported to encode for protein (e.g. alr1690 anti furA) [67], or antisense RNA could act as both cis and trans-encoded base pairing RNAs, as for E.coli GadY RNA [63].

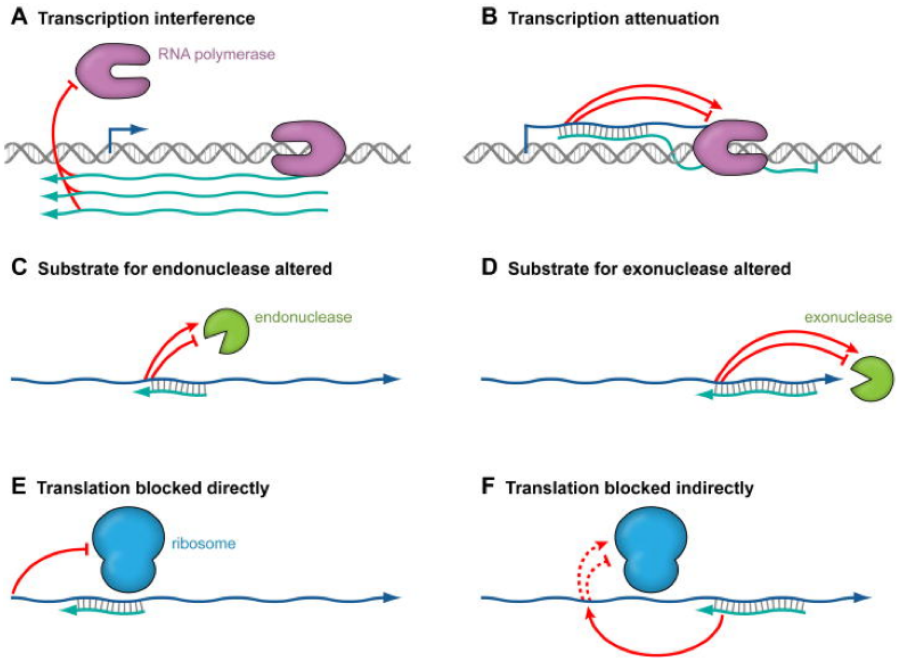

Figure 8. Mechanisms of action of antisense RNAs. Antisense RNAs can induce transcription interference (A), where transcription from one promoter blocks transcription from a second promoter by preventing RNA polymerase from either binding or extending a transcript encoded on the opposite strand. Transcription interference does not involve basepairing and does not occur when the antisense RNA is provided in trans. In transcription attenuation (B), base pairing of the antisense RNA to the target RNA causes changes in the target RNA structure ultimately affecting

transcription termination. Antisense RNAs can also affect target RNA degradation by endonucleases (C) and exonucleases (D). In these cases, base pairing between the sense and antisense RNAs can directly either generate or block a ribonuclease target site. Antisense RNAs can also indirectly affect the binding of the ribonuclease at a distance from the site of base pairing. Finally, antisense RNAs can directly block ribosome binding (E) or indirectly positively or negatively impact ribosome binding by affecting the target mRNA structure (F). The sense RNAs are indicated in dark blue while the antisense RNAs are shown in light blue (from [65]).

1.8.3 5' and 3' untranslated regions

The region between the transcriptional start site and the start codon of an mRNA is known as the 5' untranslated region (UTR). This region can vary in length, ranging from a few to several hundred bases. 5' UTRs are used by pathogenic bacteria to modify gene expression on the basis of changes in temperature, pH and the presence of metabolites. RNA thermosensor 5'UTR forms a secondary structure at low temperature masking the Shine-Dalgarno sequence at inhibiting translation, while at 37°C an alternative secondary structure is formed that allow translation of the ORF. An example is the 116 bp 5'UTR upstream of prfA mRNA in *L. monocytogenes* [68], but other thermosensors have been found in Yersinia and Salmonella spp [69]. Such sensing mechanisms are especially important for pathogens, which need to fine-tune gene expression in response to host temperature. The same mechanism is the one used in pH sensing by *E. coli* for the expression of alx gene, that is expressed highly in alkaline conditions.

One important group of 5'UTRs is riboswitches. These are metabolite-sensing regulatory RNA structures that function as sensors and regulators of various metabolic pathways in bacteria. Each class of riboswitches binds a specific metabolite through its aptamer domain and this interaction induces a structural change in the riboswitch regulatory domain that causes altered transcription or translation (Figure 9).

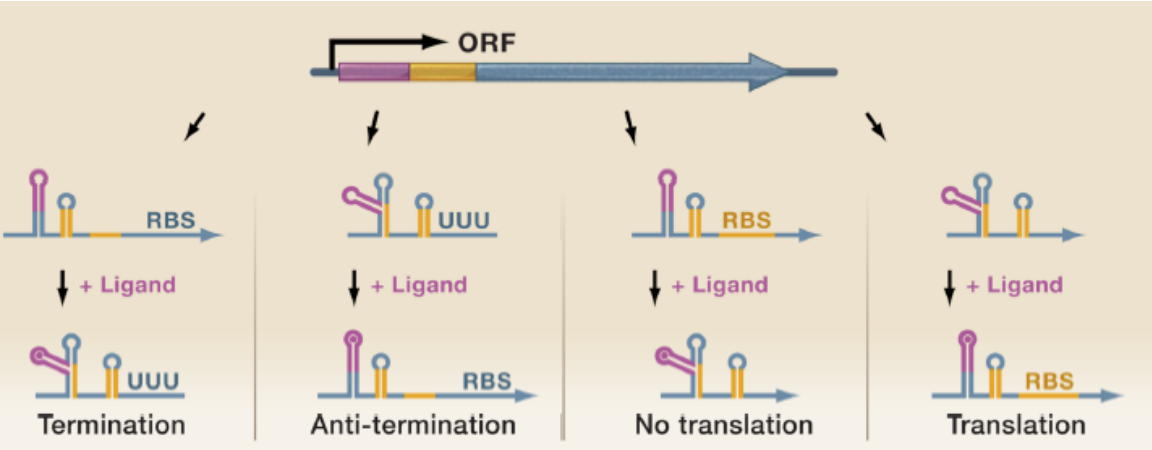

Figure 9. Regulatory functions of riboswitches. Riboswitches are composed of an aptamer region (pink) and an expression platform (orange) in the 5' UTR of an mRNA (blue). Ligand binding can result in transcriptional regulation of mRNA synthesis or translational control of protein synthesis. (Left panel) In the absence of ligand, the expression platform assumes a conformation permissive of transcription—shown here as a stem-loop lacking a U-rich region—allowing synthesis of the entire mRNA. When the ligand binds the aptamer region, a conformational change leads to the disruption of this structure and the formation of an alternative hairpin followed by a string of U residues. This alternative hairpin acts as a transcriptional terminator, inhibiting gene expression. (Middle left panel) In the absence of ligand, the riboswitch initially forms a terminator. Upon ligand binding, this terminator is disrupted, allowing transcription to continue. (Middle right panel) In the absence of ligand, the ribosome binding site (RBS) is accessible, but upon ligand binding, is sequestered into an inhibitory stem-loop, preventing translation. (Right panel) In the absence of ligand, the expression platform forms a repressive secondary structure in which the ribosome binding site is occluded. When the ligand binds to the aptamer region, the ribosome binding site is released and translation can initiate (from [43]).

At the translation level, the binding of the metabolite alters the access of the ribosome to the Shine-Dalgarno sequence. There are several different classes of riboswitches according to the metabolite they bind: cobalamin, c-di-GMP (i.e. in *Vibrio cholera*, *Clostridium difficile*, *Bacillus cereus* [70], lysine (LysRS of *Listeria monocytogenes*) [59], glycine, purine, FMN, GlmS, SAM, SAH, TPP and tetrahydrofolate [71]. Riboswitch-derived small RNAs described for *L. monocytogenes* (sreA and sreB that produce short antisense RNAs to repress the prfA mRNA) are known also in Gram negative species [72].

Toledo Arana and coworkers have identified in *L. monocytogenes* mRNAs with long overlapping 5' or 3' UTRs. In these cases, the mRNAs transcription starts or ends inside or before/after a gene located in the opposite strand. Thus the mRNA overlaps the mRNA from the convergent gene. How this overlapping UTRs affect gene expression is not clearly understood, but, as previously mentioned, it is reported that they can act as antisense RNAs for the gene located in the opposite strand [59]. This could be also a way to link neighboring gene expression, in the context of a global gene regulation.

On the other hand, a 3' untranslated region (UTR) can be generated either by the absence of a transcriptional terminator near the stop codon, or by termination read-through events. The 3'UTRs of bacterial mRNAs are thought to mainly harbor transcription termination structures, which might prevent access to exonucleases to the 3' end of the transcript but have no clear regulatory function. In *B. subtilis*, the transcript of nine genes were found to have long 3'UTRs that have high sequence similarity and form stable RNA secondary structures. The 3'UTR structures may be involved in the translation or localization of the proteins, coded by the mRNA, to specific compartments in the cell [62]. Alternatively, the long 3'UTR might protect from 3'-to-5'exonucleolytic degradation through their secondary structures. In addition to these structures, long putative 3' regulatory UTRs have been observed next to transcripts encoding certain virulence factors in *S. aureus*. This bacterium has several long 3'UTRs that give rise to sRNAs [37]. These examples suggest that large bacterial 3'UTRs might have a role in mRNA stability, mRNA localization, the generation of sRNAs ore regulation by binding trans-acting factors.

2. Results

2.1 Identification of genes that contribute to survival of Nm in an *ex vivo* blood model of infection

2.1.1. Generation and characterization of deletion mutant strains

We hypothesized that genes with enhanced expression (up- regulated) in response to incubation in human blood, previously identified using the gene-based microarray, might contribute to the survival of *Nm* in blood. 15 genes with a significant and sustained increase in expression throughout the time course of blood infection were selected for a further characterization. They encode for proteins belonging to different functional categories: transporters (tbpB, lctP), host-pathogen interaction (opc, mip, kat, nspA), surface-exposed proteins (nalP, NMB1483), transcriptional regulators (fur, NMB0595) and hypothetical proteins (NMB1946, NMB0035, NMB1840, NMB1786, NMB1064) (Table 2). Deletion mutants of each single gene were generated in the Nm strain MC58 by replacing the entire encoding sequence with an erythromycin or kanamycin resistance cassette (Figure 10A). In addition a subset of these proteins were analyzed also in another genetic background, 95N477 strain, where fHbp is expressed at low levels (data not shown), in order to investigate whether other factors that contribute to blood survival are revealed in this strain. In 95N477 strains were generated deletion mutants for the genes encoding for fHbp, LctP, TbpB, NMB1483, NspA, Kat, NMB1840, NMB1946, NMB1786 and NMB0035, using the same strategy followed for MC58.

			log_2 ratio				
NMB	**Gene**	**Annotation/Function**	**15 min**	**30 min**	**45 min**	**60 min**	**90 min**
NMB0035		P47, Lipoprotein	1.28	2.82	2.98	2.77	2.09
NMB0205	*fur*	Ferric uptake regulatory protein	0.88	1.33	1.77	1.69	1.57
NMB0216	*kat*	Catalase	1.21	2.04	3.33	3.56	2.96
NMB0460	*tbpB*	Transferrin binding protein B	1.04	1.53	1.47	1.13	0.96
NMB0543	*lctP*	L-lactate permease	1.00	0.93	1.34	1.30	1.62
NMB0595		DNA-binding response regulator	0.54	1.15	1.21	1.00	0.96
NMB0663	*nspA*	*Neisseria* surface protein A	2.03	1.61	1.85	1.49	1.13
NMB1053	*opc*	Class 5 outer membrane protein	0.71	1.04	1.28	1.44	1.55
NMB1064		Conserved hypothetical protein NUDIX	1.27	1.89	2.53	2.34	2.29
NMB1483		Putative lipoprotein	0.46	0.68	1.08	0.95	1.05
NMB1567	*mip*	Macrophage infectivity potentiator	0.42	1.51	2.21	2.03	1.60
NMB1786		Hypothetical protein	0.96	1.59	2.19	2.07	2.09
NMB1840		Conserved hypothetical protein/integral membrane protein	0.83	1.39	2.35	2.27	2.48
NMB1946		Outer membrane lipoprotein	0.68	1.31	1.62	1.51	1.46
NMB1969	*nalP*	Serine type peptidase	0.07	0.55	0.93	0.91	1.05

Table 2. Nm genes up-regulated in human blood and encoding known and putative virulence factors, that were selected for a further characterization in an *ex vivo* model of bacteremia (from [29]).

All the deletion mutant strains were characterized respect to growth in GC rich medium and they were all able to grow normally, without any evident growth defect (data not shown). In addition, a Southern Blot analysis was performed in order to verify the correct insertion of the antibiotic resistance cassette. Kanamycin or erythromycin cassettes were used as a probe. The results showed that the mutants had only one insertion of the antibiotic resistance cassette, corresponding to the gene locus to replace (Figure 10C). PCR analysis on each gene locus further confirmed the double strand recombination event and allowed to determine the orientation of the antibiotic resistance cassette (Figure 10B).

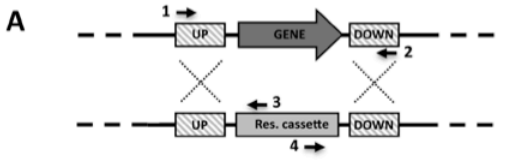

B

ko strain	resistance cassette	cassette orientation (5'-3')	approx. digestion fragment length (bp)
MC58 Δfur	Kan	→	15000
MC58 ΔnalP	Kan	→	16400
MC58 ΔfHbp	Ery	→	6250
MC58 Δ1483	Ery	→	5700
MC58 Δmip	Ery	→	9750
MC58 ΔtbpB	Ery	→	11400
MC58 ΔlctP	Ery	→	2300
95N477 ΔlctP	Ery	→	2400
95N477 ΔnspA	Ery	→	6200
95N477 Δ1483	Ery	→	4200
95N477 ΔfHbp	Ery	→	6250
95N477 ΔtbpB	Ery	→	13900

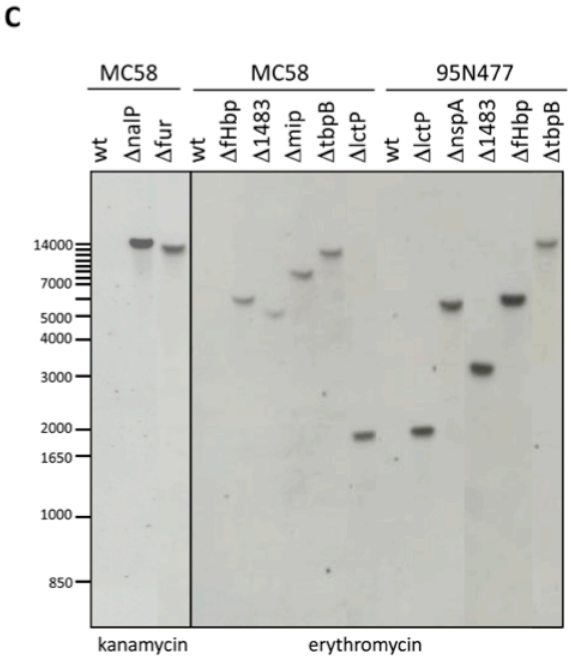

Figure 10. Characterization of the Nm deletion mutants. A. Schematic representation of the allelic replacement with the resistance cassette, used to generate the deletion mutant strains. The gene locus of each deletion mutant was amplified from the genomic DNA using primers specific for each amplicon (indicated as 1 and 2) and the PCR fragments were sequenced using the same primers and primers 3 and 4 for the antibiotic cassette Kan or Ery. **B.** The orientation of the resistance cassette for each deletion mutant, determined from sequencing. **C.** Southern blot analysis was performed using labeled Kan and Ery PCR products as probes. Genomic DNA of wild-type and deletion mutant strains was digested with *BglI*. The size of the expected fragment for each mutant is reported in panel B. The length of the fragment is approximate since *BglI* restriction site is subjected to *dam* methylation that could occur along the genomic DNA. Note that here are reported only the data of the deletion mutants that gave a phenotype in the *ex vivo* model of bacteremia, to confirm that the phenotype was not due to any other genomic alteration of the bacterial strain (from [29]).

2.1.2 Survival experiment of wild type and knock out strains in an ex vivo model of bacteremia

The MC58 wild-type and mutant strains were then incubated in human whole blood for two hours in an *ex vivo* model of bacteremia and samples were taken at various time points to assess survival through CFU determination. The fHbp mutant strain was used as a control (Figure 11A), since it has previously been described as a crucial factor for survival in human blood [31]. Nm MC58 mutant strains lacking LctP, TbpB, NalP, NMB1483, Mip and Fur were sensitive to killing by human whole blood compared to the MC58 wild-type strain (Figure 11A2–7). Bacterial counts for the other mutants were not significantly different compared to the MC58 wild-type strain (Figure 11A8–9), suggesting that these genes are not essential for Nm survival in human blood in this Nm genetic background. Mutant strains were also characterized for their growth in GC broth at 37°C in the same experimental conditions used for incubation in blood. The growth rate for the majority of the mutants was comparable to the wild-type strain (insets in Figure 11A) suggesting that the phenotype observed in blood is not attributable to a growth defect. In addition, to overcome donor variability, we tested the same mutant strains with a second blood donor and comparable results were obtained (Figure 12). LctP (NMB0543) is a lactate permease involved in the uptake of lactate, which is present in blood and is taken up by the bacterium as a carbon energy source and also converted to precursors of capsular and lipopolysaccharide sialic acid [74]. The up-regulation of lctP together with the phenotype of decreased survival that was observed for the deletion mutants in this ex vivo model (Figure 11A2) as well as in other relevant models [74], confirm the important role that this membrane transporter plays in increasing complement resistance of Nm strains. However, the fact that the lctP deletion mutant is not completely killed in human blood even after 120 minutes of incubation might suggest that other carbon sources could be utilized by the bacterium to generate phospho-enol pyruvate that in turn could be used to generate sialic acid [75]. TbpA and TbpB function as the transferrin receptor in Nm and we demonstrate that a TbpB mutant is defective in growth in human blood, suggesting that transferrin-binding is a crucial step for iron-uptake and survival under these conditions (Figure 11A3). NalP, an autotransporter lipoprotein with serine-protease activity that is involved in the cleavage of Nm surface-exposed proteins [76], was identified as being important for survival in blood (Figure 11A4). Studies published to date have not identified NalP as a

factor involved in the survival of Nm in the host and further study will be necessary to understand if NalP plays a direct role in survival of Nm (i.e., maybe by cleaving a component of the innate immune system), or an indirect role (through activity on one of its known surface targets). NMB1483, a putative surface-exposed lipoprotein annotated as a NlpD-homologue, is also involved in survival in blood (Figure 11A5). BLAST searches reveal that NMB1483 might have a metalloprotease activity and homologues of this protein are involved in the pathogenesis of *N. gonorrhoeae* and *Y. pestis* [77], [78]. Interestingly, in N. gonorrhoeae the NMB1483-homologue protects against oxidative damage mediated by hydrogen peroxide and against neutrophil-mediated killing. The mip gene is highly up-regulated during blood exposure and the results obtained with the mip deletion mutant (Figure 11A6) suggest that the protein has a role in survival of Nm in blood. The Mip lipoprotein is involved in the intracellular survival in macrophages of the closely related species *N. gonorrhoeae* [79] and the Nm Mip protein may also facilitate interaction of Nm with macrophages. The ferric uptake regulator (Fur) mutants of different pathogens (e.g. *Helicobacter pylori, Staphylococcus aureus, Listeria monocytogenes* and *Campylobacter jejuni*) are attenuated in animal models of infections [80]. Similarly, our data demonstrate that in Nm Fur plays a major role in the adaptation and survival of the bacterium in the ex vivo model of blood infection (Figure 11A7).

In strain 95N477, deletion of the fHbp gene did not significantly alter bacterial survival in blood (Figure 11B1). However, deletion of NspA in strain 95N477 had a marked effect on survival in blood (Figure 11B5), suggesting that NspA may be the main factor involved in fH binding and resistance to the alternative complement pathway in this genetic background where fHbp is expressed at very low levels. We did not examine the expression of fHbp in 95N477 in blood, however, recent work by Oriente et al. showed that fHbp is regulated in a similar manner in 16/17 strains, in an FNR dependent manner, even in strains with very low fHbp expression [81]. The NspA-related phenotype observed confirms what was recently shown in NspA mutants of a similar Nm strain with low fHbp expression [82] and suggests that the two factors might have a complementary function. The survival phenotypes obtained for LctP, TbpB and NMB1483 mutants were comparable in the two genetic backgrounds suggesting a conserved role of the function of these proteins in the survival of Nm in blood. The other 5 mutants analyzed in 95N477 (NMB1840, NMB1946, NMB1786, kat and NMB0035) were not sensitive to killing by human blood and showed comparable survivals with respect to MC58 mutants (Figure 11B6). This suggests that, despite up-regulation of the genes, these factors are not essential

for Nm survival in human blood.

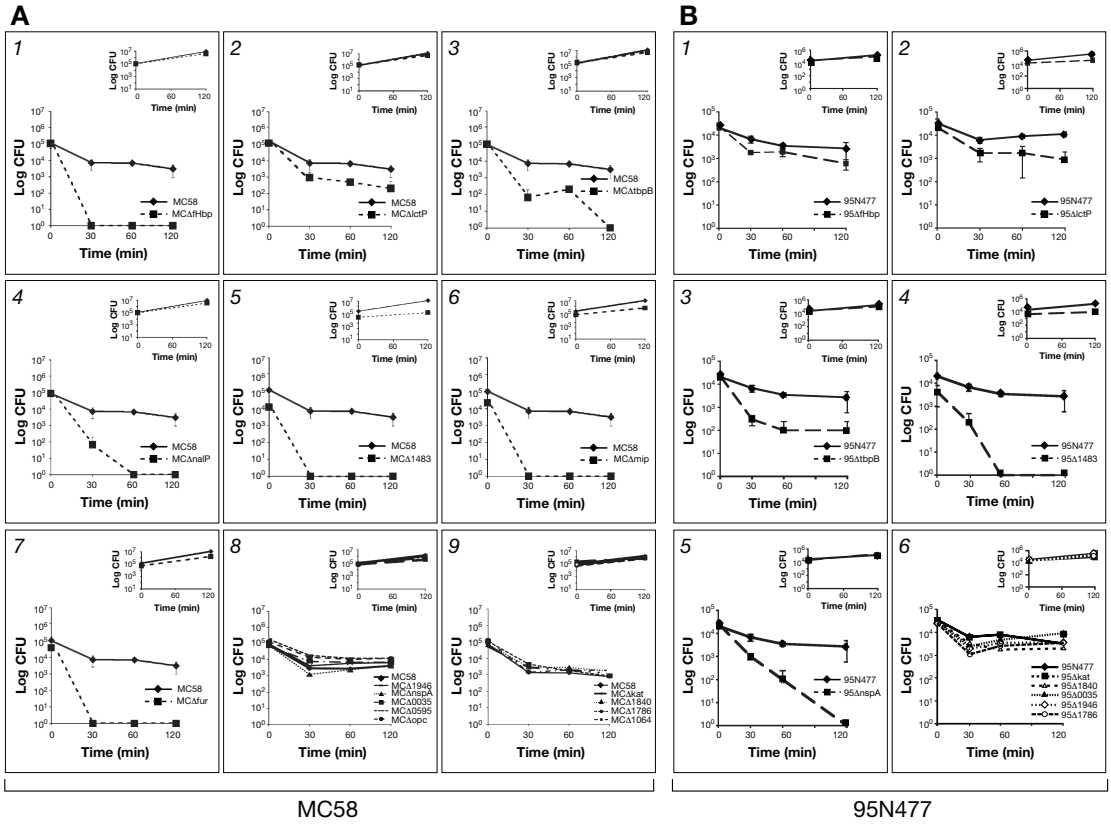

Figure 11. Survival of MC58 and 95N477 wild-type and deletion mutant strains in the *ex vivo* whole blood model of meningococcal septicemia. Deletion mutants in the genetic backgrounds MC58 (panel A) and 95N477 (panel B) of the selected up-regulated genes were tested for survival using the ex vivo whole human blood model over a time course of 120 minutes. The phenotype of the specific mutants were compared to the wild-type strain. MCΔfHbp deletion mutant was used as a control (A1). Deletion mutants with a significant sensitivity to killing by human blood respect to MC58 wild-type are reported in panels A2-7, while those that were not significantly sensitive are reported in panels A8-9. Deletion mutants with a phenotype in 95N477 genetic background are reported in panels B2-5, while those that were not significantly sensitive to whole human blood are reported in panel B6. Survival result of deletion mutant for fHbp in 95N477 is reported in panel B1. The insets of each panel represent the growth control in GC medium for the same time course of incubation as performed in whole blood (from [29]).

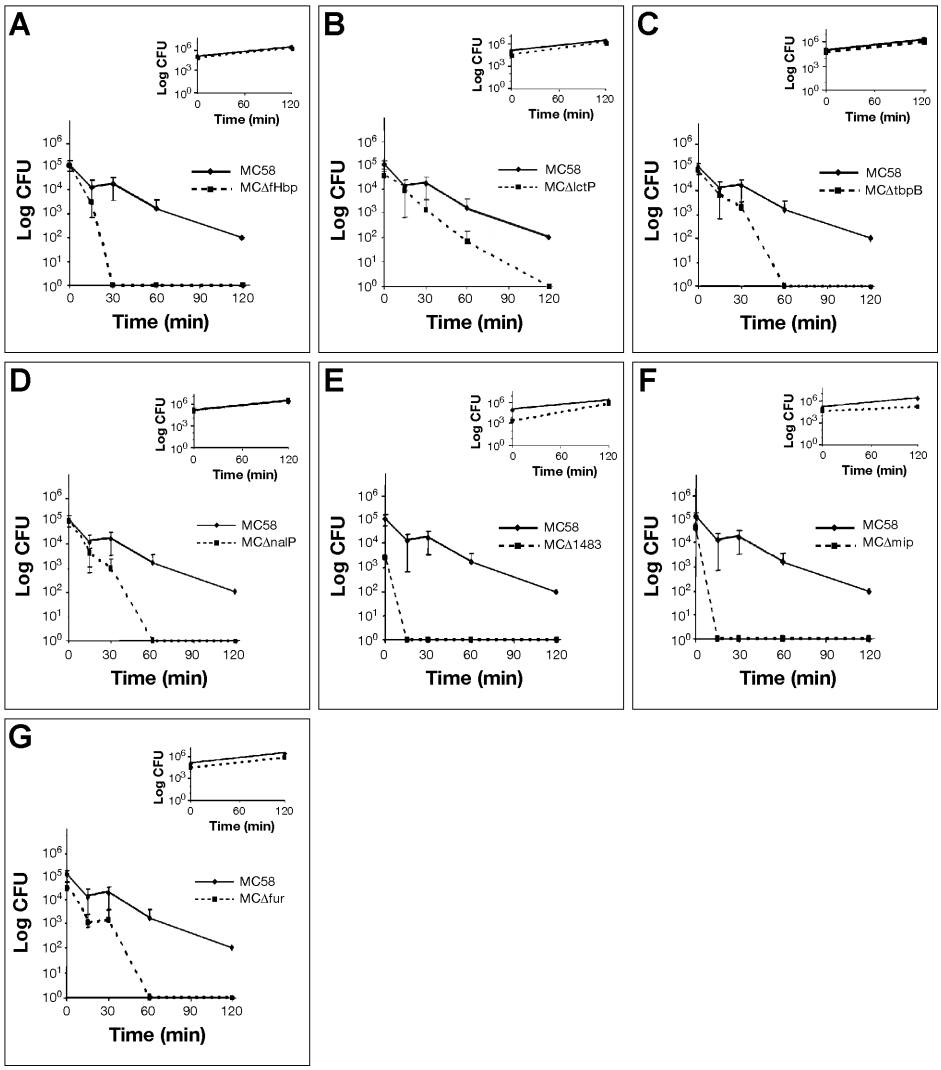

Figure 12. Survival of MC58 wild-type and deletion mutant strains in the *ex vivo* whole blood model using a second blood donor. Deletion mutants of the selected up-regulated genes were tested for survival using the *ex vivo* whole human blood model over a time course of 120 minutes. In each panel the phenotype of the specific mutant is compared to MC58 wild-type strain. The MCΔfHbp deletion mutant was used as a control. The insets of each panel represent the growth control in GC medium for the same time course of incubation as done with whole blood (from [29]).

2.1.3 Complementation experiments were able to restore the survival in blood

In order to better characterize mutant strains with a defective phenotype in blood, deletion mutants for fur, mip and NMB1483 in the MC58 genetic background and nspA in the 95N477 genetic background were complemented. The corresponding wild-type gene was inserted as a single copy in the chromosome of the mutant strains in the intergenic region between Nmb1428 and Nmb1429, under the control of a constitutive promoter. In this way, strains MCD-Cfur, MCD-Cmip, MCD-C1483 and 95D-CnspA were obtained. Wild-type, mutant and complementing strains were tested for growth in whole blood and in GC rich medium as a control. As shown in Figure 13, the survival in blood was restored in all the complementing strains confirming the role played by these factors in the survival of Nm in human blood.

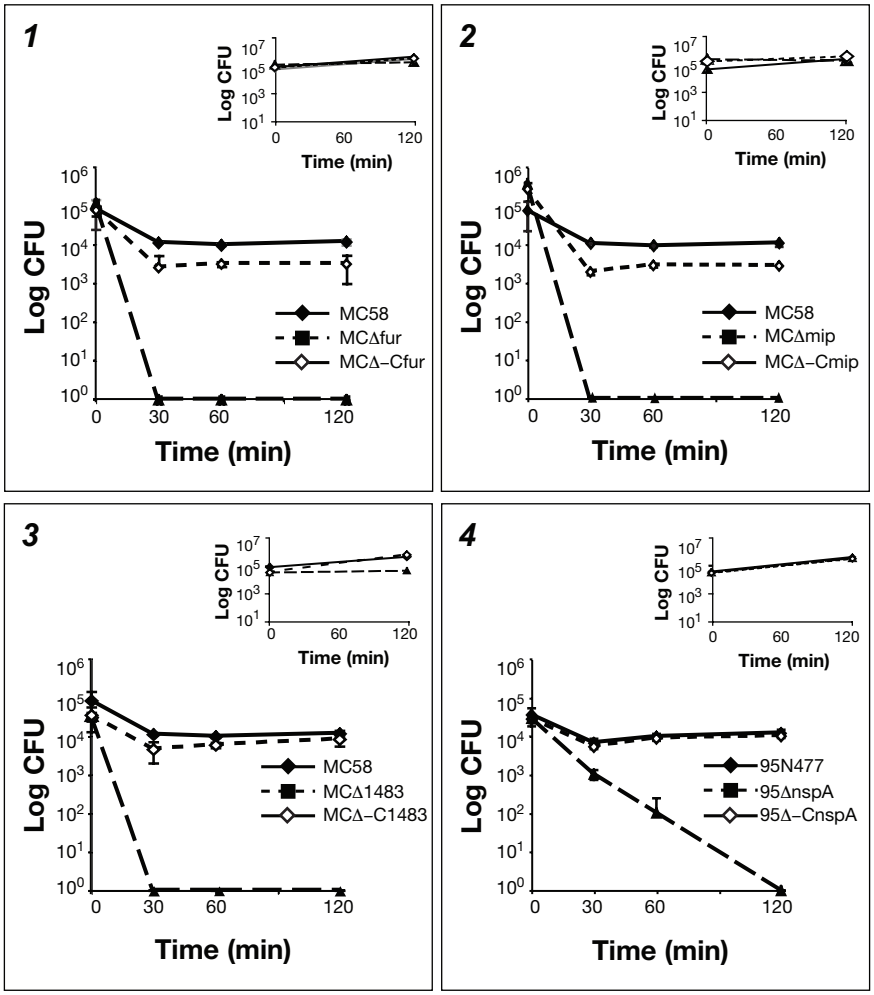

Figure 13. Survival of MC58 and 95N477 complementing strains in the *ex vivo* whole blood model of meningococcal septicemia. Results show the survival of the wild-type, deletion mutant and complementing strains in human whole blood for *fur* (panel 1), *mip* (panel 2) and *NMB1483* (panel 3) in MC58 and *nspA* (panel 4) in 95N477. The insets of each panel represent the growth control in GC medium for the same time course of incubation as performed in whole blood (from [29]).

2.2 Identification of new Nm transcript, differentially expressed during incubation in human whole blood

2.2.1 Analysis of the whole transcriptome of Nm using an oligonucleotide high density tiling microarray

Due to the design of the array, the previous analysis, performed with a 60-mer Nm oligonucleotide microarray that contained probes designed only in the coding sequence of each ORF, allowed to detect only the changes in gene expression profiles. Hence, the investigation was broadened to the whole transcriptome of *Nm*, using a customized 60-mer high density tiling oligonucleotide microarray. The array contained probes designed in the coding sequence of the ORFs (present also in the microarray used in the previous analysis) and probes covering tail-to-tail the antisense strand of each ORF and all the intergenic regions in both strands (Figure 14A).

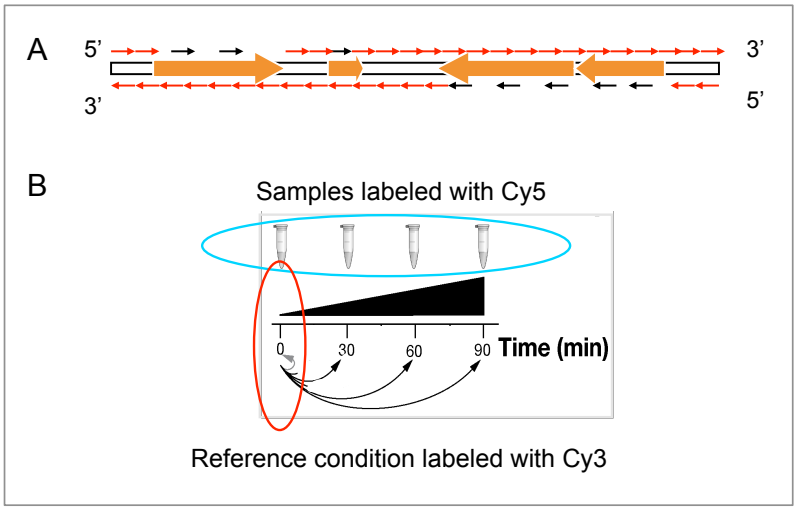

Figure 14. A. Microarray design. The customized high-density oligonucleotide tiling microarray was designed to contain probes covering all ORFs of MC58 > 300 bp with at least 2 probes/ORF (smaller ORFs are covered tail-tail). In addition, it has probes covering intergenic regions tail-tail both sense/antisense and probes covering antisense filament of ORFs **B. Experimental design.** Human blood isolated from three different donors was incubated with Nm and RNA extracted at the indicated time points (samples from each time point was done in triplicate and then pooled). Time 0 was used as the reference time point.

Freshly isolated whole venous blood collected from three healthy human volunteers (one male and two female) was used. Nm MC58 bacteria (approximately 10^8, grown in GC medium to early exponential phase) were mixed with blood from each donor in order to mimic disease. Analysis of growth in the blood by colony forming unit (CFU) counting showed that bacterial numbers increased approximately 3-fold over a 90-minute incubation period and that there was no significant difference in the number of CFU between the three donors (Figure 15A). In order to evaluate the adaptation of Nm to human blood, samples were collected at four different time points (each time point consisted of triplicate cultures): immediately after mixing bacteria with blood (time 0, reference point), and after 30, 60 and 90 minutes incubation at 37°C (Figure 14B). Total RNA extracted at each time point consisted of a mix of eukaryotic and prokaryotic RNA. Since eukaryotic RNA can compete with bacterial RNA during cDNA synthesis and fluorochrome labeling, we used a procedure that simultaneously removes mammalian rRNA and mRNA. With this procedure, we were able to significantly enrich the samples for Nm prokaryotic RNA (Figure 14B). We then applied an *in vitro* transcription amplification/labeling step [32] to produce amplified-labeled cRNA that was then used in competitive hybridization experiments with a 60-mer Nm oligo-microarray. Transcriptional changes throughout the course of Nm incubation in human blood were defined by comparison of expression levels at various time points against time 0 (Figure 14B). The analysis was performed considering the data set resulting from each single experiment (e.g. each single donor) and also the merge of the three data sets.

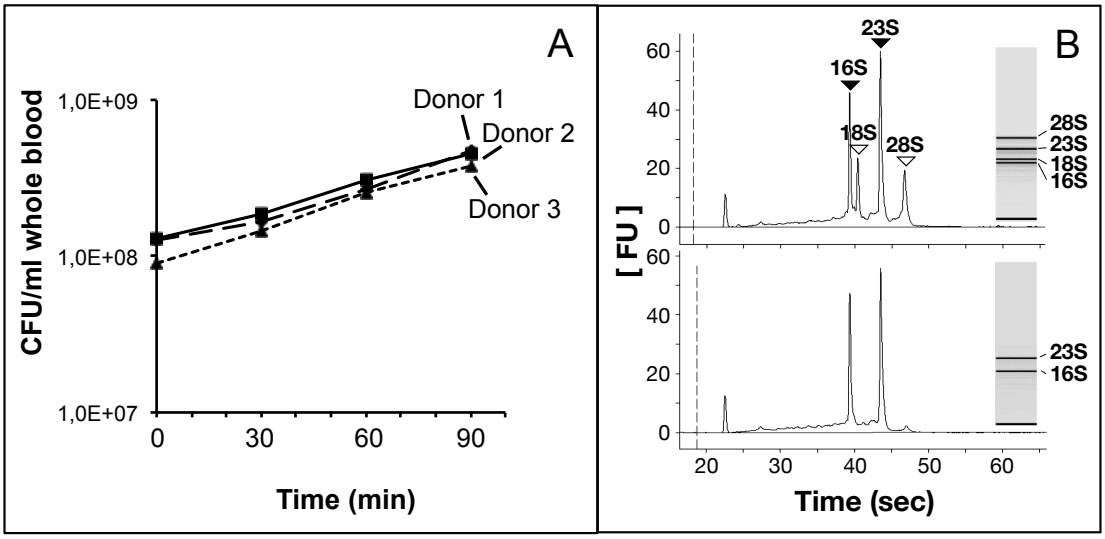

Figure 15. Growth of Nm in human whole blood and RNA analysis. A. Number of bacteria during incubation with human blood. The CFU/ml per single donor is shown during a time course experiment. **B.** Analysis of isolated total RNA and enriched Nm RNA using a BioAnalyzer 2100 (Agilent). **Upper panel:** Total RNA collected from Nm incubated in human whole blood, bacterial RNA (shaded arrowheads) and eukaryotic RNA (open arrowheads) are indicated. **Lower panel:** Enriched bacterial RNA.

2.2.2. Identification of new transcribed regions specifically expressed during incubation in human whole blood

The merge dataset was analyzed using a dedicated in-house developed bioinformatics tool. This tool, called SAD as Signal Areas Detector, allowed detecting close intensity-correlated probe regions. These boxes of correlated-probe regions were then manually inspected along the genome using the Artemis software, in order to map transcriptional units, considering both the coding and non-coding regions. In addition, the borders of the transcriptional units were manually curated.

The transcriptional units were classified considering the genomic position and the orientation of the probes that were part of every single unit. In this way, it was possible to identify four different groups of transcripts: small intergenic RNAs, antisense RNAs, 5' and 3' untranslated regions (UTRs) and operons.

Since the experimental procedure was based on a competitive hybridization experiment to compare the transcriptome of *Nm* at different time points of incubation in human blood respect to time 0, the analysis was performed considering the M value, that is the log2 ratio between the two signals (Cy5 for each time point of incubation and Cy3 for reference condition at time 0).

In particular a transcriptional unit was defined to be differentially expressed if the average M value of all the probes of the unit was above the background, set as < -0.68 for down regulation and > 0.68 for up regulation (the background was set up comparing t0 vs t0). For probes designed tiling in the antisense strand of coding region the background was set as < -0.91 for down regulation and > 0.91 for up regulation.

As expected and also taking into account the design of the array, the expression profile showed a strong correlation with the positions of previously annotated ORFs. The transcriptional profile of annotated ORFs was consistent with the one obtained in previous experiments using a gene-based oligonucleotide microarray [29]. In addition, the analysis revealed numerous signals located in intergenic regions and in the antisense strand of annotated ORFs. According to the time course analysis, at 60 minutes of incubation in blood, most of the transcripts were differentially expressed.

Overall nearly 25% of the probes designed in the intergenic regions gave a signal above the background and, in particular, 194 intergenic transcripts were identified with a consistent signal during the time course experiment.

The analysis of the antisense strand for each ORF revealed that 14,7 % of the genes had a signal in the opposite strand, with 278 transcripts identified. In addition, for 89 genes the probes designed soon up or downstream the coding sequence gave a signal above the background and similar to the probes in the coding sequence. It means that for these genes the transcription started upstream and/or ended downstream the coding sequence leading to a 5' and/or 3' untranslated region (UTR). Finally 143 transcriptional units contained both probes in the coding sequences of adjacent genes and probes in intergenic regions, suggesting the presence of operons. All detected transcripts are listed in Table S1-4. It is important to notice that the protocol used allowed only the identification of differentially expressed transcripts, i.e. transcripts that changed their expression profile during a time course experiment in whole human blood and are therefore detected in a competitive hybridization experiment.

The different classes of transcripts will be analyzed and discussed in the next paragraphs.

2.2.3 Intergenic small RNAs

In addition to expression of known coding regions, a consistent number of transcriptional units mapped in intergenic regions. The criteria used for the analysis were: (i) no annotated transcription according to the published GeneBank annotation of the genome (Tettelin 2000), (ii) higher signal level than neighboring probes, (iii) higher signal than the corresponding antisense strand, (iv) no cross-hybridization of the probes in the unit with other regions in the genome. This screening resulted in the identification of 194 transcripts, which are listed in Table S1. They have a median length of 126 nt and range from 60 nt (corresponding to a single probe) to 440 nt, and none of them corresponds to known tRNAs.

From the list of these small RNAs (sRNA), a subpanel of regulated transcripts was selected for experimental confirmation using a modified 5'-3'RACE (rapid amplification of cDNA ends) protocol, that allowed simultaneous determination of 5' and 3' ends [59]. The experiments were performed using total RNA, extracted at time 0 for down regulated small RNAs, or after 60 minutes of incubation in human whole blood for up regulated small RNAs. RACE results confirmed the presence of seven small RNA molecules (called Bns as Blood-induced Neisserial Small RNA) in our samples and in all cases, the results correlated with tiling array signals (Figure 16). Moreover, this protocol allowed obtaining the exact sequence of the RNA molecule that gave a signal in the tiling array. The sequences were analyzed respect to the conservation among different species considered as reference of the neisserial population using Geneious software. In addition, for each small RNA, bioinformatics tools were used to predict the promoter, the possible target mRNAs and the presence of a Rho-independent transcription terminator (Figure 16, panel c).

A Bns1

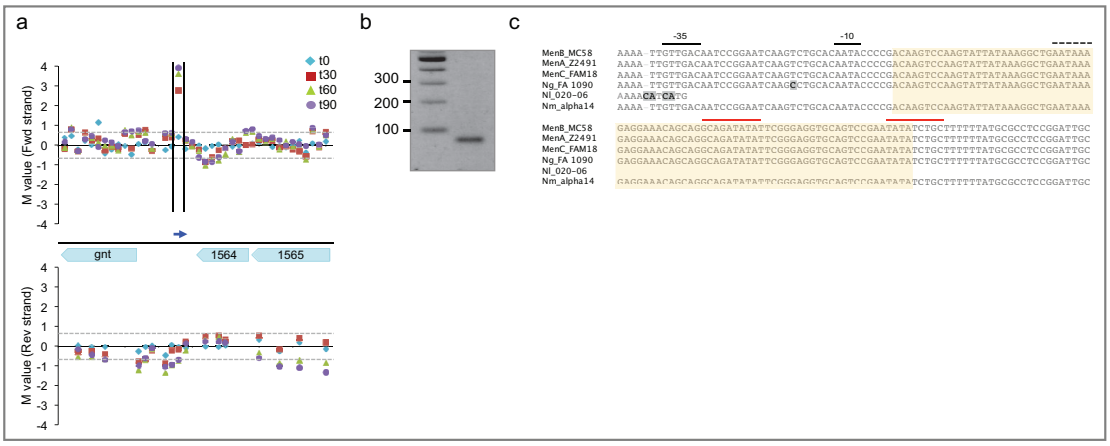

B Bns2

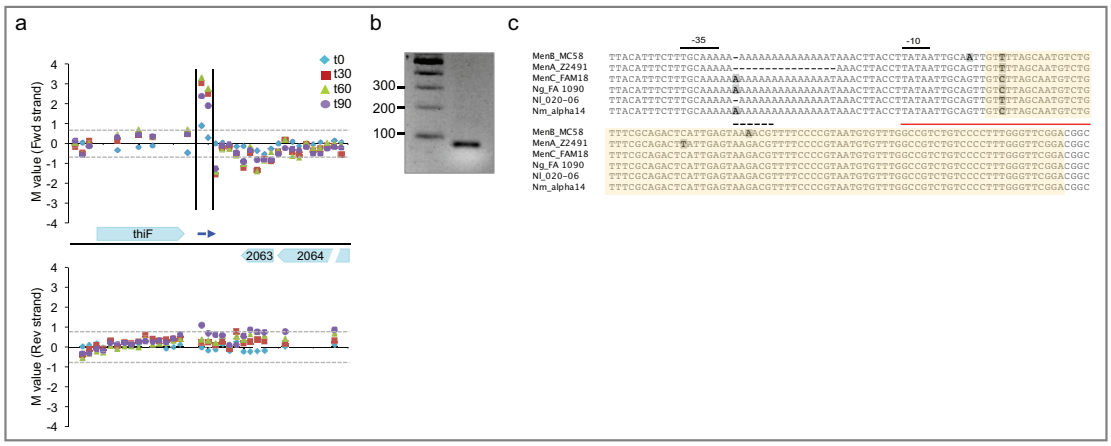

C Bns3

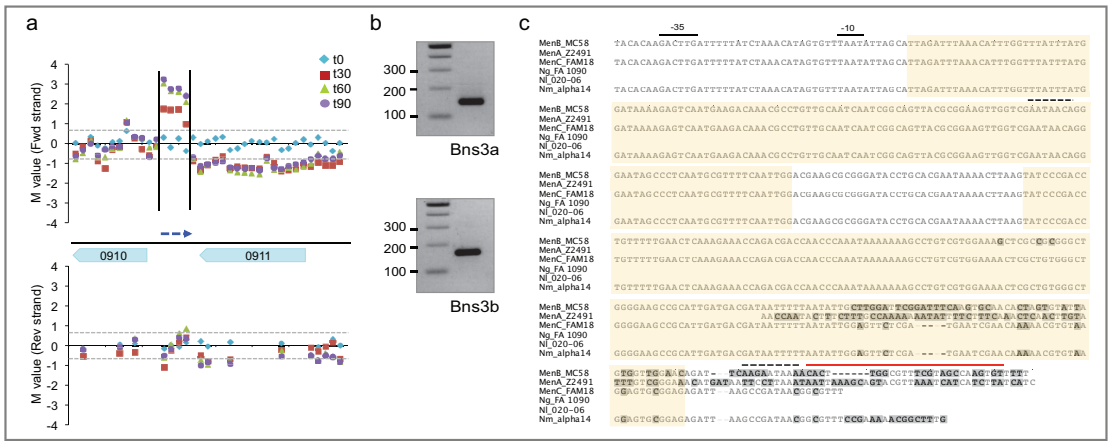

(see next page)

D Bns4

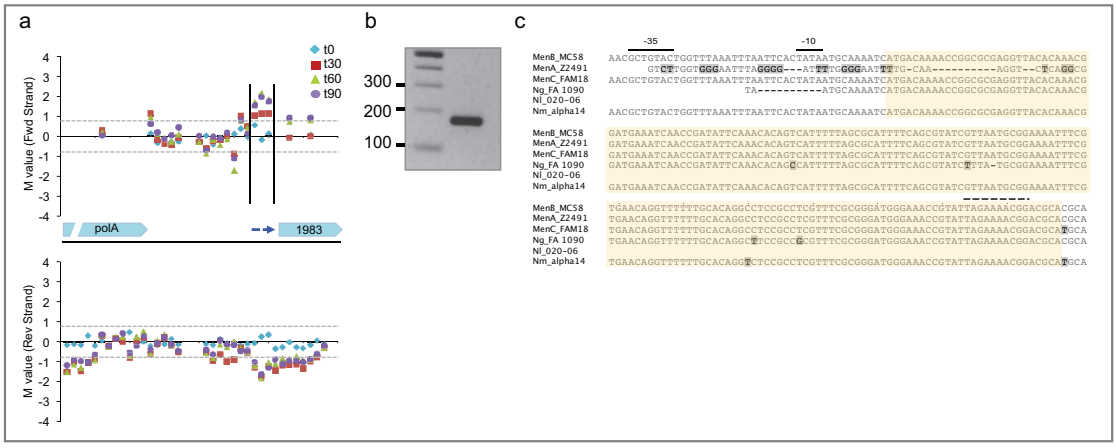

E Bns5

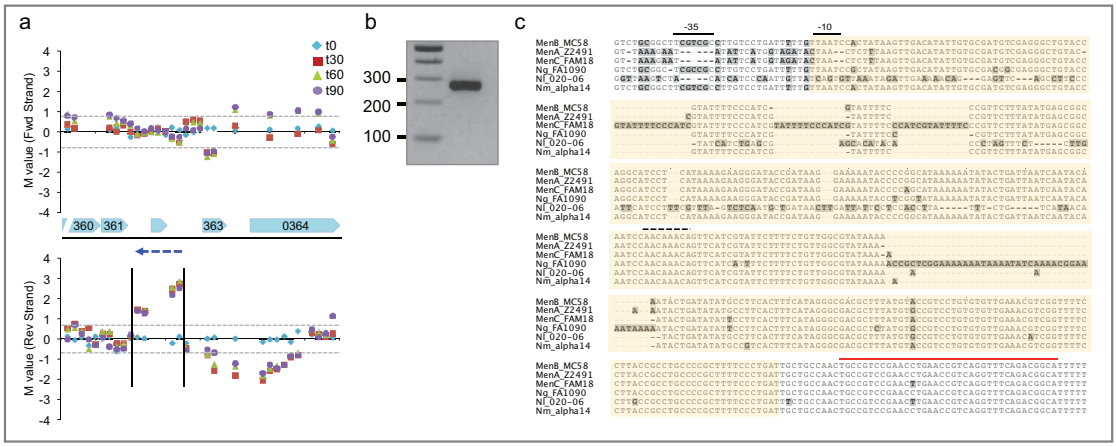

F Bns6

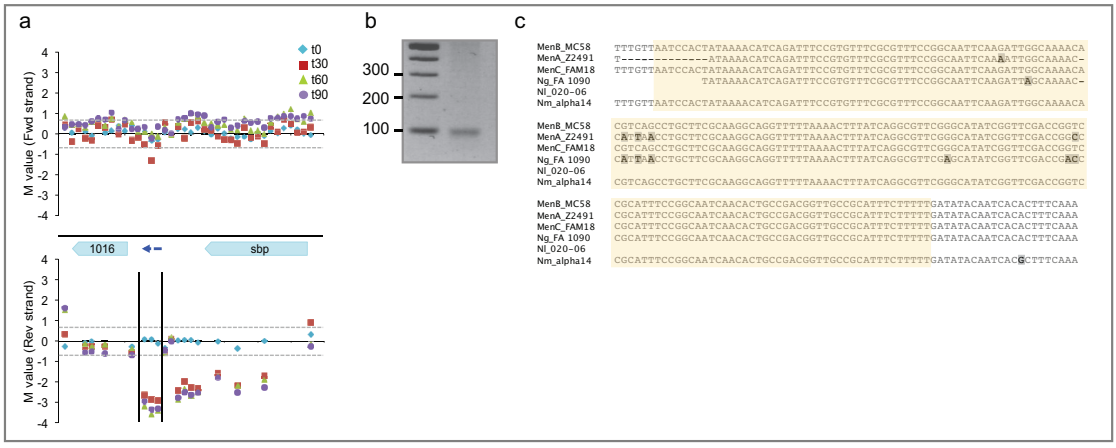

(see next page)

G NrrF

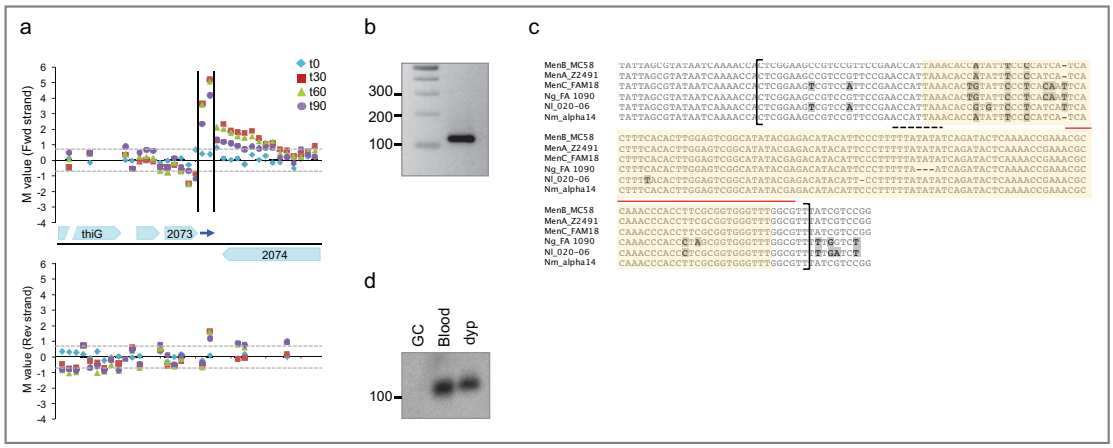

Figure 16. Small intergenic RNAs. For each small RNA, the transcriptional map obtained by high density tiling array is reported (panel a): the plot shows in y axis the normalized M value (log2 ratio of the two channels, Cy5 for samples recovered at 30, 60 and 90 minutes of incubation in blood and Cy3 for reference condition at time 0) for positive strand (Fwd; F) and negative strand (Rev; R). The scheme of the genomic position is in x axis. Annotated ORFs are in blue arrows, detected transcripts in dashed blue lines. The signal background is delimited by dashed grey lines. Each dot corresponds to the average of intensity signals for one probe from three independent biological repetitions. For each probe are reported four dots in different colours, corresponding to the four time points of the time course (blue rhomb for t0; red square for t30; green triangle for t60; purple circle for t90). For each small RNA, the RACE result is reported next to the 100 bp ladder (panel b). The sequence determined by RACE analysis was compared in different neisserial genomes (*N. meningitidis* serogroups A, B and C, *N. gonorrhoeae, N. lactamica* and *N. meningitidis alpha14*) (panel c; not conserved nucleotides are in grey). The sequence obtained by sequencing the RACE PCR product is underlined by a light orange box. In the sequence are reported also the predicted promoter (black line), the predicted terminator (red line) and the putative Hfq- binding site (dashed black line). For NrrF small RNA we reported in panel d the Northern Blot results, showing the same level of expression during incubation in human blood and in condition of iron starvation. A. Bns1 (IG *NMB1563-NMB1564*); B. Bns2 (IG *NMB2062-NMB2063*); C. Bns3 *(IG NMB0910-NMB0911*); D. Bns4 (*IG NMB1982-NMB1983*); E. Bns5 (IG *NMB0361-NMB0363*); F. Bns6 (IG *NMB1016-NMB1017*); G. NrrF (*IG NMB2073-NMB2074*)

One of these sRNAs mapped in the intergenic region (IG) between *NMB2073* and *NMB2074*. The sequence obtained with RACE amplification showed that this small RNA corresponded to NrrF, a recently identified small RNA, highly induced under iron

starvation [83]; [84]. The presence of NrrF in our sample was confirmed also by Northern Blot and the expression of NrrF in human blood was comparable to the one observed in *in vitro* condition of iron-starvation using dipyridyl (Figure 16G). This result confirmed the ability of the array to detect the presence of small RNAs in our sample and demonstrated that NrrF was highly expressed in an *ex vivo* model of bacteremia. In addition, the up regulation of NrrF in blood could be linked to the observed up regulation in blood of its known targets *sdhA* and *sdhC* (data not shown).

Going through the other six transcripts identified, Bns1 (IG *NMB1563-NMB1564*) is 77 nt long and corresponds to one probe highly up regulated (M value=3 at t60; Figure 16A). Sequence alignment showed that it is conserved in all neisserial species analyzed, except for *N. lactamica.* In the prediction of target mRNA, the best hit was *NMB0429*. This gene is annotated as a small hypothetical protein, was found to be part of the same operon together with *prpB* (2-methylisocitrate lyase) and *pprC* (methylcitrate synthase) and was strongly up regulated in blood (Figure 21B; Table S4).

Bns2 (IG *NMB2062-NMB2063*) is 85 nt long and it is conserved in all the genomes analyzed (Figure 16B). it has a predicted Rho independent terminator and promoter sequence. Putative targets are *siaB* (*NMB0069*), which was not regulated in blood, and the type IV pilin protein *NMB0547*, which was not regulated, while its antisense RNA was up regulated (Table S2). Interestingly, Bns2 mapped in the same intergenic region of the small RNA mc05, identified by Mellin and coworker [84] as a putative Fur-regulated small RNA and confirmed by RT-PCR.

In the intergenic region between *NMB0910* and *NMB0911*, four up regulated probes met the specifics used. This region is part of a putative prophage in *Nm* serogroups B and C [85]. RACE analysis, performed using two pairs of primers, annealing in the first two or the latter two probes, showed the presence of two distinct RNA molecules, named Bns3a and Bns3b (Figure 16C). As expected, among the genomes considered, the sequences are conserved only in *Nm* group C FAM18 and *Nm* alpha14, where the prophage is present, although in a different chromosomal locus. Since the search for promoter and Rho-independent terminator sequences resulted only in one putative promoter before the first probe and a terminator inside the latter probe (Figure 16C, panel c), the sequence was probably transcribed as one and then processed somehow. Among the putative target mRNAs for Bns3a, the best hit is *NMB2149*, coding for a hypothetical protein that was down regulated in blood, while the other targets *NMB0366* and *NMB1396* were not differentially expressed. On the other hand, Bns3b is predicted to base pair with *NMB0835*

(a putative type I restriction enzyme, down regulated in blood), *NMB1771* (coding for a hypothetical protein, up regulated in blood), *minD* (*NMB0171*), which was not regulated, and also *NMB0607*. The last mRNA codes for a protein-export protein SecD that was not regulated in blood, but was down regulated in Hfq deletion mutant [40]. So, here we reported two meningococcal small RNAs transcribed from a prophage DNA element that can potentially regulate bacterial genes, as already described for *sprD* sRNA of *S. aureus* [58] and *dicF* [87] and *ipeX* [88] of *E. coli.* In addition, this finding might support the involvement of bacteriophages in bacterial pathogenesis [89], [90].

Bns4 is a 175 nt sRNA (IG *NMB1982-NMB1983*), confirmed by RACE and conserved in all neisserial species analyzed except for *N. lactamica* (Figure 16D). Predicted mRNA targets are *NMB0077*, *NMB1258*, *purA* and *NMB1111*, which were not regulated during incubation in blood.

In addition, RACE analysis, performed using a pair of primers designed in two up-regulated probes mapped in the intergenic region IG *NMB0362-NMB0363*, resulted in a longer RT-PCR product, comprising other two probes in IG *NMB0361-NMB0362* (Figure 16E). This 273 nt small RNA, Bns5, is conserved in *MenA*, *N. gonorrhoeae* and *N. meningitidis alpha 14* strains and has a predicted a Rho-independent terminator at the end of the sequence obtained with RACE protocol. As it is, in *MenB* MC58 strain, it should be considered antisense to NMB0362, which, however, codes for a hypothetical small ORF of 81 bp, that could be misannotated. The prediction of target mRNAs resulted in *NMB1435* (a drug resistance translocase), not regulated in blood, and a putative isomerase *NMB1338* and *prrC (NMB0832)*, that were both not regulated but had a down regulated asRNA (Table S2).

Lastly, RACE analysis on total RNA extracted at time 0, confirmed the expression of a down regulated small RNA, Bns6, that mapped in the intergenic region between *NMB1016* and *NMB1017* (Figure 16F). Bns6 was strongly down regulated during the incubation in blood and the sequence is not conserved in *N. lactamica.* The bioinformatics analysis performed could not allow predicting a promoter or terminator sequence, but in the search for putative target mRNAs the most interesting hit is *tonB* 5' end (*NMB1730*), which was strongly up-regulated in human blood as an operon together with *NMB1728* and *NMB1729* (Table S4).

In the analysis of the six new small RNAs identified, a putative consensus for Hfq binding was found in five of them (Figure 16, panel c). This is not surprising, since potential contact sites of Hfq in sRNAs have a weak conservation at nucleotide level [50];

moreover, there are many examples of Hfq-independent sRNAs in other Hfq-expressing bacteria, like *vrrA* in *V. cholerae* [51] and *symR* in *E. coli* [91].

Among the expressed intergenic regions, one of them corresponded to *N. meningitidis* tmRNA NmtmRNA1 (IR *NMB1015-NMB1016*, 1030802-1031164c, Table S1), slightly up regulated during incubation in human blood. tmRNA is a structural housekeeping RNA that binds to damaged mRNA and, in other bacterial pathogens, it is reported to have different phenotypes; interestingly, in *S. typhimurium*, the corresponding deletion mutant is attenuated in various infection models [92], [93].

Small RNAs are reported to regulate gene expression both positively and negatively [94], [50]. This could help to explain the diverse level of expression of sRNAs and putative mRNA targets that we observed during incubation of *N. meningitidis* in human blood, as in some cases sRNAs and their putative target RNA were both up or down regulated, while in other cases, their expression was inversely related.

2.2.4 Antisense RNAs

By mapping the transcriptional units in the genome, nearly 14,7% of the genes had a signal in the antisense strand. In a detailed analysis, 278 antisense RNAs were transcribed and differentially expressed during incubation in human blood; of them, 25% were up regulated and 75% were down regulated (Table S2).

Antisense transcripts detected in this study correspond typically to cis-encoded antisense RNAs, i.e. encoded in the same DNA locus of their complementary putative targets. If there is a regulatory function of asRNAs, it appears likely that the expression level of an asRNA is somehow coupled to the expression level of the corresponding mRNA. In our time course experiment, it was possible to identify different types of correlation in the expression levels between a mRNA and its corresponding antisense transcript (Figure 17): in 23,6% of genes, they were either up or down regulated; in 40,6% of genes, the mRNA was not differentially expressed, while the antisense RNA could be either up or down regulated; finally in 35,8% of cases, the two transcripts were inversely regulated. Interestingly, in 32,9% of cases the antisense was downregulated and the corresponding mRNA was up regulated, while only in 2,9% we observed the upregulation of asRNA and downregulation of mRNA (the list of all detected antisense transcripts and the relative expression data are reported in Table S2).

A

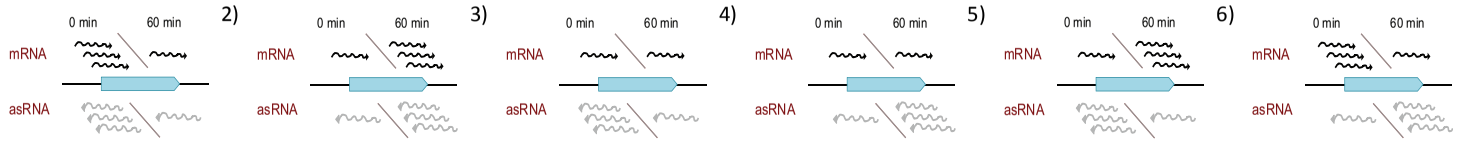

B

						antisense RNA M value (log2 cy5/cy3)				mRNA M value (log2 cy5/cy3)				tested	
strand	ORF	annotation/function	start	end	length (nt)	t0	t30	t60	t90	t0	t30	t60	t90	by RT-PCR	Notes
1) Down reg. asRNA - Down reg. mRNA															
F	*NMB0211 (sdaA)*	L-serine dehydratase	212612	213377	765	0,12	-1,24	-1,64	-1,66	-0,13	-1,07	-1,30	-1,11	yes	
F	*NMB0846*	LPS biosynthesis protein-related protein	873200	873971	771	0,13	-1,00	-1,15	-0,77	-0,12	-1,40	-1,84	-1,84		
F	*NMB0881 (cysT)*	sulfate ABC transporter, permease protein	902256	903037	781	-0,53	-1,80	-1,29	-1,32	0,23	-2,30	-2,21	-2,82		a, e
F	*NMB1260 (res)*	type III restriction EcoPI enzyme	1268749	1270358	1609	-0,40	-2,24	-2,02	-1,87	0,24	-0,48	-1,03	-1,06		
F	*NMB1279*	putative lytic murein transglycosylase B	1292447	1293034	587	-0,23	-0,55	-0,93	-0,80	0,26	-0,92	-1,31	-1,31		
F	*NMB1488 (gabD)*	succinate-semialdehyde dehydrogenase	1536578	1536970	392	0,28	-1,12	-1,19	-1,14	0,11	-1,26	-0,61	-0,25		b
R	*NMB1923*	hypothetical protein	2021447	2021824	377	-0,40	-2,05	-2,16	-2,00	0,07	-0,88	-2,19	-1,89	yes	
2) Up reg. asRNA - Up reg. mRNA															
F	*NMB0176 (dadA)*	D-amino acid dehydrogenase	172293	173637	1344	0,28	0,77	1,16	1,16	0,05	0,78	2,42	2,32	yes	a
F	*NMB0177*	putative sodium/alanine symporter	173710	174194	484	0,10	0,55	1,16	0,89	0,09	0,78	2,42	2,32	yes	a, e
R	*NMB0432*	conserved hypothetical protein	442691	443421	730	-0,32	0,80	1,37	1,15	0,16	0,87	1,46	1,28		a, e
R	*NMB0535 (gluP)*	glucose/galactose transporter	556577	557256	679	-0,14	1,28	1,35	0,95	0,24	1,42	2,07	2,49		
R	*NMB0954 (gltA)*	citrate synthase	966338	967074	736	-0,17	1,25	1,46	1,25	-0,29	1,46	2,05	2,37	yes	a, f
F	*NMB1729 (exbB)*	biopolymer transport protein	1812316	1812762	446	-0,23	1,00	0,86	1,48	-0,04	2,00	2,19	2,18	yes	a
F	*NMB1796*	hypothetical protein, predicted flavoprotein	1884457	1884993	536	0,17	0,95	1,16	1,30	0,14	1,41	2,15	1,91		c, d, f
F	*NMB1995 (glnB)*	nitrogen regulatory protein P-II	2101506	2101883	377	0,54	2,07	2,07	1,91	0,09	1,79	2,25	3,11	yes	
3) Down reg. asRNA - Not reg. mRNA															
F	*NMB0068 (siaC)*	polysialic acid capsule biosynthesis	77585	78033	448	-0,05	-1,21	-1,41	-1,40	0,10	-0,23	-0,53	-0,50		
F	*NMB0839 (pmbA)*	part of proposed TldE/TldD complex	865720	866446	726	-0,40	-0,50	-1,54	-0,88	0,05	0,24	0,40	0,42		b
F	*NMB0884 (sodB)*	superoxide dismutase B	904896	905622	726	-0,30	-1,61	-1,68	-1,60	0,07	-0,29	-0,33	-0,28	yes	d, f
R	*NMB1432 (aroA)*	3-phosphoshikimate 1-carboxyvinyltransferase	1471364	1472575	1211	0,02	-1,33	-1,35	-1,52	0,03	0,63	-0,17	-0,19		b
F	*NMB1650 (lrp)*	leucine-responsive regulatory protein	1717671	1718206	535	0,17	-2,41	-2,75	-2,59	0,20	0,38	0,34	-0,07	yes	
4) Up reg. asRNA - Not reg. mRNA															
F	*NMB0547*	type IV pilin protein	571717	572500	783	0,28	1,60	1,88	1,38	0,23	0,18	0,25	0,13		
R	*NMB1297*	membrane-bound lytic murein transglycosylase D	1314470	1315394	924 *	-0,30	-0,60	1,31	1,34	-0,24	0,27	0,53	0,22		
F	*NMB1686 (prfA)*	peptide chain release factor 1	1763089	1764192	1103	0,25	0,78	1,23	1,37	0,08	0,04	0,16	0,48	yes	
R	*NMB1704 (lgtF)*	beta-1,4-glucosyltransferase	1780632	1781200	568	0,08	0,45	1,11	1,19	-0,13	0,50	-0,14	-0,31	yes	
5) Down reg. asRNA - Up reg. mRNA															
F	*NMB0401 (putA)*	proline dehydrogenase	405787	409660	3873	0,20	-1,12	-1,64	-1,67	0,04	1,12	1,50	1,06		a
R	*NMB0430-0431*	2-methylisocitrate lyase/methylcitrate synthase	440814	442421	1607 *	-0,30	-1,60	-1,28	-1,21	0,05	1,81	3,32	3,57		a, d, e, f
R	*NMB0752*	putative bacterioferritin-associated ferredoxin	782018	783020	1002 *	0,05	-1,59	-1,87	-1,98	0,10	1,73	2,98	2,75	yes	e
F	*NMB1395*	alcohol dehydrogenase, zinc-containing	1424406	1425258	852	-0,30	-2,08	-1,90	-2,30	0,18	0,25	0,72	1,04		
F	*NMB1786*	conserved hypothetical protein	1872643	1872894	251	0,17	-0,90	-1,34	-1,40	0,16	1,12	1,75	1,23	yes	a
R	*NMB1975*	sodium/chloride-dependent transporter	2073041	2074262	1221	-0,45	-0,97	-1,34	-1,51	-0,30	0,93	1,33	1,18		
6) Up reg. asRNA - Down reg. mRNA															
R	*NMB0614*	putative oxidoreductase	643843	644836	993	-0,10	-0,12	1,70	2,27	0,11	0,14	-0,84	-0,80		a
F	*NMB0747*	conserved hypothetical protein	778625	779180	555	0,14	1,05	1,01	0,76	-0,05	0,63	-0,71	-0,75		
F	*NMB1985 (app)*	adhesion and penetration protein	2084678	2087747	3069	0,50	0,98	1,24	1,24	-0,03	-0,88	-1,93	-1,81	yes	

* in this case, the transcript is antisense to more than one gene

Figure 17. *(see next page)*

Figure 17. Cis-antisense RNAs. A. Schematic representation of different types of correlation between the sense mRNA and corresponding cis-antisense RNA transcriptional profiles: 1) both sense and antisense RNAs are down regulated; 2) both sense and antisense RNAs are up regulated; 3) the mRNA is not differentially expressed while the cis-antisense RNA is down regulated; 4) the mRNA is not differentially expressed while the cis-antisense RNA is up regulated; 5) the mRNA is up regulated while the cis-antisense RNA is down regulated; 6) the mRNA is down regulated while the cis-antisense RNA is up regulated. **B.** In the table is reported a sub-panel of Nm antisense RNAs identified and differentially expressed during incubation in human blood. Examples of different types of correlation between mRNA and antisense RNA expression are shown. For each antisense RNA are defined: the strand (forward for 5'-3' genomic orientation and reverse for the opposite strand); the gene to which the RNA is antisense with annotation and function of the ORF; the start and the end of the signal; the length of the signal; the transcriptional profile of antisense RNA and mRNA, reported as M value (log2 ratio between the two channels, Cy5 for 30, 60 and 90 minutes of incubation in blood and Cy3 for reference condition at t0); if the transcript was tested by RT-PCR.

Notes: a. gene part of differentially expressed operon; b. located at the 5' end of the gene; c. located at the 3' end of the gene; d. protein deregulated in Hfq mutant [30]; e. gene deregulated in Hfq mutant [40]; f. protein deregulated in Hfq mutant [39].

Moreover, the relative expression of each mRNA and its cis-encoded antisense RNA could be followed over a certain period of time. Considering the dynamic of expression changes of the antisense RNAs during the time course experiment, some asRNAs showed a rapid increase in expression after 30 minutes with a subsequent stable up regulation. Analogously, another group showed a stable down- regulation within 30 minutes. On the contrary, in other cases the dynamic was different: antisense showed up- regulation or down-regulation at 30 minutes, but the expression levels were reduced during the incubation time, as reported in our previous work for the expression profile dynamics of the genes differentially expressed in blood [29].

The presence of antisense RNA molecules in our sample was confirmed by specific RT-PCR [96]. The reverse transcription was perfomed using a reverse primer specific only for the antisense RNA, followed by digestion with RNase H and a subsequent PCR with a specific pair of primers (Figure 18A). Using this approach, 16 asRNAs were tested in total RNA samples extracted at t0 (for down regulated transcripts) or t60 (for up-regulated transcripts) (Figure 18B).

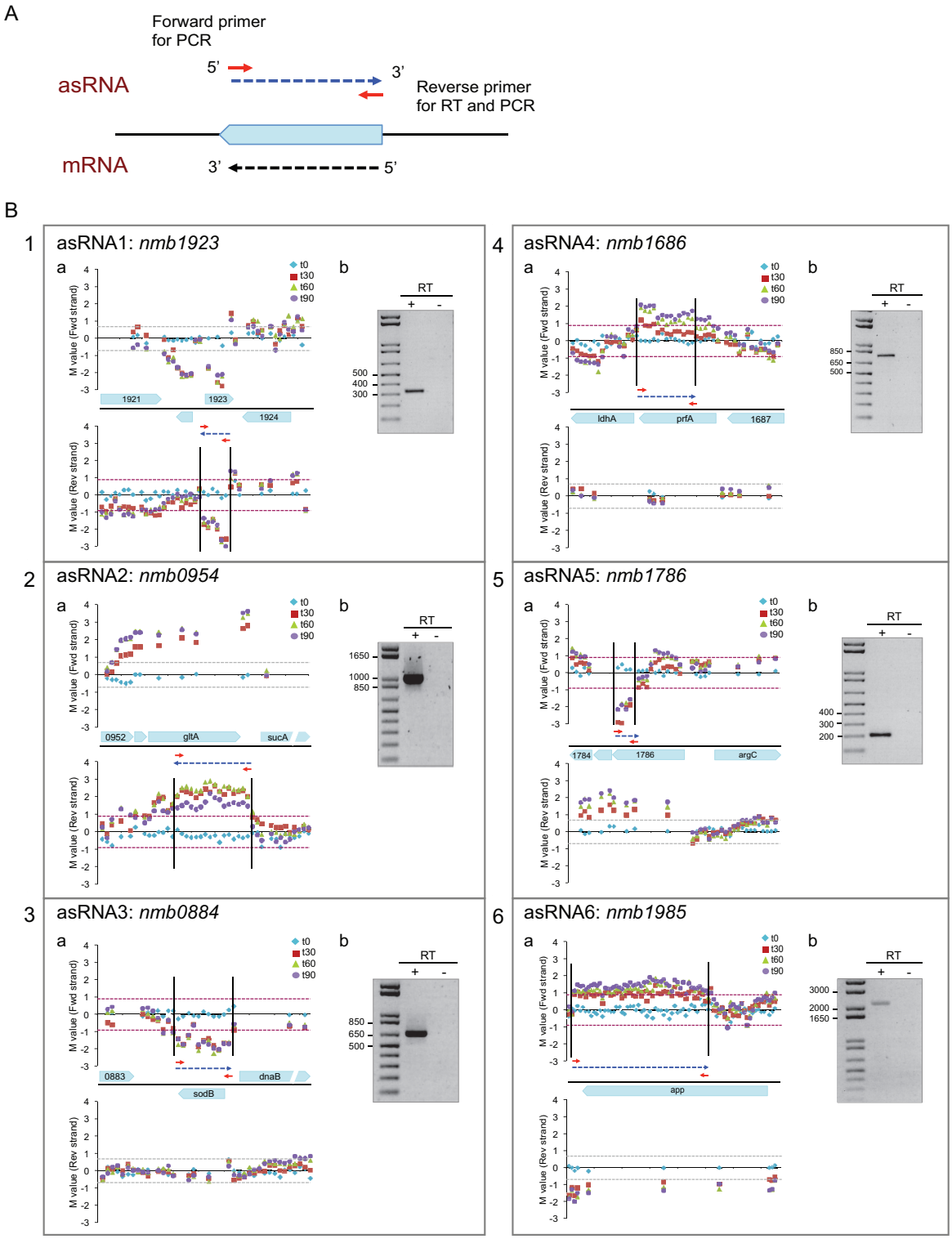

Figure 18. *(see next page)*

Figure 18. Detection of identified cis-antisense RNAs by RT-PCR. A. Scheme of the RT-PCR strategy used to confirm the presence of cis-antisense transcripts in total RNA extracted after incubation of Nm in human whole blood. The reverse transcription was performed using a primer specific only for the antisense RNA, and then a PCR reaction was used to amplify and detect the transcript. **B**. Examples of cis-antisense RNAs confirmed by RT-PCR that corresponds to the different types defined in Figure 17. For each antisense RNA are reported the transcriptional map (panel a) and the RT-PCR results (panel b). In the transcriptional map, the signal background for probes in the coding sequence is delimited by dashed grey lines; the one for antisense probes is delimited by dashed red lines. 1) Cis-antisense RNA to *NMB1923*; expected amplicon size 380 bp. 2) Cis-antisense RNA to *NMB0954*; expected amplicon size 1014 bp. 3) Cis-antisense RNA to *NMB0884*; expected amplicon size 650 bp. 4) Cis-antisense RNA to *NMB1686*; expected amplicon size 780 bp. 5) Cis-antisense RNA to *NMB1786*; expected amplicon size 240 bp. 6) Cis-antisense RNA to *NMB1985*; expected amplicon size 2200 bp.

Among all the antisense transcripts identified, some of them corresponded to genes potentially involved in virulence and pathogenesis. As an example, *NMB0752* is a putative bacterioferritin-associated ferrodoxin, strongly up regulated in blood (M value 2,98); on the contrary its asRNA was down regulated (M value -1,59). It suggests that the protein is necessary for the bacterium in blood and is regulated by a transcript that therefore needs to be down regulated. Moreover, it is reported that ferredoxin is important for *E. coli* pathogenesis; in fact it affects the secretion of CNF1 across the inner membrane of meningitis-causing strain K1 and is involved in invasion of HBMEC [97].

There are several other examples of up-regulation of the mRNA and down regulation of the corresponding asRNA: the alcohol dehydrogenase *NMB1395*, the proline dehydrogenase *NMB0401*, the sodium- and chloride-dependent transporter *NMB1975* (Figure 17B) and the hypothetical protein *NMB1786* (Figure 18B.5) to cite some of them. On the contrary, for *app* (adhesion and penetration protein; *NMB1985*) (Figure 18B.6), the asRNA was up regulated while the mRNA was down regulated. In other cases, as already mentioned, both transcripts were up regulated, for example *glnB* (nitrogen regulatory protein P-II 1; *NMB1995*), the D-amino acid dehydrogenase *NMB0176* (Figure 17B) and *gltA* (type II citrate synthase; *NMB0954*) (Figure 18B.2). In the case of *gltA*, the M value for mRNA was 2,05 and for the asRNA was 1,25 at t60. However, considering the A value (not reported in Table S2), that is the log of the product of the intensities of the two channel Cy5 and Cy3), it was 4 for mRNA and 2,2 for asRNA. This means that, unless

both transcripts were up regulated in blood, there were much more mRNA molecules at t60 respect to asRNA. The same reasoning can be applied in cases where both transcripts are down regulated, as for *NMB0846*, *NMB1279*, *NMB1260*, *NMB1488* (Figure 17B) and *NMB1923* (Figure 18B.1). Nevertheless, in about 40,6 % of the cases, only the antisense RNA was differentially expressed. For example, for the *lgtF* (*NMB1704*) and *prfA* (*NMB1686*) (Figure 18B.4) the antisense RNA was up regulated. On the contrary, for *pmbA* (*NMB0839*), *aroA* (*NMB1432*) and *siaC* (*NMB0068*) the antisense RNA was down regulated (Figure 17B). Interestingly, a cis-antisense transcript corresponding to the superoxide dismutase *sodB* (*NMB0884*, Figure 18B.3) was down regulated. This finding is consistent with the deregulation of the protein observed in Hfq deletion mutants [40], [39] and support the idea that the expression of *sodB* is post-transcriptionally regulated, perhaps by its cis-encoded antisense RNA. This finding is not surprising since Lorenz and colleagues reported the presence of Hfq aptamers in many antisense RNAs in *E.coli*, suggesting that Hfq might regulate the expression of a large number of genes via interaction with cis-antisense RNAs [99]. Other cases of antisense RNAs to ORFs deregulated in Hfq deletion mutants are reported as notes in Figure 2.B.

Another example is the asRNA of *lrp* (*NMB1650*, Figure 17B), strongly down regulated during the incubation in blood. *Lrp* is a leucine-binding transcriptional regulator not differentially expressed in blood, but the down-regulation of the antisense RNA suggests instead that the gene was somehow regulated in blood. In literature there are other examples of antisense RNAs shown to regulate the synthesis of transcription regulators, either positively (like *gadY* of *E. coli* acting on the stability of *gadX* mRNA [63], or *arnA* of *C. glutamicum* on cg1935 [100] or negatively (like alr1690 of *Anabaena sp*. on *furA*) [101].

In some cases antisense RNAs corresponded to genes that were part of an operon, for example the asRNA to *NMB0432*, that seems to be cotrascribed with *NMB0433*. The same cases were the asRNA to *putA* (*NMB0401*) and *exbB* (*NMB1729*; Figure 17B) Interestingly, for the operon *NMB1652-NMB1653*, a down regulated asRNA for *NMB1652* and an up-regulated asRNA for *NMB1653* were detected (Table S2).

These different types of regulation could be explained according to the potential mechanism of action of antisense RNAs: in the majority of cases, antisense RNA action entails post-transcriptional inhibition of target RNA function but, in few cases, activating mechanisms have been found too [63]. As a general statement, if antisense transcripts were

acting as negative cis-regulatory elements, the signal levels of sense and antisense ratio would expected to be inversely correlated [62].

On the contrary, it is not trivial to assign a functional correlation when both sense and antisense are regulated in the same way, or only the antisense RNA is differentially expressed, as observed in most cases during the incubation in blood. It has been proposed that the expression of a target is repressed as long as the transcription of the regulator exceeds the transcription of the target and its expression increases linearly when the mRNA concentrations outruns that of the regulator; only mRNA that is present at higher levels than its cis-acting antisense antagonist is translated, so translation of certain genes starts only when the mRNA concentration reaches a certain level [102]. Therefore, the asRNA might facilitate a temporal delay of gene expression and a faster expression cutoff due to codegradation with its target [103]. This kind of regulation is advantageous especially when fast responses are needed, as it is the case of adaptation to human blood, once the bacteria have reached the blood stream.

The high level of meningococcal antisense RNAs in our data is consistent with the fact that, as expected for regulatory factors, asRNAs respond to changes in the environment [59], [104], [105]. In addition, for the cases where the expression of antisense RNA was regulated in blood, while the corresponding mRNA was not, we can speculate that, since the antisense RNA expression is anyway affected by the incubation in blood, the gene could be in some way involved in growth and survival of meningococcus in human blood. In the cases of asRNAs corresponding to genes part of an operon, asRNAs can be utilize by bacteria to set temporal gene expression thresholds for genes within an operon and implement a quantitative adjustment of the mRNA amounts [63], [106], [107], [108].

2.2.5 5' and 3' untranslated regions (UTRs)

The mapping of the identified transcriptional units in the genome showed the presence of a 5' and/or 3' untranslated region (UTR) within the transcripts of 89 genes (Table S3). The length of these regions is variable and ranges from 60 to 530 nt. Due to the use of 60-mer oligonucleotides as probes for the microarray, only UTRs longer than 60 nt were identified. In total, 25 5' UTRs, 36 3' UTR were identified; in addition, 12 transcripts comprised both a 5' and 3' UTR. Two 5'UTRs and five 3'UTRs were confirmed

experimentally by performing an RT-PCR with specific pairs of primers in order to discriminate the presence of a long transcript, comprising the UTR (for the PCR, it was used total RNA collected at time 0 for down regulated transcripts, or after 60 minutes of incubation in blood for up regulated transcripts) (Table 2; Figure 19).

								M value (log2 cy5/cy3)			
strand	ORF	annotation/function	start	end	overlap	UTR	length (nt)	t0	t30	t60	t90
Down regulated genes											
F	*NMB1452*	conserved hypothetical protein	1500497	1503255	*NMB1453-NMB1454*	3'	1617	-0,16	-1,84	-2,44	-2,39
Up regulated genes											
R	*NMB0615 (amtB)*	putative ammonium transporter	645065	646584		5'	210	0,04	2,45	3,28	3,42
F	*NMB0983 (purH)*	Purine ribonucleotide biosynthesis	998362	1000469		3'	531	0,22	2,78	2,43	2,08
F	*NMB1070 (leuA)*	2-isopropylmalate synthase	1090259	1092068		5'	253	0,12	1,30	1,87	2,03
R	*NMB1647*	putative amino acid symporter	1713234	1715531	*NMB1646*	3'	791	0,02	2,32	2,53	2,97
F	*NMB1710*	glutamate dehydrogenase	1786070	1787743	*NMB1711*	3'	345	0,07	3,10	3,07	3,16
F	*NMB1712*	L-lactate permease-related protein	1788748	1789214		3'	168	0,08	2,73	3,42	3,26
F	*NMB1840*	conserved hypothetical protein	1941540	1942748	*NMB1841*	3'	701	-0,07	1,01	2,24	2,46

Table 2. In the table is reported a sub-panel of Nm transcript containing an untranslated region at 5'- or 3'-end, that were confirmed by RT-PCR. For each transcript are defined: the strand (forward for 5'-3' genomic orientation and reverse for the opposite strand); the ORF of the transcript; the start and the end of the transcriptional unit; the length of the UTR; the transcriptional profile of the transcript during the time course experiment, reported as M value (log2 ratio between the two channels, Cy5 for 30, 60 and 90 minutes of incubation in blood and Cy3 for reference condition at t0).

In our analysis, 16 5'UTR could potentially have this regulatory activity (Table S3), but by using RFAM, any known function was assigned. However, a 253 nt 5'UTR was identified in the mRNA of LeuA (NMB1070) (Table 2). *LeuA* is a 2-isopropylmalate synthase involved in leucine biosynthesis and future experiments could classify its 5'UTR as a new riboswitch, able to regulate the expression of the gene according to the availability of leucine (as reported for other aminoacids, i. e. glycine and lysine). Interestingly, a similar mechanism has been proposed for the 5' UTR of leucyl-tRNA synthetase (named as Teg73) of *S. aureus* [1]. The same could be the case of 210 nt 5'UTR of *amtB* (*NMB0615*) (Figure 19B) that is a putative ammonium transporter.

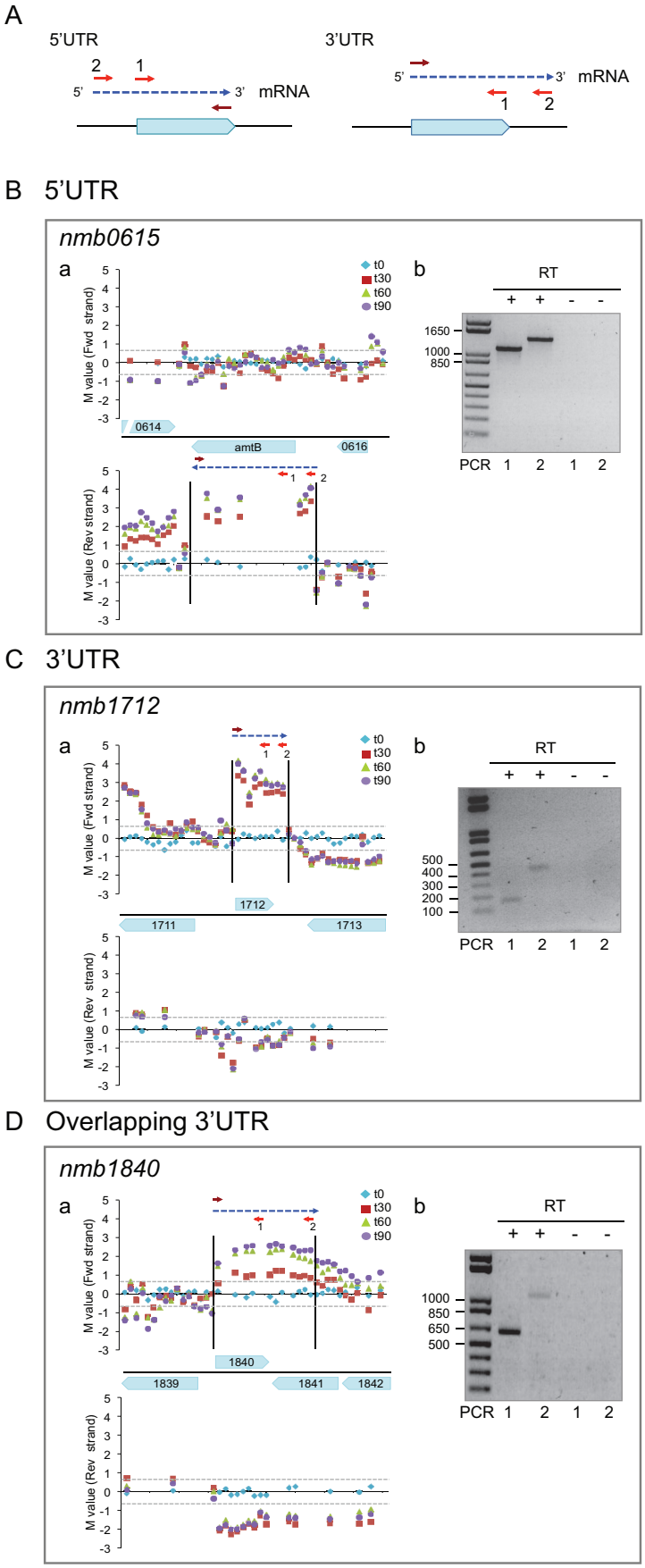

Figure 19. *(see next page)*

Figure 19: Detection of identified 5' and 3' untranslated regions (UTRs) by RT-PCR. A. Scheme of the RT-PCR strategy used to confirm the presence of 5' and 3' untranslated regions in RNA transcripts extracted after incubation of Nm in human whole blood. We used two pairs of primers, one to amplify only the coding sequence as a positive control (1) and one to amplify the entire transcript (corresponding to the signal obtained from the tiling array) in order to confirm the presence of a 5' or 3' untranslated region (2). **B-D.** Here is reported an example of 5'UTR (B. *NMB0615* (*amtB*); expected amplicon size PCR1 1100 bp and PCR2 1350 bp), 3'UTR (C. *NMB1712*; expected amplicon size PCR1 187 bp and PCR2 463 bp) and overlapping 3' UTR (D. *NMB1840*; expected amplicon size PCR1 620 bp and PCR2 1070 bp). For each example, the transcriptional map (panel a) and the results of the RT-PCR (panel b) are shown.

On the other hand, 3'UTRs of bacterial mRNAs are thought to mainly harbor transcription termination structures, which might prevent access to exonucleases to the 3' end of the transcript but have no clear regulatory function. In our analysis of *Nm* transcriptome, several genes, differentially expressed in blood, possessed a 3'UTR. Two of them, *NMB1712* and *NMB0983* 3'UTRs, were confirmed by RT-PCR (Figure 19C, Figure 20). Interestingly, the 3'UTR of *NMB0983* seemed to be present in our sample also as a small RNA (called Bns7); in fact, the RACE analysis, performed using a pair of primers designed in the sequence corresponding to the 3'UTR, led to a RT-PCR product of 236 bp (Figure 20), that could derive from an independent promoter, or from the processing of the longer transcript.

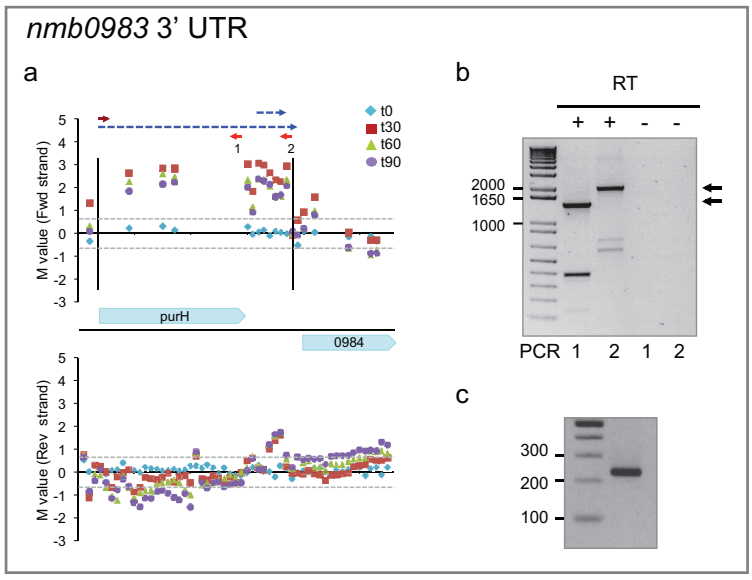

Figure 20. *(see next page)*

Figure 20. *NMB0983* 3' UTR. Microarray analysis revealed the presence of a 3' untranslated region in the mRNA coding for *NMB0983*, up regulated during incubation in whole human blood (transcriptional map reported in panel a). RT-PCR analysis confirmed the presence of a long transcript (panel b. Expected amplicon size for PCR1 is 1405 bp and for PCR2 is 1984 bp). However, RACE analysis, performed using primers designed in the 3'UTR, showed the presence in blood sample of a small RNA corresponding to this region, called Bns7 (panel c).

In 21 cases, the transcripts ended inside or after a gene located in the opposite strand. Thus, the transcript extended over the convergent gene, leading to an overlapping UTR (overall 18 overlapping 3' UTR and 3 overlapping 5' UTRs were identified). The transcription of a long 3'UTR for *NMB1710*, *NMB1647* (Table 2) and *NMB1840* (Figure 19D) was confirmed experimentally by RT-PCR. How this overlapping UTRs affect gene expression is not clearly understood, but it is reported that they can act as antisense RNAs for the gene located in the opposite strand [59]. This could be also a way to link neighboring gene expression, in the context of a global gene regulation. In our cases, *NMB1710* long 3'UTR overlapped with the downstream gene *NMB1711* (M value 0,95 at t60). *NMB1710* codes for the glutamate dehydrogenase *gdhA*, while *NMB1711* belongs to *gntR* family transcriptional regulators. It suggests that the long 3'UTR, which is antisense to *NMB1711*, is used as a connection between two metabolic pathways. The 3'UTR of *NMB1840* (coding for an hypothetical protein) overlapped for 701 nt with *NMB1841*. It is worth noting that *NMB1841* seemed to be coexpressed with *NMB1842* as a putative operon (Table S4) and they code respectively for a mannose-1-phosphate guanylyltransferase and a putative 4-hydroxyphenylacetate 3-hydroxylase, involved in different metabolic pathways. Lastly, the long 3'UTR of *NMB1647* overlapped for 791 nt with *NMB1646*. It is interesting to notice that *NMB1646* is a putative hemolysin, not differentially expressed in blood while another putative meningococcal hemolysin *NMB2091* was slightly up-regulated, suggesting a precise regulation of the activity of the two proteins when bacteria were grown in human blood.

In the context of adaptation to blood it is worth also to mention *NMB1452* 3'UTR (Table 2). This 3'UTR of 1617 nt was strongly down-regulated (M value -2,5) and overlapped with *NMB1453* and *NMB1454*. *NMB1454* is a ferredoxin and is not differentially expressed in blood. On the contrary, as mentioned before, another putative bacterioferritin-

associated ferrodoxin (*NMB0752*) was upregulated, while its antisense is down regulated. This suggests a fine tune regulation of this system in *Neisseria meningitidis*.
An example of long 5'UTR is *NMB269* transcript that overlapped for 384 nt to *NMB0270* (Table S3); the two genes codes respectively for a competence protein and a putative BioH protein and STRING 9.0 database predicts a functional association between the two proteins.

2.2.6 Differentially expressed operons

The gene expression data obtained from probes designed in the coding sequence of the ORFs were used to define the operon map of differentially expressed genes during incubation in human blood.
From the list of transcriptional units, determined using the chipSAD software, operon transcripts were identified by applying the following rules: (i) similar M value for all the probes designed in the coding sequence of adjacent genes; (ii) similar M value for the probes designed in the intergenic regions between adjacent genes and the probes inside the genes, when present; (iii) statistical significance of the signal of the probes considered as part of the same transcriptional unit. Starting from the chipSAD results, the transcriptional units were manually curated also considering the presence of Rho-independent terminators and 143 regulated operons were identified: nearly 63% consisted of two genes, while in some cases a single transcriptional unit contained four genes, or more, clustered together (Table S4). The presence in our samples of long regulated transcripts, corresponding to operons, was confirmed by RT-PCR with specific primers, in order to amplify both the entire operon and the intergenic regions between adjacent genes, using primers designed inside the genes, in divergent orientation. (Figure 21A).

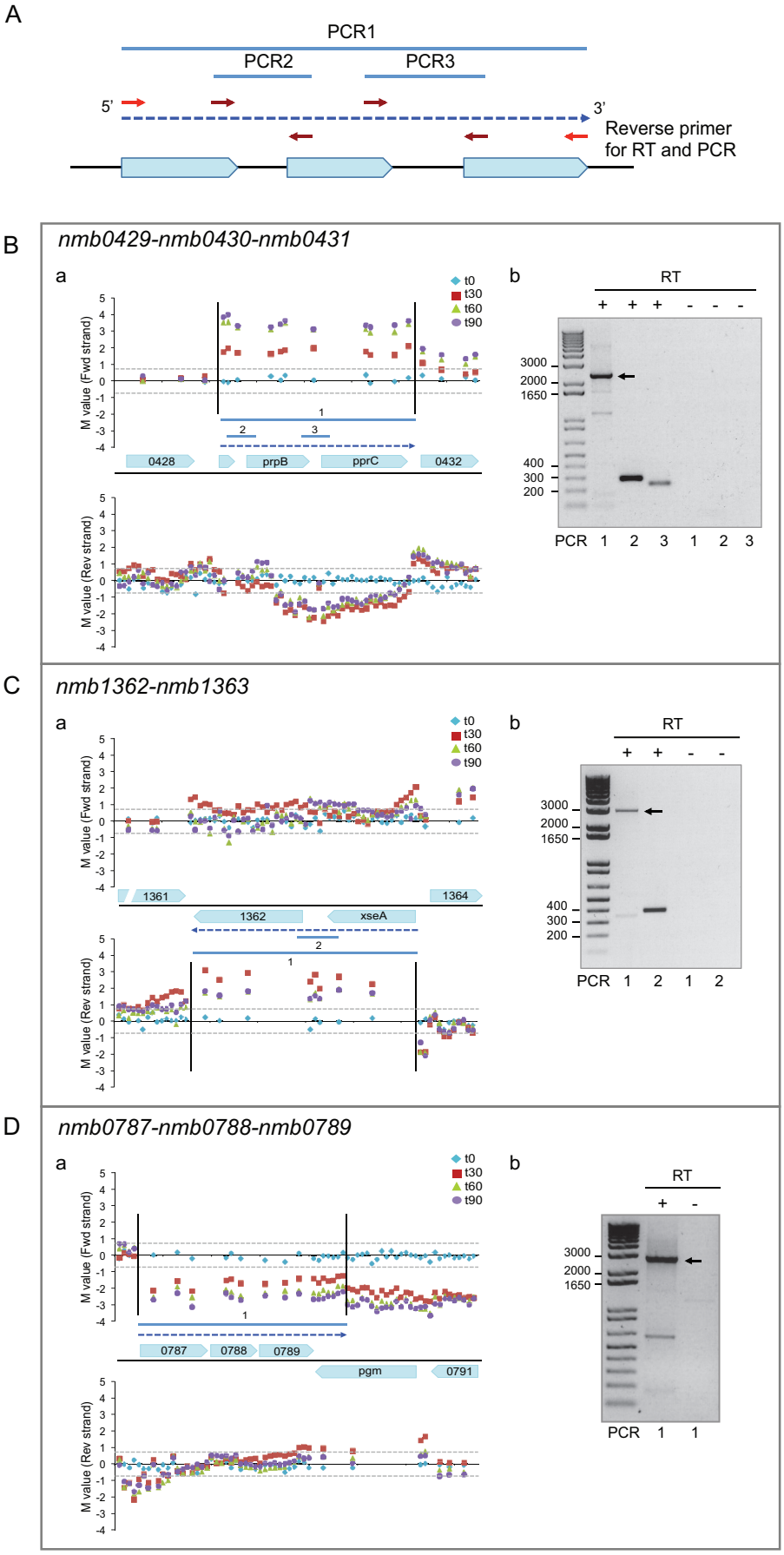

Figure 21. *(see next page)*

Figure 21. Detection of differentially expressed operons by RT-PCR. A. Scheme of the RT-PCR strategy used to confirm the presence of long transcripts, referred as operons, in total RNA extracted after incubation of Nm in human whole blood. Reverse transcription was performed using a primer designed at the end of the detected transcript. Then, PCR analysis was performed using the same cDNA sample in order to amplify the entire transcript (PCR1) and the intergenic regions between adjacent genes (PCR2 and PCR3). **B-C.** Here we reported an example of the detected operons. For each example, we reported the transcriptional map (panel a) and the results of the RT-PCR (panel b). B. Long transcript for *NMB0429-NMB0430-NMB0431*, expected amplicon size: PCR1 2330 bp; PCR2 300 bp; PCR3 256 bp. C. Long transcript for *NMB1362-NMB1363*, expected amplicon size: PCR1 3000 bp; PCR2 414 bp. D. Long transcript for *NMB0787-NMB788-NMB0789*, expected amplicon size: PCR1 2700 bp. In this case, since there is no intergenic space between the genes, only one PCR was performed and it allowed detecting a long transcript that partially overlapped to *NMB0791*, in the opposite strand.

For example, the three genes *NMB0429*, *NMB0430* and *NMB0431* were part of the same transcriptional unit containing both probes inside the genes and probes in the intergenic regions (Figure 21B). *NMB0429* is annotated as a small hypothetical protein of 34 aa, that could be misannotated. *NMB0430* and *NMB0431* code respectively for PrpB (2-methylisocitrate lyase) and PprC (methylcitrate synthase) and were all strongly up regulated in blood. Interestingly, *NMB0429* sequence is the best hit as target mRNA for Bns1. Moreover, an antisense transcript for *prpB* and *pprC* was detected (Figure 17B). In addition, PrpB and PprC proteins were deregulated in Hfq deletion mutant [1], [40], [39]. We can therefore speculate that these three genes are part of the same operon, involved in the methylcytrate synthesis pathway, and could be regulated by different RNA molecules to define precisely the expression level in particular growing condition, like human blood. Significantly, in *M. tuberculosis*, this metabolic pathway is required for growth on fatty acids, in macrophages, and in mice [109].

Another case is the transcriptional unit that includes the genes *NMB1728*, *NMB1729* and *NMB1730* (Table S4). The genes code respectively for the biopolymer proteins ExbD and ExbB and the TonB protein and are involved in the release into the periplasm of ligands bound by correlated outer membrane proteins. This system is required for heme utilization and virulence in various bacteria [110], [111]. The analysis showed the up regulation of this operon during incubation in human blood; in addition an up-regulated antisense transcript to *NMB1729* was detected (Figure 17B). Moreover, *NMB1730* was identified as

a target sequence for Bns6. All these finding suggested a fine tuned regulation of the expression of this system during incubation in human blood.

Because functionally related genes are generally clustered in operons, identification of operon is critical for gene function elucidation. With this regard, in some cases the identified transcriptional units corresponded to an annotated ORF clustered with hypothetical proteins, as for example *NMB0432-acnA*, *folB-NMB1064* and *leuD-NMB1035* (Table S4). This analysis suggests not only that these genes are somehow involved in growth and survival in human blood, but also that their activity can be correlated. The same reasoning can be applied to adjacent genes with known function, as the long transcriptional unit that include the putative oxalate/formate antiporter *NMB1362* and the exodeoxyribonuclease VII large subunit *eseA* (*NMB1363*), reported in Figure 21C.

Interestingly, in 8 cases the transcriptional unit extended to adjacent non-coding region, acting as an antisense to the genes mapped in the opposite strand. Two examples were: *NMB0787-NMB0788-NMB0789* that has long 3'UTR overlapping with *NMB0790* (Figure 21D) and *cstA-NMB1494* that has a long 5'UTR overlapping with *NMB1492* (Table S4).

We checked the correspondence of the operons identified with a list of predicted *N. meningitidis* MC58 operons available in DOOR database [112]. The analysis showed that, using our approach, we were able to identify 33 transcriptional units not predicted by the DOOR algoritm, while for 49 transcriptional units the operon organization was different; the remaining 61 transcripts were correspondent.

It is important to underline that, the fact that we found the same signal in adjacent genes (not previously predicted to be part of an operon) means that they are transcriptionally correlated, but, in case there is not a probe designed in the intergenic regions between the genes, we can just speculate that they are part of the same operon. Further experiments will be necessary to confirm these findings.

3. Discussion

Characterization of the bacterial transcriptome during host-pathogen interactions is a fundamental step for understanding infectious processes caused by human pathogens. Some steps of Nm-host interactions have been analyzed by microarray expression profiling. However, despite its importance in the disease process, little is known about how Nm adapts to permit survival and growth in blood. A previous analysis of the transcriptional profile of a Nm strain, in an *ex vivo* human whole blood model of infection, showed how this bacterium adapts to enable survival and growth in blood. Nm undergoes a rapid, adaptive response and, as a consequence, bacterial metabolism and virulence pathways are remodeled resulting in enhanced survival, which could enable bacterial dissemination and proliferation. In particular, genes belonging to different functional classes (energy metabolism, amino acid biosynthesis, transport and binding proteins) were differentially expressed.

In the work presented here, through mutagenesis studies of a subset of up-regulated genes, we were able to identify new proteins important for survival in human blood and also to identify additional roles of previously known virulence factors in aiding survival in blood. Nm mutant strains lacking the genes encoding the hypothetical protein NMB1483 and the surface-exposed proteins NalP, Mip and NspA, the Fur regulator, the transferrin binding protein TbpB, and the L-lactate permease LctP were sensitive to killing by human blood.

These results showed that different bacterial factors contribute to survival in blood with diverse mechanisms. LctP is involved in the uptake of lactate present in blood and is taken up by the bacterium as a carbon energy source and also converted to precursors of capsular and lipopolysaccharide sialic acid [74]. The phenotype of decreased survival that was observed for the deletion mutants in the *ex vivo* model of bacteremia confirm the important role that this membrane transporter plays in increasing complement resistance of Nm strains. TbpB functions as transferrin receptor together with TbpA, and the fact that a TbpB mutant is defective in growth in human blood suggested that transferrin-binding is a crucial step for iron-uptake and survival under these conditions. NalP, an autotransporter lipoprotein with serine-protease activity that is involved in the cleavage of Nm surface-

exposed proteins [76] was identified for the first time as important for survival in blood, even if further study will be necessary to better define how it contributes to survival. NMB1483 is a putative surface-exposed lipoprotein annotated as a NlpD-homologue, and interestingly, in *N. gonorrhoeae* the NMB1483-homologue protects against oxidative damage mediated by hydrogen peroxide and against neutrophil-mediated killing [77]. The Mip lipoprotein is involved in the intracellular survival in macrophages of the closely related species N. gonorrhoeae; the results obtained with the mip deletion mutants suggests that the Nm Mip protein may also facilitate interaction of Nm with macrophages. The ferric uptake regulator (Fur) mutants of different pathogens is well known as an important virulence factor [80]; our data demonstrate that in Nm Fur plays a major role in the adaptation and survival of the bacterium in the *ex vivo* model of blood infection and also suggest a complex regulation of gene expression during this step of pathogenesis. In addition, mutagenesis studies in an additional neisserial strain showed the contribution of NspA, suggesting that NspA may be the main factor involved in fH binding and resistance to the alternative complement pathway in this genetic background where fHbp is expressed at very low levels.

The data of gene-expression array suggested the presence of a complex regulatory network that controls the changes in expression seen upon exposure to blood. In this work, in order to broaden the analysis to the whole transcriptome, total neisserial transcriptome was analyzed in a time course experiment of incubation in human whole blood, using a high-density tiling microarray. The application of chipSAD tool to high-density tiling array data allowed the identification of new transcripts -small intergenic RNAs, cis-antisense RNAs, 5' and 3' untranslated regions and operons- differentially expressed in human blood. This findings extend our knowledge on the whole transcriptome of Nm; previously, other research groups have shown the expression of small regulatory RNAs with a role in bacterial pathogenesis [83], [84], [113] and proteomic and transcriptomic analysis of Hfq deletion mutant suggested the presence of a small RNA network in this bacterium [30], [40], [39]. Here we also showed, for the first time, an extensive antisense transcription when Nm was incubated in human whole blood. This means, not only that also *Nm* might use antisense transcription to regulate gene expression, but that these riboregulators contribute to adaptation of the bacteria to grow and survive in human blood. In fact, antisense RNAs to genes of various metabolic pathways were identified; some others corresponded to genes potentially involved in neisserial pathogenesis (as for example the asRNA for *app*, the ferredoxin *NMB0752* and the citrate synthase *NMB0954*). Moreover,

some sRNAs, which can potentially regulate genes involved in bacterial metabolism (as Bns1 for the methylcitrate synthesis pathway) and transport and binding (as Bns6 for the regulation of *tonB* gene), were strongly up regulated during incubation in human blood. The time course analysis allowed monitoring the changes in transcription profile over 90 minutes of incubation in human blood. This study showed different types of correlation between the expression of an asRNA and the corresponding mRNA. In about 40,6% of cases, only the asRNA was differentially expressed. This might means that the corresponding genes, although not differentially expressed in our analysis, are indeed regulated somehow during incubation in blood. This suggests that there could be more genes, than the ones already described, implicated in this step of the pathogenesis that is worth to further investigate. In addition, it is important to notice that we performed a bacterial population study; it could be interesting to perform the same analysis in a single cell transcriptome study, to verify what happens inside a single bacterium. The RNA regulatory circuit appears very complex. In fact, the expression of some genes was regulated at different levels: they might be co-expressed with the adjacent gene, have a cis-acting antisense RNA and the transcript could be also target of a small RNA.

In the field of Nm pathogenesis, this complete analysis of neisserial whole transcriptome in human blood significantly increases the knowledge of how this bacterium responds to human blood and causes sepsis. The findings reported in this study could also be helpful to identify the function of gene products annotated as hypothetical proteins and understand the regulation of vaccine antigens in blood. Moreover, it open the way for a further characterization of the identified regulatory RNAs as new virulence factors and key elements in the pathogenesis of meningococcus.

4. Materials and Methods

4.1 Construction of isogenic deletion mutants and complementing strains

To generate isogenic deletion mutants, target genes were truncated by replacing the gene sequence with an erythromycin (Ery) or kanamycin (Kan) resistance cassette. Approximately 800 bp fragments of the flanking regions of target genes were amplified by PCR from Nm MC58 genomic DNA. Primers used for generation of flanking regions are listed in Table S5. Upstream regions were generated with XbaI and SmaI restriction sites, while downstream regions with SmaI and XhoI restriction sites. Restriction enzymes were purchased from New England Biolabs. The purified PCR fragments were digested and co-ligated into the pBluescript (pBS-KS vector) (Novagen) and transformed into E. coli DH5-a using standard techniques. Resulting plasmids were digested with SmaI to insert the erythromycin or kanamycin cassette. All constructs generated to delete the target genes are listed in Table S6. Once subcloning was complete, plasmid DNA was linearized using ApaI and naturally competent Nm MC58 and 95N477 strains were transformed. Transformants were then selected on plates containing erythromycin at 5 mg/ml or kanamycin at 100 mg/ml. Deletion of the target gene was verified by colony PCR analysis using primer pairs to amplify a PCR product inside each gene locus (Table S5). In addition, the primers 1 and 2 (Figure 10A and Table S5) were used to confirm, by sequencing, the correct insertion and orientation of antibiotic resistance cassettes within the deletion region. Furthermore, the sequencing permitted verification that there were no variations in the sequences of the adjacent genes (used as flanking regions) due to the recombination event. The amplified PCR fragments were sequenced using the primers 1 and 2 specific for each gene region and the primers 3 and 4 specific for the antibiotic cassette used to generate the KO strains (Kan or Ery) (Figure 10A and Table S5). Southern blots analysis was performed to verify that all the deletion mutants have no off-target insertions of the antibiotic resistance cassettes. The genes to be complemented were cloned into the pCom- pRBS vector [114]. Forward primers include a NdeI restriction site and reverse primers contain a NsiI restriction site. The pairs of primers used to amplify the different genes are indicated in Table S5. PCRs were performed on Nm MC58 (for genes:

NMB1483 and mip) or 95N477 (for gene nspA) genomic DNA using the Platinum Taq High Fidelity DNA polymerase (Invitrogen). Each PCR product was digested with NdeI and NsiI enzymes, and cloned into the NdeI/NsiI sites of the pCom-pRBS vector. Resulting plasmids were checked by sequencing and are listed in Table S6. Plasmid DNA was linearized using SpeI and used to transform respective isogenic deletion mutants. The genes were inserted in the intergenic region between the NMB1428 and NMB1429 genes and the recombination event occurs between the upstream and downstream region of this locus, allowing the insertion of chloramphenicol resistance cassette and the gene of interest under the control of a constitutive promoter. Transformants were then selected on plates containing chloramphenicol at 5 mg/ml and insertion of the target gene was verified by colony PCR using primers designed on the regions flanking the site of recombination as previously described [114]. The various deletion mutant and complementing strains were also analyzed for growth kinetics in GC broth with respect to the wild-type strains.

4.2 Southern blot analysis

Genomic DNA of Nm wild-type and deletion mutant strains were isolated using Dneasy blood and tissue extraction kit (Qiagen) according to the manufacturer's instructions. Two mg of genomic DNA was digested with BglI overnight and purified using a PCR purification kit (Qiagen). Southern Blot was performed using the ECL Direct Nucleic Acid Labeling and Detection Systems (GE Healthcare) according to the manufacturer's instructions. Briefly, digested DNA was separated in a 0.8% agarose gel and blotted to Hybond N+ membrane (Amersham). The blots were hybridized with the probes generated by PCR using High Fidelity DNA Polymerase (Invitrogen) and labeled with HRP (horseradish peroxidase). The probes were a 1019 bp-Kan (amplified using the primers SB_Kan Fw and SB_Kan Rv) or a 1018 bp Ery fragment (amplified using the primers SB_Ery Fw and SB_Ery Rv) (Table S5).

4.3 Ex vivo whole blood model of meningococcal bacteremia

Nm MC58 and 95N477 wild-type, deletion mutants and complementing strains (Table S7) were grown on GC agar plates at 37uC overnight. Bacteria were harvested into GC liquid medium to an OD = 600 nm of 0.05 and grown to mid-log phase (OD 0.5-0.6) then diluted to approximately 106, 105 or 104 CFU/ml in a total volume of 100 ml of GC liquid medium in a 96 well/plate. The assay was started by the addition of 100% whole human blood (190 ml), supplied by two different donors (a male and a female) to the bacterial suspension (10 ml) in a 96 well/plate. Cultures were incubated at 37uC/5%CO2 with gentle agitation, at various time points (30, 60 and 120 minutes) an aliquot of the sample was removed and the number of viable bacteria determined by plating serial dilutions onto MH agar and incubating overnight at 37 C° /5% CO2. Experiments were performed in duplicate. We used the diluted 100 ml culture as the control time 0 (T0). Whole venous blood, collected from healthy individuals and anti-coagulated with heparin (5 U/ml), was used for whole blood experiments [95].

4.4 Bacterial strains and growth conditions

Serogroup B Nm strains (MC58, 95N477 and their isogenic derivatives) and *Escherichia coli* DH5α strains used in this study are listed in Table S7. Nm strains were grown on GC agar plates or in GC broth at 37°C in 5% CO_2. *E. coli* strains were cultured in Luria-Bertani (LB) agar or LB broth at 37 °C. Antibiotics were added when required; erythromycin was added at 5 μg/ml for selection of isogenic Nm strains. Ampicillin and erythromycin were added at final concentration of 100 μg/ml for *E. coli*. For *E.coli* white/blue selection, used in TOPO-TA cloning kit, IPTG and X-gal were added to LB agar according to manufacturer's instructions. Nm strains were grown overnight on GC agar plates and cultured in GC broth to early exponential phase. Approximately 10^8 bacteria were pelleted by centrifugation at 4000 rpm for 5 minutes and resuspended in an equal volume (1ml) of freshly isolated human blood maintained at 37°C. Whole blood infected with bacteria was incubated for 0, 30, 60 and 90 minutes with gentle shacking to avoid sedimentation. Samples were then treated with RNA protect bacteria reagent (Qiagen) immediately after adding bacteria to whole blood (time 0) and for each time point

to 90 minutes. Cells were harvested by centrifugation and stored at -80°C until bacterial RNA isolation. Each time point was represented by three samples from which RNA was purified separately. CFU counts were obtained for Nm cultures immediately before time course initiation (time 0) and 30, 60 and 90 minutes of incubation. The time course experiments were performed independently with three different blood donors.

4.5 Human whole blood

Heparinized human venous blood was collected from 3 healthy volunteers (a male and two females, ages ranged from 25 to 31 years). Heparin was used at concentration of 5U/ml. Heparin was used in preference to ethylenediaminetetraacetic acid (EDTA) as an anti-coagulant agent because EDTA chelates divalent cations, which would influence cellular functions during *Neisseria*-blood cell interactions. Heparin is commonly used in blood models of infection for Neisseria [95] and while heparin has been reported to affect complement activation, it is not know to alter gene expression in Neisseria.

4.6 Isolation and enrichment of bacterial RNA

For RNA isolation, the samples were incubated with 5 volumes of Erythrocyte Lysis (EL) buffer (Qiagen) for 15 minutes on ice and centrifuged at 4°C and 4500 rpm for 6 minutes. Total RNA (bacterial and eukaryotic RNA) was isolated by enzymatic lysis using lysozyme (Sigma) at 0.4 mg/ml final concentration, vortexed and incubated at room temperature for 5 minutes. RNA isolation was completed with the RNeasy Mini Kit (Qiagen) according to the manufacturer's protocol. DNA contamination was avoided by on-column treatment with RNase-Free DNase Set (Qiagen) and post-treatment with recombinant DNase I (Roche) according to manufacturer's instructions. Absence of bacterial DNA was confirmed by PCR with primers specific for *NMB1591*. RNA concentration and integrity was assessed by measurement of the A260/A280 ratios and electrophoretic analysis with an Agilent 2100 Bioanalyzer (Agilent Technologies).
Finally, three total RNA aliquots corresponding to each time point were pooled and used for the bacterial RNA enrichment procedure. Total RNA obtained at this step, extracted at

time 0 and 60 minutes of incubation, was used also for Northern Blot analysis, 5'-3' RACE and RT-PCR. Enrichment of bacterial RNA was performed using the MICROBEnrich kit (Ambion) according to manufacturer's instructions. Enriched-bacterial RNA was assessed by electrophoretic analysis with an Agilent 2100 Bioanalyzer. Enriched-bacterial total RNA was used as template for cRNA synthesis (amplification and labelling reaction).

4.7 RNA amplification and labeling

Enriched-bacterial RNA was amplified and labeled using the MessageAmp II Bacteria kit (Ambion). The kit employs an *in vitro* transcription (IVT)-mediated linear amplification system to produce amplified RNA (cRNA). Briefly, 100 ng of total RNA from each time point was used as template for the synthesis reaction. An initial polyadenylation step was performed. The tailed RNA was reverse transcribed (cDNA synthesis) in a reaction primed with an oligo (dT) primers bearing a T7 promoter. The resulting cDNA was then transcribed with T7 RNA Polymerase to generate antisense RNA (cRNA) in an *in vitro* reaction for 14 hours at 37°C. The cRNA was labeled by including Cyanine 3-CTP (Cy3) and Cyanine 5-CTP (Cy5; Perkin Elmer, Boston, MA) nucleotides in the IVT reaction.
The cRNA was then fragmented in fragmentation buffer (Agilent Technologies) at 60°C for 30 minutes before hybridization. Competitive hybridizations were conducted with 825 ng of Cy3-labelled cRNA reference (bacteria in contact with whole blood at time 0) versus 825 ng Cy5-labelled cRNA of each time point (30, 60 and 90 minutes). cRNAs were hybridized onto the microarray slides for 17 hours at 65°C, washed and scanned with an Agilent scanner following the Agilent Microarray protocol.

4.8 Microarray design and analysis

The customized oligonucleotide high-density tiling array, used in this work, was designed *in house* and produced with the Agilent *in-situ* technology. In detail, the chromosome of *N. meningitidis* strain (MC58) (GenBank AE002098) was subdivided on the basis of its ORF predictions in coding and non-coding regions, considering small ORFs (<300 bp) as non-coding anyway, this both on the forward or reverse strands. Non-coding regions were the

basis for the tiling probes selection; the tiling design selected 60 bp probes shifted of 10 bp. Instead, coding portions of the chromosome (predicted ORFs with length > 300 bp), were selected for designing a low-density set of probes adding to the previous a rejection criterion in presence of possible cross homologies. Finally, 36869 probes for non-coding portions of the chromosome and 6877 probes for coding portions were selected and, in addition, control probes specific of the Agilent technology were included in the final 4x44k custom chip design. After data acquisition, the slide normalization was performed by lowess algorithm as implemented by the Agilent Feature Extraction software v.9.5.3. Before any other analysis we computed an average on replicated probes signals M=*Log2(Cy3/Cy5)* and A=*Log2(Cy3*Cy5)/2* within each slide. Then, M probe signals of the experimental replicas at each time point were compared by principal component analysis as described in the following paragraph. This approach together with the *a posteriori* homology check allowed identifying a set of 3099 probes as noisy and 4375 probes as non-specific. After this 'quality check' comparison the average signals at the level of each time point were computed merging together the slides of the different donors. These average dataset are the basis of any further transcriptional analysis at the level of the entire chromosome as described in the paragraph after the following.

4.9 Bioinformatic analysis of the identified transcripts

4.9.1 Sequence conservation, promoter prediction and target prediction of the identified small intergenic RNAs

All the small RNA transcripts detected in intergenic regions by mapping the tiling array results in the Artemis annotation environment were analyzed with regard to location, features, potential function and previous identification in literature. The following criteria were applied: (i) no annotated transcription according to the published GeneBank annotation of the genome [73], (ii) higher signal level than neighboring probes, (iii) higher signal than the corresponding antisense region, (iv) no cross-hybridization of the probes in the unit with other regions in the genome. The set of small RNAs was checked also for the correspondance with known tRNA (http://cmr.jcvi.org/).

Then, for each intergenic small RNA transcript, several analyses were performed. The conservation of the sequence was checked among different species used as reference of the neisserial population: MC58 (*N. meningitidis* group B), Z2491 (*N. meningitidis* group A), FAM18 (*N. meningitidis* group C), *N. meningitidis* alpha14, *N. gonorrhoeae* FA 1090 and *N. lactamica* 020-06. The sequences were analyzed and aligned using Geneious software.
For each small RNA, the presence of a putative promoter at the 5'-end (http://www.fruitfly.org/seq_tools/promoter.html) and of a Rho-independent terminator of transcription at 3'-end (a list of *N. meningitidis* MC58 strain Rho-independent terminator is available at) were checked.
In addition, the putative target mRNAs for each small RNA were determined using TargetRNA tool ().

4.9.2 Motif analysis of the identified UTRs with Rfam database

For 5' and 3' untranslated regions (UTRs) analysis, the presence of known functional RNA motifs was checked by using Rfam database ().

4.9.3 Comparison of the identified operons with the in silico prediction by Door algorithm

Operons that were putatively detected by the observed transcription signal were compared against an *in silico* prediction of operon boundaries in the MC58 chromosome as reported in the Database of prOkaryotic OpeRons (DOOR,).

4.10 Simultaneous mapping of 5'- and 3'-ends of RNA molecules (5'-3' RACE)

The basis of the approach is the simultaneous mapping of 5'- and 3'-RNA ends by RACE (Rapid Amplification of cDNA Ends) using circularized RNAs (Protocol adapted from [59]).

10 ug of total RNA was split in two aliquots. Both aliquots were incubated for 1 hour at 37ºC with or without the Tobacco Acid Pyrophosphatase, (TAP) (Epicentre biotechnologies) in the correnspondingbuffer (20U of TAP enzyme in 50ul reaction volume). This step allows discriminating a 5'- end generated by transcription initiation, from a 5'-end provided by RNA processing. RNA was purified by acid-phenol and chloroform extractions and ethanol precipitation. 250 ng of the TAP+ and TAP- treated RNAs were incubated with 20 U of T4 RNA ligase I (New England Biolabs) in the presence of 1X RNA ligase Buffer, 8% DMSO, 10 U of RNase Inhibitor, 1 U of DNase I (Roche) and RNase-free water in a total volume of 25 µl at 17ºC overnight. Ligated RNA was purified by acid-phenol and chloroform extractions and ethanol precipitation and resuspended in 10 ul of RNase-free water. Ligated RNA was used to perform an RT-PCR reaction using specific outward primers (Table S5) and the SuperScript One-Step RT-PCR kit (Invitrogen). The specific outward primers were designed one adjacent to the other, so that the size of the PCR product obtained should correspond to the real size of the sRNA analyzed. RT-PCR products were checked on a 3% TAE-agarose gels and the bands only present in the TAP+ reactions and corresponding to the expected size were purified using Gel Extraction kit (QIAGEN) and clone using TOPO TA Cloning kit (Invitrogen). 10 clones for each transformation were analyzed by PCR using M13 forward and reverse primers and the plasmids containing the expected size of insert were sent to sequencing.

4.11 Northern Blot analysis

Northern blot analysis was carried out using the Northern-Max kit (Ambion) according to the manufacturer's instructions. A total of 5 ug of RNA from a pooled sample of total RNA, extracted at time 0 and 60 min. of incubation of *N. meningitidis* in human whole blood, was fractionated on a 1% agarose-formaldehyde gel and transferred onto nylon

membrane (BrightStar®-Plus Nylon Membrane, Ambion) through capillary blotting. Then, 2 pmol of a specific oligonucleotides were radioactively end-labelled by using T4 polynucleotide kinase (New England Biolabs, Inc.) and 4 pmol of [γ-^{32}P]ATP (6,000 Ci/mmol; Perkin-Elmer) and were used as probe. Hybridization was performed at 37°C, low-stringency washes at room temperature.

4.12 RT-PCR to detect antisense RNAs, 5' and 3'UTRs and operons

Specific RT-PCR was performed using total RNA extracted at t0 (for down regulated transcripts) and t60 minutes of incubation in human blood (for up regulated transcripts). Total RNA was previously treated with DNase I (Roche) and checked for the absence of residual genomic DNA. Reverse transcription was performed using Superscript II (Invitrogen) and specific primers (Table S5). For antisense RNA detection, we used reverse primers designed to be complementary only to antisense RNA and not mRNA. For detection of 3'UTR we used two different primers designed one inside the coding sequence of the gene and one that matched the last probe of the transcriptional unit, which gave a signal in the tiling array analysis. 500 ng of total RNA were incubated with 1 ul dNTP mix 10mM each (Invitrogen), 2 pmoles of gene-specific primer, 1X First –Strand Buffer, 2 ul 0,1 M DTT, 1 ul RNaseOUT 40 U/ul (Invitrogen) and 1 ul Superscript II RT (200 U), according to manufacture's instruction. We added also a sample without RT polymerase as negative control. After reverse transcription, cDNA samples were treated with 1ul (2U) of *E. coli* RNase H (New England Biolabs) and incubated at 37°C for 20 min. RNase H was inactivated for 20 min. at 65°C. 2 ul of each sample (including also the RT negative control, not treated with RNase) was used for PCR reaction with Platinum Taq polymerase (Invitrogen) using specific primers (Table S5). RT-PCR products were checked on a 1% TAE-agarose gels.

5. References

1. Stephens DS, Greenwood B, Brandtzaeg P (2007) Epidemic meningitis, meningococcaemia, and Neisseria meningitidis. Lancet 369: 2196–2210. doi:10.1016/S0140-6736(07)61016-2.

2. BRANHAM SE (1953) Serological relationships among meningococci. Bacteriol Rev 17: 175–188.

3. Rosenstein NE, PERKINS BA, Stephens DS, POPOVIC T, Hughes JM (2001) Meningococcal Disease. N Engl J Med 344: 1378–1388. doi:10.1056/NEJM200105033441807.

4. Maiden M, Bygraves J, Feil E, Morelli G, Russell J, et al. (1998) Multilocus sequence typing: A portable approach to the identification of clones within populations of pathogenic microorganisms. P Natl Acad Sci Usa 95: 3140–3145. doi:10.2307/44811.

5. Parkhill J, Achtman M, James KD, Bentley SD, Churcher C, et al. (2000) Complete DNA sequence of a serogroup A strain of Neisseria meningitidis Z2491. Nature 404: 502–506. doi:10.1038/35006655.

6. Schoen C, Blom J, Claus H, Schramm-Glueck A, Brandt P, et al. (2008) Whole-genome comparison of disease and carriage strains provides insights into virulence evolution in Neisseria meningitidis. P Natl Acad Sci Usa 105: 3473–3478. doi:10.1073/pnas.0800151105.

7. Hilse R, Hammerschmidt S, Bautsch W, Frosch M (1996) Site-specific insertion of IS1301 and distribution in Neisseria meningitidis strains. J Bacteriol 178: 2527–2532.

8. Stephens DS (2009) Biology and pathogenesis of the evolutionarily successful, obligate human bacterium Neisseria meningitidis. Vaccine 27 Suppl 2: B71–7. doi:10.1016/j.vaccine.2009.04.070.

9. Bogaert D, Hermans PWM, Boelens H, Sluijter M, Luijendijk A, et al. (2005) Epidemiology of nasopharyngeal carriage of Neisseria meningitidis in healthy Dutch children. Clin Infect Dis 40: 899–902. doi:10.1086/428351.

10. Brandtzaeg P, Hogasen K, Kierulf P, Mollnes T (1996) The excessive complement activation in fulminant meningococcal septicemia is predominantly caused by alternative pathway activation. J Infect Dis 173: 647–655.

11. Molesworth AM, Cuevas LE, Connor SJ, Morse AP, Thomson MC (2003) Environmental risk and meningitis epidemics in Africa. Emerging Infect Dis 9: 1287–1293.

12. Kahler CM, Martin LE, Stephens DS, 6 (1998) The (alpha2-->8)-linked polysialic acid capsule and lipooligosaccharide structure both contribute to the ability of serogroup B Neisseria meningitidis to resist the bactericidal activity of normal human serum. Infect Immun 66: 5939–5947.

13. Takahashi H, Carlson RW, Muszynski A, Choudhury B, Kim KS, et al. (2008) Modification of lipooligosaccharide with phosphoethanolamine by LptA in Neisseria meningitidis enhances meningococcal adhesion to human endothelial and epithelial cells. Infect Immun 76: 5777–5789. doi:10.1128/IAI.00676-08.

14. Holst J, Feiring B, Naess LM, Norheim G, Kristiansen P, et al. (2005) The concept of "tailor-made," protein-based, outer membrane vesicle vaccines against meningococcal disease. Vaccine 23: 2202–2205. doi:10.1016/j.vaccine.2005.01.058.

15. Sharip A, Sorvillo F, Redelings MD, Mascola L, Wise M, et al. (2006) Population-based analysis

of meningococcal disease mortality in the United States: 1990-2002. Pediatr Infect Dis J 25: 191–194. doi:10.1097/01.inf.0000202065.03366.0c.

16. Aguilera J-FJ, Perrocheau AA, 5 (2002) Outbreak of serogroup W135 meningococcal disease after the Hajj pilgrimage, Europe, 2000. Emerging Infect Dis 8: 761–767.

17. Boisier P, Nicolas P, Djibo S, Taha M-K, Jeanne I, et al. (2007) Meningococcal meningitis: unprecedented incidence of serogroup X-related cases in 2006 in Niger. Clin Infect Dis 44: 657–663. doi:10.1086/511646.

18. Shepard CW, Rosenstein NE, Fischer M, Active Bacterial Core Surveillance Team (2003) Neonatal meningococcal disease in the United States, 1990 to 1999. Pediatr Infect Dis J 22: 418–422. doi:10.1097/01.inf.0000066876.77453.04.

19. van Deuren M, Brandtzaeg P, van der Meer JW (2000) Update on meningococcal disease with emphasis on pathogenesis and clinical management. Clin Microbiol Rev 13: 144–66, table of contents.

20. Hackett S, Guiver M, Marsh J, Sills J, Thomson A, et al. (2002) Meningococcal bacterial DNA load at presentation correlates with disease severity. Arch Dis Child 86: 44–46.

21. Ovstebo R, Brandtzaeg P, Brusletto B, Haug KBF, Lande K, et al. (2004) Use of robotized DNA isolation and real-time PCR to quantify and identify close correlation between levels of Neisseria meningitidis DNA and lipopolysaccharides in plasma and cerebrospinal fluid from patients with systemic meningococcal disease. Journal of clinical microbiology 42: 2980.

22. Waage A, Brandtzaeg P, Halstensen A, Kierulf P, Espevik T (1989) The complex pattern of cytokines in serum from patients with meningococcal septic shock. Association between interleukin 6, interleukin 1, and fatal outcome. J Exp Med 169: 333–338.

23. Hackett SJ, Thomson AP, Hart CA (2001) Cytokines, chemokines and other effector molecules involved in meningococcal disease. J Med Microbiol 50: 847–859.

24. Moller A, Bjerre A, Brusletto B, Joo G, Brandtzaeg P, et al. (2005) Chemokine patterns in meningococcal disease. J Infect Dis 191: 768–775. doi:10.1086/427514.

25. SUN Y-H (2000) Functional genomics of Neisseria meningitidis pathogenesis: 1–5.

26. Nolte OO, Rickert AA, Sonntag HGH, 5 (2002) A modified ex vivo human whole blood model of infection for studying the pathogenesis of Neisseria meningitidis during septicemia. FEMS Immunol Med Microbiol 32: 91–95. doi:10.1111/j.1574-695X.2002.tb00539.x.

27. Sprong T, Brandtzaeg P, Fung M, Pharo AM, Høiby EA, et al. (2003) Inhibition of C5a-induced inflammation with preserved C5b-9-mediated bactericidal activity in a human whole blood model of meningococcal sepsis. Blood 102: 3702–3710. doi:10.1182/blood-2003-03-0703.

28. Welsch JA, Granoff D (2007) Immunity to Neisseria meningitidis group B in adults despite lack of serum bactericidal antibody. Clin Vaccine Immunol 14: 1596–1602. doi:10.1128/CVI.00341-07.

29. Echenique-Rivera H, Muzzi A, Del Tordello E, Seib KL, Francois P, et al. (2011) Transcriptome analysis of Neisseria meningitidis in human whole blood and mutagenesis studies identify virulence factors involved in blood survival. PLoS Pathog 7: e1002027. doi:10.1371/journal.ppat.1002027.

30. Fantappiè L, Metruccio MME, Seib KL, Oriente F, Cartocci E, et al. (2009) The RNA chaperone Hfq is involved in stress response and virulence in Neisseria meningitidis and is a pleiotropic regulator of protein expression. Infect Immun 77: 1842–1853. doi:10.1128/IAI.01216-08.

31. Seib KL, Serruto D, Oriente F, Delany I, Adu-Bobie J, et al. (2008) Factor H-binding protein is important for meningococcal survival in human whole blood and serum and in the presence of the

antimicrobial peptide LL-37. Infect Immun 77: 292–299. doi:10.1128/IAI.01071-08.

32. Francois P, Garzoni C, Bento M, Schrenzel J (2007) Comparison of amplification methods for transcriptomic analyses of low abundance prokaryotic RNA sources. J Microbiol Methods 68: 385–391. doi:10.1016/j.mimet.2006.09.022.

33. Haft DH, Loftus BJ, Richardson DL, Yang F, Eisen JA, et al. (2001) TIGRFAMs: a protein family resource for the functional identification of proteins. Nucleic Acids Res 29: 41–43.

34. Toledo-Arana A, Solano C (2010) Deciphering the physiological blueprint of a bacterial cell: revelations of unanticipated complexity in transcriptome and proteome. Bioessays 32: 461–467. doi:10.1002/bies.201000020.

35. Somerville GA, Proctor RA (2009) At the crossroads of bacterial metabolism and virulence factor synthesis in Staphylococci. Microbiol Mol Biol Rev 73: 233–248. doi:10.1128/MMBR.00005-09.

36. Toledo-Arana A, Dussurget O, Nikitas G, Sesto N, Guet-Revillet H, et al. (2009) The Listeria transcriptional landscape from saprophytism to virulence. Nature 459: 950–956. doi:10.1038/nature08080.

37. Beaume M, Hernandez D, Farinelli L, Deluen C, Linder P, et al. (2010) Cartography of methicillin-resistant S. aureus transcripts: detection, orientation and temporal expression during growth phase and stress conditions. PLoS ONE 5: e10725. doi:10.1371/journal.pone.0010725.

38. Sharma CM, Hoffmann S, Darfeuille F, Reignier J, Findeiß S, et al. (2010) The primary transcriptome of the major human pathogen Helicobacter pylori. Nature 464: 250–255. doi:10.1038/nature08756.

39. Pannekoek Y, Huis in 't Veld R, Hopman CTP, Langerak AAJ, Speijer D, et al. (2009) Molecular characterization and identification of proteins regulated by Hfq in Neisseria meningitidis. FEMS Microbiol Lett 294: 216–224. doi:10.1111/j.1574-6968.2009.01568.x.

40. Mellin JR, McClure R, Lopez D, Green O, Reinhard B, et al. (2010) Role of Hfq in iron-dependent and -independent gene regulation in Neisseria meningitidis. Microbiology (Reading, Engl) 156: 2316–2326. doi:10.1099/mic.0.039040-0.

41. Beisel CL, Storz G (2010) Base pairing small RNAs and their roles in global regulatory networks. FEMS Microbiol Rev 34: 866–882. doi:10.1111/j.1574-6976.2010.00241.x.

42. Gripenland J, Netterling S, Loh E, Tiensuu T, Toledo-Arana A, et al. (2010) RNAs: regulators of bacterial virulence. Nature Publishing Group 8: 857–866. doi:10.1038/nrmicro2457.

43. Waters LS, Storz G (2009) Regulatory RNAs in bacteria. Cell 136: 615–628. doi:10.1016/j.cell.2009.01.043.

44. Sharma CM, Darfeuille F, Plantinga TH, Vogel J (2007) A small RNA regulates multiple ABC transporter mRNAs by targeting C/A-rich elements inside and upstream of ribosome-binding sites. Genes Dev 21: 2804–2817. doi:10.1101/gad.447207.

45. Vecerek B, Moll I, Bläsi U (2007) Control of Fur synthesis by the non-coding RNA RyhB and iron-responsive decoding. EMBO J 26: 965–975. doi:10.1038/sj.emboj.7601553.

46. Hammer BK, Bassler BL (2007) Regulatory small RNAs circumvent the conventional quorum sensing pathway in pandemic Vibrio cholerae. P Natl Acad Sci Usa 104: 11145–11149. doi:10.1073/pnas.0703860104.

47. Prévost K, Salvail H, Desnoyers G, Jacques J-F, Phaneuf E, et al. (2007) The small RNA RyhB activates the translation of shiA mRNA encoding a permease of shikimate, a compound involved in siderophore synthesis. Mol Microbiol 64: 1260–1273. doi:10.1111/j.1365-2958.2007.05733.x.

48. Urban JH, Vogel J (2008) Two seemingly homologous noncoding RNAs act hierarchically to activate glmS mRNA translation. PLoS Biol 6: e64. doi:10.1371/journal.pbio.0060064.

49. Papenfort K, Vogel J (2010) Regulatory RNA in bacterial pathogens. Cell Host Microbe 8: 116–127. doi:10.1016/j.chom.2010.06.008.

50. Vogel J, Luisi BF (2011) Hfq and its constellation of RNA. Nature Publishing Group 9: 578–589. doi:10.1038/nrmicro2615.

51. Song T, Mika F, Lindmark B, Liu Z, Schild S, et al. (2008) A new Vibrio cholerae sRNA modulates colonization and affects release of outer membrane vesicles. Mol Microbiol 70: 100–111. doi:10.1111/j.1365-2958.2008.06392.x.

52. De Lay N, Gottesman S (2008) The Crp-activated small noncoding regulatory RNA CyaR (RyeE) links nutritional status to group behavior. J Bacteriol 191: 461–476. doi:10.1128/JB.01157-08.

53. Johansen J, Eriksen M, Kallipolitis B, Valentin-Hansen P (2008) Down-regulation of outer membrane proteins by noncoding RNAs: unraveling the cAMP-CRP- and sigmaE-dependent CyaR-ompX regulatory case. J Mol Biol 383: 1–9. doi:10.1016/j.jmb.2008.06.058.

54. Urbanowski ML, Stauffer LT, Stauffer GV (2000) The gcvB gene encodes a small untranslated RNA involved in expression of the dipeptide and oligopeptide transport systems in Escherichia coli. Mol Microbiol 37: 856–868.

55. Novick RP, Ross HF, Projan SJ, Kornblum J, Kreiswirth B, et al. (1993) Synthesis of staphylococcal virulence factors is controlled by a regulatory RNA molecule. EMBO J 12: 3967–3975.

56. Novick RPR, Geisinger EE (2007) Quorum sensing in staphylococci. Annu Rev Genet 42: 541–564. doi:10.1146/annurev.genet.42.110807.091640.

57. Bardill JP, Zhao X, Hammer BK (2011) The Vibrio cholerae quorum sensing response is mediated by Hfq-dependent sRNA/mRNA base-pairing interactions. Mol Microbiol: –. doi:10.1111/j.1365-2958.2011.07655.x.

58. Chabelskaya S, Gaillot O, Felden B (2009) A Staphylococcus aureus Small RNA Is Required for Bacterial Virulence and Regulates the Expression of an Immune-Evasion Molecule. PLoS Pathog 6: e1000927–e1000927. doi:10.1371/journal.ppat.1000927.

59. Toledo-Arana A, Dussurget O, Nikitas G, Sesto N, Guet-Revillet H, et al. (2009) The Listeria transcriptional landscape from saprophytism to virulence. Nature 459: 950–956. doi:10.1038/nature08080.

60. Güell M, van Noort V, Yus E, Chen W-H, Leigh-Bell J, et al. (2009) Transcriptome complexity in a genome-reduced bacterium. Science 326: 1268–1271. doi:10.1126/science.1176951.

61. Filiatrault MJ, Stodghill PV, Bronstein PA, Moll S, Lindeberg M, et al. (2010) Transcriptome analysis of Pseudomonas syringae identifies new genes, noncoding RNAs, and antisense activity. J Bacteriol 192: 2359–2372. doi:10.1128/JB.01445-09.

62. Rasmussen S, Nielsen HBR, Jarmer H (2009) The transcriptionally active regions in the genome of Bacillus subtilis. Mol Microbiol 73: 1043–1057. doi:10.1111/j.1365-2958.2009.06830.x.

63. Opdyke JA, Kang JG, Storz G (2004) GadY, a small-RNA regulator of acid response genes in Escherichia coli. J Bacteriol 186: 6698.

64. Dühring U, Axmann IM, Hess WR, Wilde A (2006) An internal antisense RNA regulates expression of the photosynthesis gene isiA.

65. Thomason MK, Storz G (2010) Bacterial antisense RNAs: how many are there, and what are they

doing? Annu Rev Genet 44: 167–188. doi:10.1146/annurev-genet-102209-163523.

66. Shearwin KEK, Callen BPB, Egan JBJ (2005) Transcriptional interference--a crash course. Trends Genet 21: 339–345. doi:10.1016/j.tig.2005.04.009.

67. Silby MW, Levy SB (2008) Overlapping protein-encoding genes in Pseudomonas fluorescens Pf0-1. Plos Genet 4: e1000094–e1000094. doi:10.1371/journal.pgen.1000094.

68. Johansson J, Mandin P, Renzoni A, Chiaruttini C, Springer M, et al. (2002) An RNA Thermosensor Controls Expression of Virulence Genes in Listeria monocytogenes. Cell 110: 551–561.

69. HOE N, GOGUEN J (1993) Temperature Sensing in Yersinia-Pestis - Translation of the Lcrf Activator Protein Is Thermally Regulated. J Bacteriol 175: 7901–7909.

70. Sudarsan N, Lee ER, Weinberg Z, Moy RH, Kim JN, et al. (2008) Riboswitches in eubacteria sense the second messenger cyclic di-GMP. Science 321: 411–413. doi:10.1126/science.1159519.

71. Smith AM, Fuchs RT, Grundy FJ, Henkin T (2010) Riboswitch RNAs: regulation of gene expression by direct monitoring of a physiological signal. RNA biology 7: 104.

72. Vogel JR, Bartels V, Tang T-H, Churakov G, ger JGS-J, et al. (2003) RNomics in Escherichia coli detects new sRNA species and indicates parallel transcriptional output in bacteria. Nucleic Acids Res 31: 6435–6443. doi:10.1093/nar/gkg867.

73. Tettelin H, Saunders NJ, Heidelberg J, Jeffries AC, Nelson KE, et al. (2000) Complete genome sequence of Neisseria meningitidis serogroup B strain MC58. Science 287: 1809-1815.

74. Exley RM, Goodwin L, Mowe E, Shaw J, Smith H, et al. (2005) Neisseria meningitidis lactate permease is required for nasopharyngeal colonization. Infect Immun 73: 5762.

75. Leighton MP, Kelly DJ, Williamson MP, Shaw JG (2001) An NMR and enzyme study of the carbon metabolism of Neisseria meningitidis. Microbiology 147: 1473–1482.

76. van Ulsen P, van Alphen L, Hove ten J, Fransen F, van der Ley P, et al. (2003) A Neisserial autotransporter NalP modulating the processing of other autotransporters. Mol Microbiol 50: 1017–1030. doi:10.1046/j.1365-2958.2003.03773.x.

77. Stohl EAE, Criss AKA, Seifert HSH (2005) The transcriptome response of Neisseria gonorrhoeae to hydrogen peroxide reveals genes with previously uncharacterized roles in oxidative damage protection. Mol Microbiol 58: 520–532. doi:10.1111/j.1365-2958.2005.04839.x.

78. Tidhar A, Flashner Y, Cohen S, Levi Y, Zauberman A, et al. (2008) The NlpD Lipoprotein Is a Novel Yersinia pestis Virulence Factor Essential for the Development of Plague. PLoS ONE 4: e7023–e7023. doi:10.1371/journal.pone.0007023.

79. Leuzzi R, Serino L, Scarselli M, Savino S, Fontana MR, et al. (2005) Ng-MIP, a surface-exposed lipoprotein of Neisseria gonorrhoeae, has a peptidyl-prolyl cis/trans isomerase (PPIase) activity and is involved in persistence in macrophages. Mol Microbiol 58: 669–681. doi:10.1111/j.1365-2958.2005.04859.x.

80. Carpenter BM, Gancz H, Gonzalez-Nieves RP, West AL, Whitmire JM, et al. (2008) A single nucleotide change affects fur-dependent regulation of sodB in H. pylori. PLoS ONE 4: e5369–e5369. doi:10.1371/journal.pone.0005369.

81. Oriente F, Scarlato V, Delany I (2010) Expression of factor H binding protein of meningococcus responds to oxygen limitation through a dedicated FNR-regulated promoter. J Bacteriol 192: 691–701. doi:10.1128/JB.01308-09.

82. Lewis LAL, Ngampasutadol JJ, Wallace RR, Reid JEAJ, Vogel UU, et al. (2009) The meningococcal vaccine candidate neisserial surface protein A (NspA) binds to factor H and enhances meningococcal resistance to complement. CORD Conference Proceedings 6: e1001027–e1001027. doi:10.1371/journal.ppat.1001027.

83. Metruccio MME, Fantappiè L, Serruto D, Muzzi A, Roncarati D, et al. (2009) The Hfq-dependent small noncoding RNA NrrF directly mediates Fur-dependent positive regulation of succinate dehydrogenase in Neisseria meningitidis. J Bacteriol 191: 1330–1342. doi:10.1128/JB.00849-08.

84. Mellin JR, Goswami S, Grogan S, Tjaden B, Genco CA (2007) A novel fur- and iron-regulated small RNA, NrrF, is required for indirect fur-mediated regulation of the sdhA and sdhC genes in Neisseria meningitidis. J Bacteriol 189: 3686–3694. doi:10.1128/JB.01890-06.

85. Hotopp JCD, Grifantini R, Kumar N, Tzeng YL, Fouts D, et al. (2006) Comparative genomics of Neisseria meningitidis: core genome, islands of horizontal transfer and pathogen-specific genes. Microbiology 152: 3733–3749. doi:10.1099/mic.0.29261-0.

86. Nolte O, Rickert A, Ehrhard I, Ledig S, Sonntag HG (2002) A modified ex vivo human whole blood model of infection for studying the pathogenesis of Neisseria meningitidis during septicemia. FEMS Immunol Med Microbiol 32: 91-95

87. Faubladier M, Bouche JP (1994) Division inhibition gene dicF of Escherichia coli reveals a widespread group of prophage sequences in bacterial genomes. J Bacteriol 176: 1150.

88. Castillo-Keller M, Vuong P, Misra R (2006) Novel mechanism of Escherichia coli porin regulation. J Bacteriol 188: 576.

89. Tinsley CR, Bille E, Nassif X (2006) Bacteriophages and pathogenicity: more than just providing a toxin? Microbes Infect 8: 1365–1371. doi:10.1016/j.micinf.2005.12.013.

90. Bille E, Ure R, Gray SJ, Kaczmarski EB, McCarthy ND, et al. (2007) Association of a bacteriophage with meningococcal disease in young adults. PLoS ONE 3: e3885–e3885. doi:10.1371/journal.pone.0003885.

91. Kawano M, Aravind L, Storz G (2007) An antisense RNA controls synthesis of an SOS-induced toxin evolved from an antitoxin. Mol Microbiol 64: 738–754. doi:10.1111/j.1365-2958.2007.05688.x.

92. Ansong C, Yoon H, Porwollik S, Mottaz-Brewer H, Petritis BO, et al. (2008) Global systems-level analysis of Hfq and SmpB deletion mutants in Salmonella: implications for virulence and global protein translation. PLoS ONE 4: e4809–e4809. doi:10.1371/journal.pone.0004809.

93. Julio SM, Heithoff DM, Mahan MJ (2000) ssrA (tmRNA) plays a role in Salmonella enterica serovar Typhimurium pathogenesis. J Bacteriol 182: 1558.

94. Papenfort K, Vogel J (2010) Regulatory RNA in bacterial pathogens. Cell Host Microbe 8: 116–127. doi:10.1016/j.chom.2010.06.008.

95. Ison C (2001) Whole-Blood Model. In: Pollard AJaM, M.C.J., editor. Meningococcal Vaccines: Methods and Protocols. Totowa: Human Press Inc. pp. 317-329.

96. Cummings M, McGurk C, Masters JR (2003) Rapid identification of antisense mRNA-expressing clones using strand-specific RT-PCR. Antisense and Nucleic Acid Drug Development 13: 115–117.

97. Yu H, Kim KS (2010) Ferredoxin is involved in secretion of cytotoxic necrotizing factor 1 across the cytoplasmic membrane in Escherichia coli K1. Infect Immun 78: 838–844. doi:10.1128/IAI.00674-09.

98. Pannekoek Y, Huis in 't Veld R, Hopman CTP, Langerak AAJ, Speijer D, et al. (2009) Molecular

characterization and identification of proteins regulated by Hfq in Neisseria meningitidis. FEMS Microbiol Lett 294: 216–224. doi:10.1111/j.1574-6968.2009.01568.x.

99. Lorenz C, Gesell T, Zimmermann B, Schoeberl U, Bilusic I, et al. (2010) Genomic SELEX for Hfq-binding RNAs identifies genomic aptamers predominantly in antisense transcripts. Nucleic Acids Res 38: 3794–3808. doi:10.1093/nar/gkq032.

100. Zemanová M, Kaderábková P, Pátek M, Knoppová M, Silar R, et al. (2008) Chromosomally encoded small antisense RNA in Corynebacterium glutamicum. FEMS Microbiol Lett 279: 195–201. doi:10.1111/j.1574-6968.2007.01024.x.

101. Hernández JA, Muro-Pastor AM, Flores E, Bes MT, Peleato ML, et al. (2006) Identification of a furA cis antisense RNA in the cyanobacterium Anabaena sp. PCC 7120. J Mol Biol 355: 325–334. doi:10.1016/j.jmb.2005.10.079.

102. Levine E, Zhang Z, Kuhlman T, Hwa T (2007) Quantitative characteristics of gene regulation by small RNA. PLoS Biol 5: e229–e229. doi:10.1371/journal.pbio.0050229.

103. Georg J, Hess WR (2011) cis-antisense RNA, another level of gene regulation in bacteria. Microbiol Mol Biol Rev 75: 286–300. doi:10.1128/MMBR.00032-10.

104. Mraheil MA, Billion A, Mohamed W, Mukherjee K, Kuenne C, et al. (2011) The intracellular sRNA transcriptome of Listeria monocytogenes during growth in macrophages. Nucleic Acids Res 39: 4235–4248. doi:10.1093/nar/gkr033.

105. Chinni SV, Raabe CA, Zakaria R, Randau G, Hoe CH, et al. (2010) Experimental identification and characterization of 97 novel npcRNA candidates in Salmonella enterica serovar Typhi. Nucleic Acids Res 38: 5893–5908. doi:10.1093/nar/gkq281.

106. Tramonti A, De Canio M, De Biase D (2008) GadX/GadW-dependent regulation of the Escherichia coli acid fitness island: transcriptional control at the gadY-gadW divergent promoters and identification of four novel 42 bp GadX/GadW-specific binding sites. Mol Microbiol 70: 965–982. doi:10.1111/j.1365-2958.2008.06458.x.

107. Lee E-J, Groisman EA (2010) An antisense RNA that governs the expression kinetics of a multifunctional virulence gene. Mol Microbiol 76: 1020–1033. doi:10.1111/j.1365-2958.2010.07161.x.

108. Stork M, Di Lorenzo M, Welch TJ, Crosa JH (2007) Transcription termination within the iron transport-biosynthesis operon of Vibrio anguillarum requires an antisense RNA. J Bacteriol 189: 3479–3488. doi:10.1128/JB.00619-06.

109. Upton AM, McKinney JD (2007) Role of the methylcitrate cycle in propionate metabolism and detoxification in Mycobacterium smegmatis. Microbiology 153: 3973–3982. doi:10.1099/mic.0.2007/011726-0.

110. Tauseef I, Harrison OB, Wooldridge KG, Feavers IM, Neal KR, et al. (2011) Influence of the combination and phase variation status of the haemoglobin receptors HmbR and HpuAB on meningococcal virulence. Microbiology (Reading, Engl) 157: 1446–1456. doi:10.1099/mic.0.046946-0.

111. Stojiljkovic I, Srinivasan N (1997) Neisseria meningitidis tonB, exbB, and exbD genes: Ton-dependent utilization of protein-bound iron in Neisseriae. J Bacteriol 179: 805–812.

112. Mao F, Dam P, Chou J, Olman V, Xu Y (2008) DOOR: a database for prokaryotic operons. Nucleic Acids Res 37: D459–D463. doi:10.1093/nar/gkn757.

113. Fantappiè L, Oriente F, Muzzi A, Serruto D, Scarlato V, et al. (2011) A novel Hfq-dependent sRNA that is under FNR control and is synthesized in oxygen limitation in Neisseria meningitidis. Mol Microbiol 80: 507–523. doi:10.1111/j.1365-2958.2011.07592.x.

114. Ieva R, Alaimo C, Delany I, Spohn G, Rappuoli R, et al. (2005) CrgA is an inducible LysR-type regulator of Neisseria meningitidis, acting both as a repressor and as an activator of gene transcription. J Bacteriol 187: 3421–3430. doi:10.1128/JB.187.10.3421-3430.2005.

6. Supplementary Tables

Table S1. Small intergenic RNAs identified in this study.

strand	upstream ORF	downstream ORF	start	end	length (nt)	orientation*	M value (log2 cy5/cy3) t0	t30	t60	t90
F	NMB0006	NMB0007	4113	4254	141	>>>	-0,17	0,90	1,09	1,05
F	NMB0011	NMB0012	9157	9348	191	<<<	0,25	0,48	1,14	1,25
R	NMB0011	NMB0012	9003	9284	281	<><	-0,18	-0,90	-1,02	-1,22
R	NMB0017	NMB0018	16949	17128	179	<<<	-0,01	-0,69	-0,72	-0,97
F	NMB0018	NMB0019	18150	18210	60	<><	0,31	0,76	1,60	1,63
F	NMB0020	NMB0021	19740	19800	60	<><	0,08	-0,93	-0,97	-0,81
R	NMB0035	NMB0036	34587	34721	134	>><	0,20	-0,16	-0,28	-0,17
R	NMB0087	NMB0088	99660	99720	60	>><	0,09	0,39	0,23	0,43
R	NMB0088	NMB0089	101330	101390	60	<<<	0,09	-0,45	-1,55	-1,58
R	NMB0104	NMB0105	113082	113258	176	<<<	0,15	-0,10	-0,50	-0,78
F	NMB0135	NMB0136	146330	146390	60	>>>	-0,26	0,83	0,87	0,14
F	NMB0141	NMB0142	151660	151720	60	>>>	-0,07	0,08	0,94	0,81
F	NMB0177	NMB0178	175230	175290	60	<><	-0,14	0,18	0,57	0,40
R	NMB0188	NMB0189	187080	187142	62	<<>	0,34	0,63	0,84	0,54
R	NMB0191	NMB0192	190000	190060	60	>><	-0,10	-0,67	-1,49	-1,75
F	NMB0200	NMB0201	203540	203600	60	<>>	0,36	-1,43	-1,88	-1,16
R	NMB0216	NMB0217	223188	223322	134	<<>	0,09	-0,64	-0,74	-0,74
F	NMB0277	NMB0278	281400	281460	60	<>>	0,31	-1,96	-1,93	-1,93
F	NMB0279	NMB0280	283240	283300	60	<>>	0,14	-1,90	-2,24	-1,71
R	NMB0281	NMB0282	286890	287025	135	>><	0,01	-1,67	-1,54	-1,64
R	NMB0282	NMB0283	290250	290310	60	<<>	-0,48	-1,15	-1,26	-1,69
F	NMB0308	NMB0309	318029	318247	218	>><	0,03	0,81	0,99	0,96
F	NMB0310	NMB0311	319310	319370	60	<>>	-0,19	-1,79	-2,45	-1,35
R	NMB0310	NMB0311	319290	319475	185	<<>	-0,04	-0,79	-1,21	-1,10
F	NMB0311	NMB0312	319936	320319	383	>>>	0,03	-1,41	-1,72	-1,63
F	NMB0311	NMB0312	320379	320836	457	>>>	-0,07	-1,24	-1,56	-1,57
F	NMB0317	NMB0318	329520	329580	60	<>>	-0,04	-0,01	0,96	0,76
R	NMB0322	NMB0323	333005	333134	129	>><	0,02	1,33	0,61	0,82
F	NMB0336	NMB0337	346184	346316	132	>><	0,04	-0,10	-0,47	-0,75
F	NMB0349	NMB0350	358054	358210	156	<><	-0,08	-0,81	-1,23	-1,19
R	NMB0356	NMB0357	363787	363975	188	>><	-0,14	-1,18	-1,65	-1,31
F	NMB0358	NMB0359	365870	365930	60	<>>	-0,01	0,80	1,00	1,17
R	NMB0361	NMB0362	369091	369207	116	>><	0,20	1,20	1,30	1,80
R	NMB0362	NMB0363	369308	369428	120	>><	0,30	1,50	2,50	2,40
F	NMB0422	NMB0423	432470	432530	60	>>>	-0,34	-0,64	-0,86	-0,69
F	NMB0433	NMB0434	446346	446570	224	>>>	0,05	0,68	0,98	1,23
R	NMB0435	NMB0436	449856	449985	129	>><	0,04	-1,62	-1,96	-1,96
R	NMB0442	NMB0443	455706	455835	129	<<>	0,26	-0,12	-0,27	-0,27
F	NMB0449	NMB0450	463710	463770	60	>>>	0,34	1,03	1,04	0,99
R	NMB0457	NMB0458	470110	470233	123	<<>	-0,01	-0,40	-0,43	-0,61
R	NMB0458	NMB0459	471924	472058	134	>><	0,07	0,82	1,13	0,91
F	NMB0466	NMB0467	487580	487640	60	>>>	-0,23	0,27	-1,10	-1,07
F	NMB0467	NMB0468	488016	488150	134	>>>	-0,01	0,08	-1,07	-1,11
F	NMB0479	NMB0480	501331	501390	59	>><	-0,11	-1,16	-1,75	-1,70
R	NMB0479	NMB0480	501330	501390	60	>><	0,22	1,48	1,92	2,23
F	NMB0505	NMB0506	533587	533716	129	<>>	0,12	-0,41	-0,34	-0,29
F	NMB0517	NMB0518	542330	542390	60	<>>	-0,06	-2,07	-2,43	-2,30
R	NMB0529	NMB0530	549181	549396	215	>><	-0,02	-1,18	-1,61	-1,43
R	NMB0534	NMB0535	555664	555891	227	<<>	0,05	0,13	1,35	1,51
R	NMB0538	NMB0539	560368	560491	123	<<>	-0,20	-1,43	-1,50	-1,96
R	NMB0543	NMB0544	565820	565880	60	<<<	0,27	1,41	0,74	0,73
R	NMB0544	NMB0545	566680	566803	123	<<>	0,04	0,74	0,76	0,67
R	NMB0546	NMB0547	571620	571782	162	<<<	-0,05	-0,78	-1,10	-1,12
R	NMB0560	NMB0561	589740	589800	60	<<>	-0,07	-1,27	-1,22	-1,15
R	NMB0573	NMB0574	601776	601908	132	<<>	0,49	1,15	1,91	1,62
F	NMB0582	NMB0583	611777	611971	194	<><	0,07	2,27	1,68	1,66
F	NMB0618	NMB0619	651510	651632	122	<>>	0,26	0,03	0,85	0,89
F	NMB0642	NMB0643	675510	675570	60	<>>	0,42	-1,93	-1,98	-1,95
R	NMB0659	NMB0660	686839	686962	123	>><	0,16	-1,63	-2,32	-1,86
F	NMB0671	NMB0672	700670	700730	60	>>>	-0,22	-0,57	-1,00	-1,15
F	NMB0677	NMB0678	704960	705020	60	>>>	0,25	-2,01	-1,87	-2,10
R	NMB0690	NMB0691	717730	717790	60	<<<	0,13	-2,19	-2,98	-2,70
F	NMB0711	NMB0712	743145	743274	129	<><	0,10	-0,94	-1,35	-1,05
F	NMB0711	NMB0712	742906	743023	117	<><	0,02	-0,52	-0,58	-0,55
F	NMB0717	NMB0718	748425	748494	69	<><	0,29	0,30	0,73	0,79
F	NMB0717	NMB0718	748290	748350	60	<><	0,24	1,51	1,36	0,82
F	NMB0719	NMB0720	750771	750962	191	<>>	0,15	-0,66	-0,83	-0,55
F	NMB0757	NMB0758	785559	785672	113	>>>	-0,08	-0,56	-1,18	-1,24
R	NMB0763	NMB0764	791929	792031	102	>><	-0,15	-1,63	-2,09	-2,01
F	NMB0869	NMB0870	889115	889502	387	<>>	0,02	-1,10	-0,83	-0,78
R	NMB0869	NMB0870	889450	889510	60	<<>	-0,03	0,37	0,64	0,75
R	NMB0881	NMB0882	902970	903109	139	<<>	0,27	-0,92	-0,89	-0,94
F	NMB0895	NMB0896	915993	916242	249	>>>	0,10	-1,47	-0,77	-0,71
F	NMB0898	NMB0899	918161	918352	191	>>>	-0,18	0,20	0,88	1,14
F	NMB0899	NMB0900	919085	919402	317	>>>	0,00	-1,11	-0,40	-0,19
F	NMB0899	NMB0900	919501	919624	123	>>>	-0,23	-0,48	1,01	1,38
R	NMB0899	NMB0900	919496	919625	129	>>>	0,31	0,65	1,24	1,06
R	NMB0908	NMB0909	923710	923770	60	<<<	0,04	1,87	1,32	1,55
F	NMB0910	NMB0911	925161	925436	275	<><	0,04	1,72	2,64	2,80
R	NMB0916	NMB0917	928848	928973	125	<<<	0,06	-1,03	-1,25	-1,32
R	NMB0936	NMB0937	951587	951776	189	<<>	0,13	1,26	0,76	0,96
R	NMB0940	NMB0941	955480	955540	60	<<<	-0,15	3,26	3,02	2,52
R	NMB0940	NMB0941	955111	955419	308	<<<	0,11	3,08	2,02	1,19
F	NMB0947	NMB0948	962260	962320	60	>>>	0,04	2,15	1,00	1,14
R	NMB0960	NMB0961	976396	976626	230	>><	-0,01	-0,68	-0,87	-0,79
R	NMB0963	NMB0964	983050	983110	60	>><	0,28	1,04	0,83	0,50
R	NMB0977	NMB0978	992200	992260	60	>><	0,41	-1,51	-1,57	-1,19
R	NMB0983	NMB0984	1000201	1000399	198	>>>	0,04	1,25	1,43	1,45
R	NMB0992	NMB0993	1008987	1009092	105	<<<	-0,01	-0,98	-0,84	-0,99
R	NMB0992	NMB0993	1008042	1008189	147	<<<	-0,02	-1,15	-0,96	-0,99
R	NMB0997	NMB0998	1014444	1014597	153	<<>	-0,03	-0,90	-0,86	-0,78
R	NMB0997	NMB0998	1014710	1014770	60	<<>	0,08	0,58	1,27	1,63

R	NMB0999	NMB1000	1020175	1020366	191	><	0,05	0,15	1,26	1,22
R	NMB1000	NMB1001	1021831	1022632	801	><	0,06	0,50	1,88	1,49
F	NMB1015	NMB1016	1030821	1031138	317	><	0,52	1,42	1,59	1,52
R	NMB1015	NMB1016	1030660	1030720	60	><	0,15	-2,03	-1,00	-1,11
R	NMB1015	NMB1016	1030453	1030564	111	>>	-0,01	-0,26	1,05	1,24
R	NMB1015	NMB1016	1030815	1031183	368	><	-0,16	0,39	1,49	1,61
R	NMB1016	NMB1017	1031943	1032120	177	<<	0,08	-2,77	-3,36	-3,16
R	NMB1043	NMB1044	1060210	1060270	60	><	0,17	-0,72	-1,53	-0,45
F	NMB1047	NMB1048	1064293	1064434	141	<>	0,18	0,62	1,43	1,74
R	NMB1058	NMB1059	1078360	1078420	60	<<	-0,12	-0,92	-1,17	-1,28
F	NMB1059	NMB1060	1078781	1078859	78	><	0,06	1,79	1,08	0,70
F	NMB1107	NMB1108	1121680	1121740	60	<>	-0,01	1,18	1,96	2,20
F	NMB1199	NMB1200	1201515	1201760	245	><	0,06	1,19	0,07	0,21
R	NMB1199	NMB1200	1201770	1201830	60	>>	0,27	-1,94	-2,51	-2,77
F	NMB1244	NMB1245	1251892	1252032	140	<>	0,25	-0,42	-0,58	-0,71
R	NMB1252	NMB1253	1259960	1260406	446	<<	-0,13	-1,56	-2,31	-2,31
R	NMB1252	NMB1253	1260448	1260571	123	<<	0,38	0,58	1,40	1,34
R	NMB1258	NMB1259	1267151	1267368	217	<<	-0,03	-1,03	-0,41	-0,45
F	NMB1277	NMB1278	1289981	1290076	95	<>	0,00	1,07	1,89	1,98
R	NMB1287	NMB1288	1303250	1303310	60	<<	-0,22	-0,82	-1,68	-1,67
F	NMB1298	NMB1299	1315650	1315710	60	>>	0,12	1,18	1,21	0,98
F	NMB1299	NMB1300	1317500	1317683	183	>>	-0,17	-0,99	-1,00	-0,90
R	NMB1300	NMB1301	1318422	1318556	134	><	0,09	1,08	0,82	0,26
R	NMB1363	NMB1364	1388704	1388852	148	<<	0,02	-1,05	-0,79	-0,80
R	NMB1367	NMB1368	1392028	1392214	186	<<	0,26	-0,71	-0,58	-0,41
F	NMB1368	NMB1369	1393725	1393982	257	><	-0,14	-2,27	-2,09	-2,19
R	NMB1370	NMB1371	1395472	1395598	126	<<	-0,22	-1,86	-1,82	-1,80
R	NMB1393	NMB1394	1423372	1423492	120	><	-0,01	0,85	1,17	1,02
F	NMB1417	NMB1418	1453240	1453300	60	<>	0,84	1,57	1,28	1,48
R	NMB1417	NMB1418	1452998	1453240	242	<<	0,02	0,22	1,27	1,95
F	NMB1422	NMB1423	1458540	1458600	60	>>	0,37	0,85	1,45	1,28
R	NMB1444	NMB1445	1487853	1488054	201	><	-0,07	-1,15	-1,13	-1,07
F	NMB1451	NMB1452	1499955	1500202	247	<>	0,20	-2,18	-2,55	-2,07
R	NMB1464	NMB1465	1513580	1513640	60	<<	0,18	-1,83	-2,88	-1,72
F	NMB1496	NMB1497	1542789	1543026	237	>>	0,02	-0,55	-0,79	-0,72
R	NMB1502	NMB1503	1552395	1552643	248	><	-0,03	0,91	1,00	0,95
R	NMB1522	NMB1523	1571849	1572035	186	<<	0,21	0,36	1,20	1,17
R	NMB1538	NMB1539	1591830	1591890	60	><	0,69	1,48	1,45	1,53
R	NMB1539	NMB1540	1593004	1593121	117	><	-0,14	-1,31	-1,55	-1,41
R	NMB1556	NMB1557	1616880	1616940	60	<<	0,25	-1,24	-2,17	-2,38
F	NMB1558	NMB1559	1618341	1618466	125	<>	0,26	0,79	0,88	0,88
F	NMB1563	NMB1564	1624310	1624370	60	<>	0,40	2,79	3,63	3,93
F	NMB1574	NMB1575	1636960	1637020	60	<>	-0,54	-1,14	-1,35	-1,21
F	NMB1577	NMB1578	1640560	1640620	60	<<	0,14	0,62	1,43	1,86
R	NMB1577	NMB1578	1639738	1640103	365	<<	0,22	-2,87	-3,20	-3,20
R	NMB1577	NMB1578	1640340	1640400	60	<<	-0,14	-1,13	-1,58	-1,85
R	NMB1608	NMB1609	1670547	1670816	269	><	-0,12	-1,10	-0,97	-0,93
R	NMB1608	NMB1609	1670882	1671199	317	><	-0,01	-1,06	-1,22	-1,23
R	NMB1609	NMB1610	1672896	1673022	126	<<	0,06	1,04	0,48	0,31
R	NMB1636	NMB1637	1701109	1701229	120	><	-0,22	0,32	-0,79	-0,97
R	NMB1649	NMB1650	1717367	1717597	230	<<	0,02	1,01	1,48	1,64
F	NMB1650	NMB1651	1718370	1718430	60	<>	-0,16	-2,82	-3,00	-2,99
R	NMB1711	NMB1712	1788650	1788710	60	<<	-0,17	-1,80	-2,15	-2,11
R	NMB1716	NMB1717	1796669	1796872	203	<<	0,22	-0,94	-0,60	-0,24
R	NMB1727	NMB1728	1811450	1811510	60	><	-0,18	1,38	0,98	0,96
F	NMB1730	NMB1731	1813746	1813923	177	<>	-0,08	1,36	1,51	1,48
R	NMB1734	NMB1735	1817490	1817550	60	<<	0,42	1,20	1,84	1,78
F	NMB1750	NMB1751	1832600	1832660	60	><	-0,06	0,80	1,24	1,70
F	NMB1782	NMB1783	1870550	1870610	60	<>	0,22	-1,03	-1,51	-0,80
F	NMB1787	NMB1788	1875368	1875774	406	><	-0,15	-1,14	-1,74	-1,71
F	NMB1787	NMB1788	1875894	1876023	129	><	0,01	-0,90	-1,28	-1,30
F	NMB1814	NMB1815	1907355	1907486	131	>>	-0,09	-1,49	-2,33	-2,29
F	NMB1826	NMB1827	1919790	1919850	60	<>	-0,08	-1,25	-1,95	-1,68
R	NMB1827	NMB1828	1923600	1923660	60	><	0,11	-0,86	-0,80	-0,76
F	NMB1846	NMB1847	1946990	1947050	60	>>	0,13	0,17	-0,60	-0,60
F	NMB1847	NMB1848	1951192	1951455	263	><	0,04	-0,98	-1,19	-0,99
R	NMB1847	NMB1848	1951327	1951530	203	><	-0,08	-1,12	-1,08	-1,07
F	NMB1848	NMB1849	1952402	1952528	126	<>	0,11	-0,75	-1,08	-1,19
F	NMB1863	NMB1864	1967260	1967320	60	><	-0,12	-0,25	-0,71	-0,58
R	NMB1870	NMB1871	1976226	1976354	128	><	0,23	0,80	1,01	1,26
F	NMB1880	NMB1881	1985319	1985565	246	>>	0,02	1,25	2,01	2,12
F	NMB1888	NMB1889	1991863	1991998	135	>>	0,16	-1,59	-2,05	-2,04
F	NMB1902	NMB1903	2004160	2004220	60	<>	0,11	0,56	0,47	0,38
R	NMB1903	NMB1904	2005995	2006187	192	<<	0,34	0,55	0,93	0,99
F	NMB1915	NMB1916	2013842	2013977	135	>>	0,19	-0,37	-0,72	-0,93
R	NMB1923	NMB1924	2021857	2021980	123	><	0,61	0,86	1,13	1,35
F	NMB1932	NMB1933	2031320	2031380	60	<>	0,64	0,57	1,25	0,96
R	NMB1948	NMB1949	2043524	2043659	135	<<	-0,02	0,01	0,68	1,07
R	NMB1969	NMB1970	2065478	2065604	126	><	0,21	1,33	2,08	1,95
F	NMB1982	NMB1983	2082220	2082280	60	>>	0,05	-0,40	-0,92	-0,46
F	NMB1982	NMB1983	2082428	2082653	225	>>	0,28	1,13	1,96	1,82
R	NMB1987	NMB1988	2092400	2092460	60	><	-0,17	0,39	0,72	0,95
F	NMB2035	NMB2036	2153336	2153461	125	>>	0,07	-0,27	-1,32	-1,46
F	NMB2035	NMB2036	2153697	2154125	428	>>	0,00	-0,77	-0,71	-0,58
R	NMB2035	NMB2036	2153270	2153330	60	><	0,38	0,40	0,52	0,57
F	NMB2038	NMB2039	2157340	2157400	60	>>	0,00	-1,65	-1,71	-1,64
F	NMB2039	NMB2040	2159193	2159320	127	><	0,03	-1,15	-1,11	-1,04
F	NMB2039	NMB2040	2158562	2158756	194	><	0,04	-1,33	-0,67	-0,96
F	NMB2040	NMB2041	2161880	2162083	203	<>	-0,02	-0,60	-0,87	-0,96
R	NMB2040	NMB2041	2161581	2161794	213	<<	0,26	0,86	2,01	2,71
F	NMB2050	NMB2051	2173480	2173599	119	<>	0,13	0,43	0,83	0,92
F	NMB2057	NMB2058	2179474	2179606	132	<>	0,29	0,69	0,99	1,33
F	NMB2062	NMB2063	2185395	2185523	128	><	0,52	2,63	2,91	2,02
F	NMB2073	NMB2074	2195848	2196018	170	><	0,62	4,06	3,95	3,02

R	NMB2076	NMB2077	2199720	2199780	60	<<>	0,04	-3,03	-2,54	-2,23
R	NMB2076	NMB2077	2199220	2199280	60	<<>	-0,12	-2,49	-2,46	-2,59
F	NMB2078	NMB2079	2201328	2201474	146	<>>	0,16	-1,63	-1,84	-1,84
F	NMB2086	NMB2087	2209246	2209372	126	<><	0,00	-0,18	-0,63	-0,82
R	NMB2102	NMB2103	2220580	2220640	60	><>	-0,06	-0,60	-0,43	-0,33
R	NMB2132	NMB2133	2239950	2240133	183	<<<	-0,16	1,88	0,83	0,70
F	NMB2133	NMB2134	2241677	2241889	212	<>>	-0,07	0,62	1,22	1,35
R	NMB2145	NMB2146	2257640	2257700	60	><>	0,13	0,21	1,27	1,53

* the orientation refers to upstream gene, small RNA and upstream gene in this order:
> for forward strand
< for reverse strand

Table S2. Antisense RNAs identified in this study

						antisense RNA				mRNA			
						M value (log2 cy5/cy3)				M value (log2 cy5/cy3)			
strand	gene	annotation/function	start	end	length (nt)	t0	t30	t60	t90	t0	t30	t60	t90
1) Down reg. asRNA - Down reg. mRNA													
R	NMB0210		212011	212262	251	-0,24	-1,21	-1,43	-1,49	-0,09	-1,33	-0,99	-1,08
F	NMB0211		212612	213377	765	0,12	-1,24	-1,64	-1,66	-0,13	-1,07	-1,30	-1,11
R	NMB0416	UDPRMurNAcRpentapeptide synthetase	425778	426152	374	-0,02	-1,03	-1,08	-0,54	0,07	-0,73	-0,83	-0,93
F	NMB0489	hypothetical protein	505268	506045	777 *	0,10	-0,54	-1,04	-0,70	0,14	-1,19	-1,43	-1,57
R	NMB0518		542558	542753	195	0,05	-1,58	-0,11	-0,34	0,23	-0,88	0,48	0,42
R	NMB0549	ABC transporter, ATPRbinding protein	573735	574614	879	-0,06	-1,50	-1,76	-1,62	-0,12	0,62	-0,24	-1,37
R	NMB0686		711694	711963	269	0,20	-0,71	-0,95	-1,03	-0,04	-0,86	-1,18	-1,49
R	NMB0743	ubiquinone/menaquinone methyltransferase	776380	776691	311	-0,50	-0,90	-1,14	-0,81	0,14	-0,12	-1,08	-1,00
R	NMB0763	cysteine synthase	790861	791638	777	-0,32	-0,66	-1,43	-1,61	-0,36	-1,86	-2,12	-1,47
F	NMB0765		793122	793423	301	-0,20	-0,47	-0,95	-0,76	-0,21	-0,38	-0,91	-0,61
R	NMB0787	amino acid ABC transporter,	815465	816093	628	-0,30	-1,30	-1,22	0,07	0,13	-2,09	-2,57	-2,78
F	NMB0791		818421	821805	3384 *	-0,15	-1,79	-1,89	-1,92	-0,11	0,10	-0,34	-0,68
F	NMB0794	hypothetical protein	821842	823661	1819 *	-0,15	-1,79	-1,29	-1,13	-0,01	0,43	-0,44	-0,75
F	NMB0846		873200	873971	771	0,00	-1,00	-1,15	-0,77	-0,12	-1,40	-1,84	-1,84
F	NMB0880	sulfate ABC transporter, permease protein	901403	901857	454	0,00	-0,73	-1,29	-0,71	-0,04	-2,08	-1,97	-2,82
F	NMB0881		902256	903037	781	-0,53	-1,80	-1,29	-1,32	-0,11	-2,30	-2,21	-2,82
F	NMB1023	hypothetical protein	1038648	1039069	421	0,18	-1,15	-1,22	-1,38	0,04	0,18	-0,58	-0,69
F	NMB1260		1268749	1270358	1609	-0,13	-2,24	-2,02	-1,87	0,24	-0,48	-1,03	-1,06
F	NMB1279		1292447	1293034	587	0,14	-0,55	-0,93	-0,80	0,26	-0,92	-1,31	-1,31
R	NMB1317		1335841	1338075	2234 *	0,00	-0,82	-1,18	-1,16	-0,04	-0,71	-1,49	-0,96
R	NMB1352		1375165	1375685	520	0,00	-1,87	-1,81	-1,62	-0,07	-0,23	-0,59	-0,91
F	NMB1488		1536578	1536970	392	-0,14	-1,12	-1,19	-1,14	0,11	-1,26	-0,61	-0,25
F	NMB1622		1685233	1686229	996	0,30	0,00	-1,39	0,00	0,24	-0,90	-0,79	-0,68
R	NMB1658		1731155	1732104	949	0,21	-0,64	-1,11	-1,03	-0,17	-1,26	-1,13	-0,89
F	NMB1694		1772920	1774461	1541	0,19	-1,21	-1,61	-1,66	-0,10	-0,68	-0,58	-0,57
R	NMB1719		1798253	1798875	622	-0,29	-1,72	-1,19	-1,00	0,03	-1,32	-1,29	-1,16
R	NMB1857		1961079	1961277	198	-0,01	-0,30	-0,43	-0,98	0,07	-1,23	-1,27	-1,31
R	NMB1862	ribosomal protein L11 methyltransferase	1965657	1966096	439	0,14	-0,72	-0,99	-0,71	0,03	-1,14	-1,53	-1,38
R	NMB1920	GMP synthase	2019777	2020564	787 *	0,20	-0,86	-0,93	-0,78	-0,04	0,16	-0,62	-1,38
R	NMB1921	3RketoacylR(acylRcarrierRprotein) reductase	2019777	2020564	787 *	0,20	-0,86	-0,93	-0,78	0,06	0,50	-0,37	-1,38
R	NMB1923		2021447	2021824	377	-0,12	-2,05	-2,16	-2,00	0,07	-0,88	-2,19	-1,89
F	NMB2153	hypothetical protein	2263166	2263477	311	-0,40	-0,78	-0,93	-0,81	-0,01	-0,14	-0,81	-1,14
2) Up reg. asRNA - Up reg. mRNA													
R	NMB0060		69243	70114	871	0,04	1,75	0,99	0,00	-0,13	1,23	2,59	1,75
R	NMB0084		95667	96582	915	0,03	0,54	0,93	1,16	0,20	0,82	1,34	1,61
R	NMB0085		97335	98026	691	-0,23	0,90	0,95	0,74	0,25	1,53	1,34	1,61
F	NMB0175		171319	171809	490	0,10	0,77	1,09	1,06	0,22	2,30	2,42	2,32
F	NMB0176	DRamino acid dehydrogenase small subunit	172293	173637	1344	0,28	0,77	1,16	1,16	0,05	0,78	2,42	2,32
F	NMB0177	putative sodium/alanine symporter	173710	174194	484	-0,01	0,55	1,16	0,89	0,09	0,78	2,42	2,32
F	NMB0194		193537	194086	549	0,14	0,95	1,11	0,83	0,00	1,55	1,88	2,67
R	NMB0294		303831	304563	732	0,10	1,49	1,42	0,89	0,06	1,01	1,23	0,62
R	NMB0359		366518	367436	918	0,01	1,43	1,45	1,00	0,11	1,17	1,50	0,85
R	NMB0432	hypothetical protein	442691	443421	730	-0,32	0,80	1,37	1,15	0,16	0,87	1,46	1,28
R	NMB0535		556577	557256	679	-0,14	1,28	1,35	0,95	0,24	1,42	2,07	2,49
F	NMB0593	hypothetical protein	623188	624374	1186	0,00	0,85	0,95	0,90	0,30	0,94	0,45	0,13
F	NMB0596	hypothetical protein	627861	629672	1811	0,00	0,72	1,46	1,35	-0,02	1,08	0,36	0,20
F	NMB0604		633370	634565	1195	0,00	1,17	1,17	0,79	-0,06	1,57	1,57	2,07
F	NMB0906	hypothetical protein	922455	922960	505 *	0,03	0,79	1,05	0,98	-0,44	0,84	1,51	1,22
F	NMB0907	hypothetical protein	922455	922960	505 *	0,18	0,79	1,05	0,98	0,15	0,84	1,51	1,22
R	NMB0943		956262	957174	912	0,00	0,31	1,01	0,60	-0,13	0,90	0,41	0,12
R	NMB0949	succinate dehydrogenase	962464	963021	557	-0,31	0,59	0,96	0,86	-0,10	0,70	1,15	1,32
R	NMB0954	type II citrate synthase	966338	967074	736	-0,17	1,25	1,46	1,25	-0,29	1,46	2,05	2,37
F	NMB0964		985082	985566	484	0,87	0,91	0,95	1,40	-0,05	3,06	2,68	1,68
R	NMB1063	dihydroneopterin aldolase	1081825	1082196	371 *	0,45	0,50	1,13	1,20	0,24	1,00	1,82	1,67
R	NMB1064	hypothetical protein	1081825	1082196	371 *	0,45	0,50	1,13	1,20	0,00	1,00	1,82	1,67
F	NMB1377		1405038	1406085	1047	0,18	1,30	1,40	0,78	0,36	1,79	3,22	2,55
R	NMB1398		1427266	1427631	365	0,15	0,39	1,02	0,96	0,17	0,48	1,18	1,43
F	NMB1498		1547984	1549108	1124	-0,40	1,10	0,95	0,81	0,16	0,49	0,32	0,97
F	NMB1588	3Rphosphatidyltransferase	1650941	1651575	634	0,04	0,81	1,07	1,00	0,10	0,79	0,70	1,06
F	NMB1653		1720806	1721348	542	-0,47	0,77	0,79	0,74	0,17	1,01	1,14	1,20
F	NMB1709		1785258	1785815	557	0,50	0,90	1,06	0,85	0,04	0,90	0,57	0,46
F	NMB1729		1812316	1812762	446	-0,23	1,00	0,86	1,48	-0,04	2,00	2,19	2,18
F	NMB1730		1812963	1813651	688	0,01	0,90	0,88	0,75	-0,15	2,00	2,19	2,18
F	NMB1783		1871718	1872125	407 *	0,00	0,69	1,23	1,29	0,20	1,12	1,75	1,23
F	NMB1784		1871718	1872125	407 *	-0,06	0,69	1,23	1,29	0,10	1,12	1,75	1,23
F	NMB1796		1884457	1884993	536	0,00	0,95	1,16	1,30	0,14	1,41	2,15	1,91
R	NMB1988		2093318	2093749	431	0,20	0,56	0,77	0,85	0,50	1,90	2,07	2,10
R	NMB1988		2094168	2094718	550	0,20	0,68	0,77	0,87	0,20	1,40	1,50	1,70
F	NMB1995		2101506	2101883	377	0,00	2,07	2,07	1,91	0,09	1,79	2,25	3,11
R	NMB2003	hypothetical protein	2115399	2116063	664 *	0,14	0,80	1,35	1,34	0,15	-0,64	0,75	0,72

R	NMB2004	hypothetical protein	2115399	2116063	664 *	0,00	0,80	1,35	1,34	-0,11	-0,40	0,29	0,72
F	NMB2074	hypothetical protein	2196068	2196589	521	0,00	1,36	1,18	0,57	-0,01	0,16	0,78	0,95
R	NMB2089	hypothetical protein	2210829	2211313	484 *	-0,02	0,66	1,04	0,86	0,33	0,46	1,06	0,71
R	NMB2090	phosphoheptose isomerase	2210829	2211313	484 *	0,21	0,66	1,04	0,86	0,33	-0,14	1,06	0,71
3) Down reg. asRNA - Not reg. mRNA													
R	NMB0049		48208	48858	650	0,10	-0,77	-0,98	-1,02	-0,01	-0,30	-0,40	0,27
R	NMB0056		60032	60400	368	-0,24	-1,14	-1,12	-1,09	-0,13	0,23	-0,20	-0,46
F	NMB0068	polysialic acid capsule biosynthesis protein	77585	78033	448	0,00	-1,21	-1,41	-1,40	0,10	-0,23	-0,53	-0,50
R	NMB0097		105880	106622	742	0,10	-1,69	-1,24	-1,40	0,20	0,22	-0,32	-0,34
F	NMB0104		112667	112924	257	0,14	-1,04	-0,91	-0,85	0,10	-0,13	0,50	0,67
F	NMB0174		168413	169225	812	-0,45	-1,22	-1,10	-0,44	0,20	0,46	0,45	0,23
F	NMB0192	ribonuclease HII	190675	191204	529	0,07	-0,57	-1,29	-1,22	-0,06	0,55	-0,35	-0,41
R	NMB0199		202312	202755	443	0,07	-0,85	-0,95	-1,30	0,05	0,42	0,39	0,42
F	NMB0212		213489	214825	1336	-0,15	-1,24	-1,64	-1,51	0,20	-0,26	-0,31	-0,31
R	NMB0224		231736	233255	1519	0,00	-1,50	-1,67	-1,68	0,10	0,19	0,23	0,40
F	NMB0279		282928	283125	197	0,18	-0,28	-1,14	-1,23	0,19	0,21	0,22	0,07
F	NMB0282		289316	290374	1058	-0,10	-1,34	-1,22	-0,90	0,30	0,62	0,34	0,18
R	NMB0296	CcsARrelated protein	306404	307245	841	-0,10	-1,83	-1,56	-1,30	-0,12	0,21	0,19	0,15
F	NMB0387		389028	389805	777	0,22	-1,20	-0,97	-1,28	0,03	0,26	0,50	0,61
R	NMB0408		415876	416083	207	0,02	-1,00	-0,80	-0,40	0,20	0,22	-0,32	-0,34
R	NMB0454	hypothetical protein	467056	467673	617	0,45	-0,98	-1,55	-1,68	0,08	-0,12	-0,07	-0,03
R	NMB0455	hypothetical protein	467738	468292	554	0,60	-0,98	-1,55	-1,68	0,08	-0,03	-0,37	-0,25
F	NMB0488	hypothetical protein	505268	506045	777 *	-0,20	-0,61	-1,04	-1,44	-0,11	0,09	0,40	0,23
F	NMB0495		518393	519149	756	0,11	-0,98	-0,94	-1,18	0,06	-0,31	-0,67	0,20
F	NMB0537		559056	559723	667	-0,11	-0,33	-0,94	-0,61	0,12	0,30	0,22	0,15
R	NMB0539		560499	560984	485	-0,50	-0,90	-1,11	-0,97	0,03	0,33	0,05	-0,23
F	NMB0550		575978	576355	377	0,07	-0,70	-0,90	-0,76	-0,17	0,28	-0,15	-0,45
F	NMB0563		591316	592240	924 *	-0,15	-1,15	-1,09	-0,89	0,09	-0,40	-0,58	-0,23
F	NMB0564		591316	592240	924 *	-0,10	-1,15	-1,09	-0,89	-0,08	-0,11	-0,17	-0,27
F	NMB0620	phosphoglycolate phosphatase	652924	654334	1410 *	-0,10	-1,31	-1,22	-1,24	-0,08	0,33	0,63	0,64
F	NMB0621	hypothetical protein	652924	654334	1410 *	0,22	-1,31	-1,22	-1,24	-0,08	0,23	0,63	0,24
F	NMB0637	argininosuccinate lyase	670862	671508	646	0,00	-0,76	-1,01	-1,05	0,12	0,41	-0,31	-0,36
R	NMB0674	hypothetical protein	703097	703361	264 *	-0,29	-1,18	-1,21	-1,00	-0,24	-0,26	-0,23	-0,31
R	NMB0675	cytidylyltransferase	703097	703361	264 *	-0,04	-1,18	-1,21	-1,00	0,01	-0,21	-0,23	-0,31
R	NMB0681		707706	709453	1747 *	-0,10	-1,75	-2,10	-2,14	-0,08	0,61	0,38	0,41
R	NMB0682		707706	709453	1747 *	-0,05	-1,75	-2,10	-2,14	0,15	0,46	0,00	-0,15
R	NMB0704		736131	736795	664	0,00	-0,93	-1,37	-1,31	0,19	0,34	-0,04	0,21
R	NMB0715		746972	747331	359	0,00	-1,53	-1,82	0,00	0,00	0,47	0,50	0,47
R	NMB0751	integrase/recombinase XerD	782018	783020	1002 *	0,00	-1,59	-1,87	-1,98	0,22	0,13	0,14	0,29
R	NMB0764		792100	792884	784	0,00	-1,38	-1,76	-1,77	0,06	-0,32	-0,19	-0,12
F	NMB0795		821842	823661	1819 *	0,07	-1,79	-1,26	-1,13	-0,19	0,43	0,20	0,06
F	NMB0796	hypothetical protein	821842	823661	1819 *	0,00	-1,79	-1,26	-1,13	-0,12	0,67	0,20	-0,08
F	NMB0797	hypothetical protein	821842	823661	1819 *	0,00	-1,79	-1,26	-1,13	0,00	0,67	0,24	0,28
F	NMB0806	hypothetical protein	832597	833085	488	0,00	-1,51	-1,64	-1,42	-0,10	-0,20	-0,59	-0,36
F	NMB0807	inorganic polyphosphate/ATPRNAD kinase	833667	834310	643 *	0,20	-1,51	-1,26	-0,96	0,24	0,15	-0,45	-0,04
F	NMB0808	hypothetical protein	833667	834310	643 *	0,20	-1,26	-0,94	-0,46	0,01	-0,42	-0,45	-0,68
R	NMB0819		842899	843333	434	-0,15	-1,18	-1,09	-1,19	-0,20	-0,50	-0,04	-0,13
R	NMB0820		843448	844542	1094 *	0,13	-1,18	-1,23	-1,19	0,23	-0,43	-0,04	-0,13
R	NMB0821		843448	844542	1094 *	-0,06	-1,18	-1,23	-1,19	0,23	-0,43	-0,04	-0,32
R	NMB0831		855467	855605	138	0,25	-0,99	-1,50	-1,03	0,05	0,39	0,50	0,47
R	NMB0832	anticodon nuclease	856371	856943	572	0,07	-0,99	-1,01	-1,06	0,07	-0,35	-0,63	0,15
F	NMB0839		865720	866446	726	-0,15	-0,50	-1,54	-0,88	0,30	0,24	0,30	0,42
R	NMB0843		870405	870955	550	0,00	-0,94	-0,99	-1,15	0,03	-0,13	-0,22	-0,40
F	NMB0845		872470	872801	331	0,18	-0,71	-1,28	-1,14	-0,01	0,13	0,44	-0,02
R	NMB0867		886968	887474	506	-0,10	-1,68	-2,09	-2,03	0,09	0,35	0,21	0,24
F	NMB0877		897494	898354	860	-0,10	-0,97	-1,13	-0,85	0,23	0,32	0,18	0,04
F	NMB0884		904896	905622	726	0,22	-1,61	-1,68	-1,60	0,07	-0,29	-0,33	-0,28
F	NMB0917	deathRonRcuring protein	929076	929503	427	0,02	-1,60	-1,61	-2,26	0,01	0,30	0,57	0,64
R	NMB1049		1066151	1067075	924	0,45	-1,11	-1,31	-1,19	0,24	0,47	0,64	0,51
F	NMB1051	ABC transporter, ATPRbinding protein	1069027	1070174	1147	0,60	-1,55	-1,26	-1,14	0,29	0,25	0,35	0,23
R	NMB1091	hypothetical protein	1108308	1108739	431 *	-0,20	-1,90	-2,10	-2,26	0,00	0,30	0,14	0,37
R	NMB1096		1113183	1113811	628	0,11	-0,14	-1,70	-1,51	-0,01	0,13	0,44	-0,02
R	NMB1097		1114168	1115574	1406 *	-0,11	-2,05	-2,20	-2,00	0,34	-0,06	0,60	0,57
F	NMB1204		1210109	1210292	183	-0,50	-1,01	-1,17	-1,12	0,12	0,24	0,00	0,59
F	NMB1263		1274579	1275067	488	0,07	-0,69	-1,25	-0,56	0,05	0,39	0,50	0,47
R	NMB1278		1290187	1290845	658	-0,15	-1,50	-1,68	-1,53	0,20	0,11	-0,04	0,18
F	NMB1303		1321042	1321356	314	-0,07	-1,10	-1,65	-1,44	-0,09	0,24	0,47	0,50
F	NMB1312		1329117	1329864	747	-0,15	-0,53	-1,50	-1,21	0,10	0,16	-0,48	-0,61
R	NMB1318		1335841	1338075	2234 *	-0,20	-0,82	-1,18	-1,16	-0,01	0,13	-0,03	-0,38
R	NMB1319		1335841	1338075	2234 *	0,11	-0,82	-1,18	-1,16	0,01	-0,42	-0,45	-0,68
F	NMB1338	putative isomerase	1356366	1356830	464	-0,11	-0,25	-1,07	-1,66	0,12	0,27	0,00	0,01
F	NMB1346		1369151	1369642	491	-0,50	0,56	-1,02	0,61	0,29	0,25	0,35	0,23
R	NMB1351		1373710	1374970	1260	0,07	-1,46	-1,59	-1,45	0,26	-0,15	-0,09	-0,04
R	NMB1374	tRNA pseudouridine synthase B	1398738	1399714	976	-0,15	-1,04	-1,18	-1,08	-0,04	0,33	0,03	-0,37

F	NMB1399		1428095	1428642	547	-0,07	-1,23	-1,44	-1,19	0,19	0,25	0,47	0,46
R	NMB1432		1471364	1472575	1211	0,60	-1,33	-1,35	-1,52	0,03	0,63	-0,17	-0,19
F	NMB1440	hypothetical protein	1480751	1482112	1361 *	-0,20	-0,60	-1,25	-0,96	0,22	-0,41	-0,52	-0,50
F	NMB1445		1488514	1489836	1322	0,11	-0,60	-1,71	-1,37	0,10	0,00	-0,03	-0,16
R	NMB1446	3Rdehydroquinate dehydratase	1490481	1491426	945 *	-0,11	-0,28	-1,21	-1,01	0,00	0,16	-0,19	-0,04
R	NMB1447	ATPRdependent DNA helicase	1490481	1491426	945 *	-0,50	-0,28	-1,21	-1,01	0,07	0,16	-0,44	-0,48
F	NMB1451		1498390	1498896	506	0,07	-0,98	-1,00	-1,26	-0,03	-0,36	0,55	0,51
R	NMB1467		1516951	1517512	561	-0,15	-0,55	-0,80	-0,70	-0,03	0,15	-0,01	0,14
R	NMB1573		1634538	1635271	733	0,11	-1,12	-1,81	-1,57	0,09	0,68	0,33	0,19
R	NMB1585	MarR family transcriptional regulator	1647668	1648246	578	-0,03	-1,67	-2,09	-1,93	0,10	-0,24	-0,18	-0,11
R	NMB1586	hypothetical protein	1648300	1649024	724	0,00	-1,67	-2,09	-1,93	0,33	-0,08	-0,35	-0,33
F	NMB1594		1655541	1656142	601	-0,32	-0,78	-1,40	-1,34	0,07	0,43	0,32	0,45
F	NMB1637	hypothetical protein	1701249	1702568	1319 *	0,18	-1,37	-1,80	-1,77	0,00	-0,27	-0,35	-0,35
F	NMB1638	YhbX/YhjW/YijP/YjdB family protein	1701249	1702568	1319 *	-0,13	-1,37	-1,80	-1,77	0,32	0,33	0,06	-0,18
F	NMB1650		1717671	1718206	535	0,14	-2,41	-2,75	-2,59	0,00	0,38	0,34	-0,07
F	NMB1659		1732424	1733205	781	0,00	0,00	-1,41	-1,31	-0,03	0,15	-0,01	0,14
F	NMB1679	tRNA (uracilR5R)Rmethyltransferase	1754976	1755604	628	0,00	-1,32	-1,46	-1,54	-0,01	0,13	-0,03	-0,38
F	NMB1682	DNA topoisomerase IV subunit B	1758720	1759467	747	-0,14	0,00	-0,95	-1,10	-0,04	0,16	-0,20	-0,30
F	NMB1762	putative hemolysin activation protein HecB	1842088	1842934	846	0,30	-1,62	-1,45	-0,54	0,22	-0,41	-0,52	-0,50
F	NMB1768		1850535	1851504	969	0,21	-1,14	-1,22	-1,13	0,10	0,00	-0,03	-0,16
R	NMB1797		1886208	1886573	365	0,19	-1,07	-1,01	-0,79	0,00	0,16	-0,19	-0,04
F	NMB1828		1923683	1924706	1023	-0,25	-0,33	-1,10	-0,81	0,07	0,16	-0,44	-0,48
F	NMB1831		1927732	1928623	891	-0,30	-0,53	-1,02	-0,89	-0,03	-0,36	0,55	0,51
F	NMB1859		1962012	1962933	921	0,10	-1,28	-1,72	-1,81	-0,03	0,15	-0,01	0,14
F	NMB1864		1967863	1968832	969	-0,19	-0,73	-1,27	-1,50	0,09	0,68	0,33	0,19
R	NMB1912		2011497	2011808	311	-0,27	-0,51	-0,95	-1,01	-0,23	0,38	0,19	-0,15
R	NMB2079		2201719	2202443	724	-0,27	-0,30	-0,94	-1,08	0,00	0,22	0,25	0,25
F	NMB2087		2209485	2210287	802 *	-0,03	-0,41	-1,13	-1,55	0,28	-0,62	-0,53	-0,32
F	NMB2088		2209485	2210287	802 *	0,00	-0,41	-1,13	-1,55	0,22	-0,13	0,07	0,11
4) Up reg. asRNA - Not reg. mRNA													
R	NMB0082	capsule polysaccharide modification protein	92055	93324	1269	0,00	0,57	1,03	0,95	0,07	0,12	-0,07	-0,19
F	NMB0180	UDPR3RORglucosamine NRacyltransferase	176547	177276	729	0,16	0,64	1,02	0,97	0,03	0,59	-0,06	0,40
F	NMB0351		358888	360005	1117	0,09	0,59	1,15	1,17	0,06	0,09	0,33	0,27
F	NMB0403		411429	411677	248	-0,07	0,03	1,14	1,20	0,06	0,65	0,66	0,63
F	NMB0547		571717	572500	783	0,22	1,60	1,88	1,38	0,00	0,18	0,25	0,13
F	NMB0552		579211	580316	1105	0,02	1,74	1,89	1,85	0,09	0,27	0,15	0,05
F	NMB0597	hypothetical protein	629708	631895	2187 *	0,45	-0,07	1,03	1,35	-0,02	0,55	-0,24	-0,29
F	NMB0598	Maf/YceF/YhdE family protein	629708	631895	2187 *	0,60	0,15	1,03	1,35	0,13	0,55	0,17	0,21
F	NMB0599		629708	631895	2187 *	-0,20	0,15	1,03	1,35	0,07	0,16	-0,44	-0,48
F	NMB0605		635038	635638	600	0,11	0,51	1,05	1,07	0,17	0,00	0,04	0,19
F	NMB0664		690893	691207	314	-0,11	0,16	1,02	0,96	0,19	0,37	-0,44	-0,52
F	NMB0756		783541	784525	984	-0,50	2,63	1,53	1,89	-0,10	0,42	0,67	0,41
R	NMB0829	type I restriction enzyme EcoR124II M protein	852816	854061	1245	0,07	0,41	1,21	1,00	0,10	-0,13	-0,55	-0,25
R	nmb0841		867375	867626	251	-0,15	0,46	0,79	0,61	-0,03	0,15	-0,01	0,14
F	NMB1065	crcB protein	1083023	1084269	1246 *	-0,07	1,33	1,04	1,26	0,10	0,20	-0,25	-0,51
F	NMB1066	hypothetical protein	1083023	1084269	1246 *	0,00	1,33	1,04	1,26	-0,34	0,20	-0,25	-0,41
F	NMB1075	hypothetical protein	1097591	1098497	906	0,13	1,05	0,96	0,81	0,12	0,17	0,17	-0,04
R	NMB1297		1314470	1315394	924 *	0,00	0,58	1,31	1,34	-0,24	0,27	0,53	0,22
R	NMB1298		1314470	1315394	924 *	0,18	0,58	1,31	1,34	0,13	0,27	-0,63	-0,28
F	NMB1499		1549312	1549853	541	-0,13	1,10	0,98	0,69	0,28	-0,62	-0,53	-0,32
R	NMB1571	hypothetical protein	1631419	1631844	425	0,14	0,96	1,06	1,02	0,17	-0,49	-0,27	0,71
F	NMB1686		1763089	1764192	1103	0,00	0,78	1,23	1,37	0,08	0,04	0,16	0,48
R	NMB1704	betaR1,4Rglucosyltransferase	1780632	1781200	568	0,00	0,45	1,11	1,19	-0,13	0,50	-0,14	-0,31
R	NMB1808	pilM protein	1898928	1899825	897	-0,14	1,03	1,02	0,63	0,04	0,06	-0,02	0,58
R	NMB1994		2100720	2101470	750	0,30	0,98	0,76	1,05	0,07	0,12	-0,07	-0,19
R	NMB2114		2228318	2228530	212	0,21	1,09	1,08	0,55	0,00	-0,54	0,04	0,25
R	NMB2147	hypothetical protein	2257885	2258253	368	0,19	0,54	1,18	0,96	-0,04	0,26	0,21	0,00
5) Down reg. asRNA - Up reg. mRNA													
R	NMB0016		13855	14115	260	0,00	-1,98	-1,68	-1,81	0,40	0,71	1,40	1,28
R	NMB0032		30145	30477	332	-0,14	0,00	-1,61	-0,91	0,38	0,32	1,24	0,97
R	NMB0055		59254	59933	679	0,00	-1,18	-1,42	-1,67	0,33	0,23	0,84	0,30
F	NMB0216		221825	222187	362	0,00	0,00	-1,23	0,00	0,11	4,33	2,66	4,74
R	NMB0234		242067	242330	263	0,00	-1,66	-1,27	-0,15	-0,01	1,10	0,95	0,54
R	NMB0285		292845	293865	1020	0,00	-1,41	-1,54	-1,33	0,15	1,06	0,74	0,94
R	NMB0288		297672	297956	284	0,27	-1,15	-1,52	-1,45	0,10	0,70	0,81	0,63
F	NMB0357	biosynthetic peptidoglycan transglycosylase	364125	364507	382	0,00	-1,20	-1,31	-1,46	0,24	0,57	0,81	0,78
F	NMB0358	shikimate dehydrogenase	364616	365163	547	0,00	-0,96	-1,56	-1,46	0,24	0,57	0,81	0,78
F	NMB0381		384354	384958	604	0,15	-1,02	-1,66	-1,61	0,06	-0,21	0,00	0,72
F	NMB0392		396893	397730	837	-0,50	-0,87	-1,03	-0,88	0,01	1,10	1,31	0,92
F	NMB0393		397765	398076	311	0,20	-0,87	-1,03	-0,88	0,01	1,10	1,31	0,92
F	NMB0394		399234	399485	251	-0,14	-1,10	-1,26	-0,50	0,18	1,10	1,31	1,31
F	NMB0401		405787	409660	3873	-0,14	-1,12	-1,64	-1,67	0,04	1,12	1,50	1,06
R	NMB0430	2Rmethylisocitrate lyase	440814	442421	1607 *	0,15	-1,60	-1,28	-1,21	0,05	1,81	3,32	3,57
R	NMB0431	methylcitrate synthase	440814	442421	1607 *	-0,30	-1,59	-1,28	-1,21	0,16	1,81	3,32	3,57

R	NMB0436		450074	450621	547	0,02	-1,28	-1,70	-1,37	0,00	0,42	0,62	0,77
R	NMB0441		453965	454829	864	0,30	-1,14	-1,73	-1,98	0,16	0,57	0,73	1,02
R	NMB0468		489760	491166	1406 *	-0,20	-1,16	-1,37	-1,29	0,00	0,74	0,57	0,56
R	NMB0469		489760	491166	1406 *	-0,35	-1,16	-1,37	-1,29	0,36	0,74	0,71	0,64
R	NMB0514	hypothetical protein	540558	540821	263 *	0,02	-1,42	-1,47	-1,07	0,12	0,34	0,82	0,96
R	NMB0515	hypothetical protein	540558	540821	263 *	0,02	-1,42	-1,47	0,00	-0,04	0,34	0,82	0,96
R	NMB0516	hypothetical protein	541195	541838	643	-0,18	-1,42	-1,47	0,00	-0,04	0,06	0,82	0,46
F	NMB0524		545257	545822	565	-0,50	-0,87	-0,99	-0,88	0,40	0,50	0,65	0,85
R	NMB0545		567446	569100	1654	-0,07	0,00	-1,30	0,00	0,04	0,77	0,83	0,30
F	NMB0560		589343	589650	307	0,00	-1,06	-1,17	-0,68	0,14	0,34	0,87	0,92
F	NMB0626		659205	660060	855	0,00	-0,64	-1,16	-1,40	0,24	0,71	0,10	0,24
F	NMB0689		715425	715879	454	-0,10	-0,69	-0,60	-0,67	0,13	2,01	1,81	1,34
R	NMB0698		724056	725088	1032 *	0,22	-0,42	-0,95	-1,32	-0,19	-0,15	0,88	0,98
R	NMB0699		724056	725088	1032 *	0,22	-0,42	-0,95	-1,32	0,16	0,76	0,88	0,98
R	NMB0716		747459	747761	302	-0,07	0,00	-1,13	-1,23	0,16	0,35	0,96	1,24
R	NMB0752		782018	783020	1002 *	-0,05	-1,59	-1,87	-1,98	0,10	1,73	2,98	2,75
R	NMB0753	hypothetical protein	782018	783020	1002 *	0,02	-1,59	-1,87	0,00	0,10	1,19	1,14	1,24
F	NMB0790		818421	821805	3384 *	-0,50	-1,79	-1,89	-1,92	-0,20	1,09	0,32	0,34
F	NMB0792	NadC family protein	818421	821805	3384 *	0,07	-1,79	-1,89	-1,92	0,08	0,98	1,30	1,08
F	NMB0793	hypothetical protein	818421	821805	3384 *	-0,15	-1,79	-1,89	-1,92	0,08	0,65	1,30	0,61
F	NMB0802		828930	829494	564	0,00	-0,36	-1,01	-1,29	-0,09	0,63	1,19	0,76
F	NMB0866	hypothetical protein	886101	886403	302	0,18	-0,58	-1,05	-0,88	-0,02	2,15	3,15	2,17
F	NMB0901	DRlactate dehydrogenaseRrelated protein	920822	921216	394 *	-0,10	-0,98	-1,05	-0,77	-0,09	0,97	1,51	1,20
F	NMB0902	hypothetical protein	920822	921216	394 *	-0,10	-0,98	-1,05	-0,77	0,07	0,97	1,51	1,20
F	NMB0903	hypothetical protein	920822	921216	394 *	0,22	-0,98	-1,05	-0,77	-0,04	0,84	1,51	1,22
F	NMB0915	hypothetical protein	928466	928717	251	0,02	-1,60	-1,61	-1,46	0,28	0,78	0,67	0,74
R	NMB0927		942006	942790	784	0,45	-0,39	-1,00	-0,92	-0,09	0,13	0,57	1,23
R	NMB0930		946028	946830	802	0,60	-1,28	-1,81	-1,94	0,20	0,32	0,78	0,36
R	NMB0999		1018963	1019456	493	-0,20	-1,57	-1,33	-1,08	0,19	1,32	0,41	0,40
F	NMB1021	anthranilate synthase component I	1036121	1037125	1004	0,11	-1,07	-1,22	-1,09	0,01	0,88	0,55	0,40
R	NMB1059		1078493	1078687	194	-0,11	-0,91	-0,62	-0,62	0,15	0,42	0,70	0,68
R	NMB1092	hypothetical protein	1108308	1108739	431 *	-0,50	-1,90	-2,10	-2,26	0,37	0,17	0,40	0,83
R	NMB1098		1114168	1115574	1406 *	0,07	-2,05	-2,20	-2,00	0,43	1,53	0,83	0,90
R	NMB1119	hypothetical protein	1133146	1133412	266	-0,15	-0,83	-1,00	-1,03	0,19	0,44	0,64	0,73
R	NMB1228	homoserine dehydrogenase	1233265	1234889	1624 *	-0,07	-0,80	-1,11	-0,81	0,26	0,77	0,60	0,28
R	NMB1229	hypothetical protein	1233265	1234889	1624 *	-0,05	-0,30	-1,11	-0,81	-0,24	0,77	0,60	0,28
F	NMB1244		1251237	1251605	368	0,00	-0,63	-1,23	-1,19	-0,05	1,55	1,11	0,99
F	NMB1246	hypothetical protein	1252767	1253673	906 *	0,20	-2,14	-2,12	-2,70	-0,27	0,73	0,81	0,65
F	NMB1247	riboflavin synthase subunit alpha	1252767	1253673	906 *	-0,14	-2,14	-2,12	-2,70	0,14	0,88	0,81	0,65
F	NMB1248		1254136	1254322	186	0,12	-0,26	-0,98	-1,57	0,37	0,88	0,81	0,65
F	NMB1257		1265164	1265510	346	-0,07	-2,45	-2,22	-1,42	0,36	0,05	0,53	0,73
F	NMB1277		1287764	1288968	1204	0,20	-0,81	-1,04	-0,86	0,12	0,50	0,43	0,93
F	nmb1395		1424406	1425258	852	-0,50	-2,08	-1,90	-1,98	0,18	0,25	0,72	1,04
F	NMB1441	putative ORmethyltransferase	1480751	1482112	1361 *	0,20	-0,60	-1,25	-1,40	-0,04	0,00	0,70	0,56
F	NMB1454		1503301	1504242	941 *	-0,14	-2,03	-1,81	-1,76	0,02	0,59	1,01	1,08
F	NMB1455		1503301	1504242	941 *	-0,14	-2,03	-1,81	-1,76	0,08	0,59	0,73	0,66
F	NMB1456		1503301	1504242	941 *	0,15	-2,03	-1,81	-1,76	0,08	0,59	0,73	0,66
R	NMB1458		1506542	1506721	179	-0,30	-1,00	-0,81	-1,20	0,16	2,66	2,67	2,09
R	NMB1475		1525247	1526093	846	0,02	-1,16	-1,48	-1,39	-0,06	1,75	4,72	4,18
F	NMB1483		1530172	1531530	1358	0,30	-1,14	-1,18	-1,35	-0,17	0,17	0,50	1,04
R	NMB1489		1537529	1537897	368	-0,20	-1,19	-0,95	-1,95	0,08	0,29	0,96	0,80
R	NMB1542		1600672	1600819	147	-0,35	-0,60	-1,15	-1,15	0,45	1,12	0,94	0,76
R	NMB1591		1653217	1653502	285	-0,50	-0,73	-0,97	-0,69	-0,24	0,52	1,17	0,44
R	NMB1603		1663320	1663643	323	0,02	-1,11	-1,36	-1,11	0,11	-0,07	0,60	1,10
F	NMB1652		1719852	1720426	574	-0,18	-0,78	-0,99	-1,05	0,14	1,01	1,14	1,08
F	NMB1678	aromatic amino acid aminotransferase	1753723	1754919	1196	-0,50	-1,32	-1,05	-1,19	0,13	0,88	0,65	0,73
F	NMB1688	LRasparaginase	1765110	1765906	796	-0,07	-0,95	-1,15	-0,91	0,29	0,34	0,78	0,48
F	NMB1737	putative secretion protein	1821027	1822053	1026	0,13	-1,25	-1,43	-1,44	0,25	1,16	1,62	1,27
R	NMB1748	hypothetical protein	1829675	1830127	452 *	-0,12	-1,00	-0,94	-0,51	-0,01	0,37	0,61	0,85
R	NMB1749	hypothetical protein	1829675	1830127	452 *	-0,12	-1,00	-0,94	-0,51	0,00	0,37	1,00	0,85
R	NMB1750		1831699	1832198	499	0,00	-2,07	-2,19	-2,46	-0,06	0,81	1,00	0,85
R	NMB1761		1840961	1841260	299	-0,24	-1,41	-1,05	-0,88	-0,04	0,34	0,67	0,94
F	NMB1782	hypothetical protein	1870162	1870294	132	0,10	-0,96	-0,95	-0,44	-0,11	0,24	0,36	1,23
F	NMB1786	hypothetical protein	1872643	1872894	251	0,17	0,00	-1,34	-1,40	0,16	1,12	1,75	1,23
F	NMB1792		1881167	1882187	1020 *	0,00	-1,44	-1,85	-1,44	0,35	1,05	0,87	1,00
F	NMB1793		1881167	1882187	1020 *	0,13	-1,44	-1,85	-1,91	-0,02	1,05	1,48	1,00
R	NMB1801		1888984	1889384	400	0,28	-0,75	-1,04	-0,83	-0,05	0,55	0,70	0,80
F	NMB1838		1939234	1939665	431	-0,19	-0,82	-1,03	-0,94	0,00	0,68	0,21	0,12
R	NMB1880		1984337	1984956	619	0,16	-1,02	-1,29	-1,29	0,26	1,14	1,73	1,76
R	NMB1881		1985448	1986483	1035 *	-0,11	-1,17	-1,35	-1,17	-0,28	0,32	0,69	0,57
R	NMB1882		1985448	1986483	1035 *	0,14	0,00	-1,35	-1,17	0,21	0,61	0,69	0,57
R	NMB1890	hypothetical protein	1992641	1993006	365	-0,14	-0,60	-1,09	-0,67	0,17	0,09	0,68	0,07
R	NMB1975		2073041	2074262	1221	0,00	-0,97	-1,34	-1,51	-0,30	0,93	1,33	1,18
R	NMB1983		2082751	2083409	658	-0,26	-1,25	-0,97	-1,09	0,07	-0,09	0,84	0,97

	F	NMB2018	hypothetical protein	2137814	2138837	1023 *	0,00	-1,65	-1,30	-1,29	-0,03	0,58	0,84	0,64
	F	NMB2019	phosphopantetheine adenylyltransferase	2137814	2138837	1023 *	0,00	-1,65	-1,30	-1,29	0,09	0,58	0,84	0,64
	R	NMB2070		2194077	2194325	248	0,21	-1,27	-0,95	-0,55	0,18	0,07	0,46	0,71
	R	NMB2077		2199712	2200376	664	-0,87	-0,90	-1,60	-1,58	0,25	1,35	0,95	0,98
	F	NMB2096	malate:quinone oxidoreductase	2215833	2216910	1077 *	-0,09	-1,00	-1,28	-1,38	0,00	0,29	0,76	1,33
	F	NMB2097		2215833	2216910	1077 *	-0,09	-1,00	-1,28	-1,38	-0,08	0,68	0,76	1,33
	F	NMB2127	putative protease	2235025	2235877	852 *	-0,23	-1,16	-1,32	-1,31	-0,03	0,30	1,31	1,22
	F	NMB2128	CinARrelated protein	2235025	2235877	852 *	-0,21	-1,16	-1,32	-1,31	0,08	0,35	1,06	0,96
	F	NMB2132		2238495	2239070	575	0,00	-0,74	-1,38	-1,53	-0,26	2,01	0,65	0,35
	F	NMB2133		2240892	2241455	563	-0,16	0,78	0,83	0,75	0,60	1,40	1,25	1,80
	R	NMB2158		2267241	2267991	750	-0,13	-0,57	-1,38	-1,70	0,21	1,05	0,79	0,65
6)	**Up reg. asRNA - Down reg. mRNA**													
	R	NMB0083		93659	94640	981	0,40	0,57	1,03	0,95	0,03	-0,20	-0,56	-0,70
	R	NMB0614	putative oxidoreductase	643843	644836	993	-0,10	-0,12	1,70	2,27	0,11	0,14	-0,84	-0,80
	F	NMB0747		778625	779180	555	0,14	1,05	1,01	0,76	-0,05	0,79	-0,71	-0,75
	R	NMB0825	putative ADPRheptose synthase	848045	848655	610	0,06	0,64	1,19	1,43	-0,15	-0,93	-0,72	-0,36
	F	NMB1122		1134140	1134867	727	0,00	0,77	0,95	1,01	0,11	-2,08	-1,76	-0,83
	R	NMB1285	phosphopyruvate hydratase	1302210	1302811	601 *	-0,42	0,55	1,19	1,45	-0,03	0,12	-0,69	-0,94
	R	NMB1286	hypothetical protein	1302210	1302811	601 *	-0,19	0,55	1,19	1,45	-0,11	0,16	-0,69	-0,94
	F	NMB1430	greA	1470483	1471168	685	0,20	0,44	0,76	0,86	-0,04	-0,31	-0,77	-0,68
	F	NMB1985		2084678	2087747	3069	0,02	0,98	1,24	1,24	-0,03	-0,88	-1,93	-1,81

*in this case the transcript is antisense to more than one gene

Table S3. 5' and 3' untranslated regions (UTR) identified in this study.

							M value (log2 cy5/cy3)			
strand	gene	start	end	UTR	UTR length	overlap	**t0**	**t30**	**t60**	**t90**
F	NMB0016	13854	14231	5'/3'	75/72		0,40	0,40	1,40	1,28
R	NMB0028	24229	24561	3'	82		0,06	2,81	3,23	2,52
F	NMB0032	29965	30572	3'	82		0,23	0,23	1,24	0,97
F	NMB0036	34718	36434	3'	456	NMB0037	-0,05	1,33	1,02	1,15
F	NMB0085	96793	98130	3'	97		0,24	1,53	1,92	2,06
F	NMB0102	110518	111134	5'	95		0,06	0,92	0,30	1,15
F	NMB0189	187362	187875	3'	90		0,37	0,67	0,55	0,56
R	NMB0194	193571	195059	5'	66		0,08	1,55	1,88	2,67
F	NMB0205	205820	206322	3'	60		0,15	1,10	1,33	1,20
F	NMB0210	212010	212411	5'	60		0,05	-1,33	-0,99	-1,08
R	NMB0211	212781	214158	5'	60		-0,15	-1,18	-1,28	-1,11
R	NMB0216	221323	223028	5'/3'	60/114		-0,05	4,33	2,66	4,74
R	NMB0269	271751	272926	5'	384	NMB0270	-0,01	0,63	1,11	1,10
F	NMB0307	316334	317465	5'	80		0,04	0,60	0,93	0,79
F	NMB0313	323429	325019	3'	130		0,06	1,82	1,57	1,52
R	NMB0337	345653	347374	3'	720	NMB0336	0,16	1,09	1,13	1,20
R	NMB0377	378384	379592	5'	60		0,15	1,00	1,39	1,12
F	NMB0436	449981	451092	3'	375	NMB0437	0,04	0,29	0,62	0,77
F	NMB0439	451884	454050	3'	1018	NMB0440	-0,02	0,24	0,74	0,80
F	NMB0441	454053	455169	3'	306	NMB0442	0,01	0,57	0,81	1,02
F	NMB0508	535920	536312	3'	124		-0,05	1,31	0,89	1,13
R	NMB0517	541946	542322	5'/3'	115/100	NMB0516	-0,13	-1,12	-0,89	-1,27
R	NMB0543	563942	565743	5'/3'	60/141		0,10	1,91	1,97	2,18
F	NMB0579	607120	607858	3'	123		-0,14	-1,46	-1,37	-1,26
R	NMB0586	618298	619288	5'	60		0,12	3,28	3,15	2,46
R	NMB0596	627926	629828	3'	88		0,06	1,16	0,29	0,32
R	NMB0604	633421	634553	5'	60		-0,11	1,30	1,71	2,07
F	NMB0606	636271	636634	3'	96		-0,04	0,92	0,99	0,99
R	NMB0615	645065	646584	5'	210		0,04	1,22	2,77	2,82
R	NMB0663	690175	690820	3'	123		0,21	2,16	1,43	1,24
F	NMB0702	732372	734649	5'	193		0,11	0,67	1,03	1,02
F	NMB0729	761371	761860	3'	185		-0,03	0,45	0,72	0,81
R	NMB0741	773727	775669	5'/3'	243/250		0,07	0,80	1,07	0,91
F	NMB0763	790688	791762	3'	139		-0,17	-1,86	-2,12	-1,47
R	NMB0790	817641	819392	3'	310	NMB0789	-0,19	0,88	0,45	0,31
F	NMB0800	826764	827184	3'	141		0,03	0,87	1,07	1,37
F	NMB0900	919659	920742	3'	183	NMB0901	0,01	-1,50	-1,38	-1,48
F	NMB0924	936572	937466	5'	73		0,05	0,83	1,58	1,38
F	NMB0943	956269	957275	3'	124		-0,05	0,88	0,32	0,12
F	NMB0945	959573	959821	3'	91		-0,15	0,20	-0,84	-1,17
F	NMB0983	998362	1000469	3'	531		0,22	2,36	2,13	1,78
R	NMB0993	1009247	1009492	3'	60		-0,10	-2,78	-3,88	-3,21
F	NMB0998	1014959	1018891	5'/3'	88/103		-0,04	1,52	1,30	1,30
R	NMB1017	1032251	1033618	3'	312		-0,12	-2,06	-2,32	-2,44
R	NMB1048	1064486	1066080	5'	130		-0,16	-1,76	-1,45	-1,64
F	NMB1070	1090259	1092068	5'	253		0,12	1,30	1,87	2,03
F	NMB1074	1095130	1096094	3'	60		0,16	2,20	2,70	2,58
R	NMB1077	1099006	1099730	5'/3'	60/102		0,15	-1,13	-1,07	-1,37
R	NMB1088	1107106	1107435	5'	120		0,17	0,62	1,52	1,73
R	NMB1244	1250432	1251622	3'	546	NMB1243	-0,05	1,55	1,11	0,99
R	NMB1279	1291193	1293491	3'	1052	NMB1278	0,14	-0,99	-1,66	-1,75
F	NMB1281	1295171	1299432	3'	126		-0,08	-0,67	-0,80	-1,06
F	NMB1293	1309265	1309928	5'	336	NMB1292	0,12	0,08	1,12	1,09
R	NMB1311	1327942	1329052	3'	820	NMB1310	0,11	0,51	-1,08	-1,34
F	NMB1352	1375168	1375934	5'/3'	139/187	NMB1353	-0,05	-0,34	-0,79	-1,06
F	NMB1359	1382356	1383431	3'	69		0,02	-0,96	-1,87	-2,04
F	NMB1364	1388847	1390061	3'	366	NMB1365	0,07	0,80	1,06	1,07
F	NMB1368	1391970	1393661	5'/3'	229/96		-0,10	-2,81	-2,83	-3,30
F	NMB1371	1395599	1396872	3'	82		0,05	1,09	1,37	1,41
F	NMB1383	1409374	1409944	3'	60		-0,23	-0,69	-0,81	-0,76
R	NMB1400	1429302	1431669	3'	133		-0,04	2,19	1,81	1,76
F	NMB1452	1500497	1503255	3'	1617	NMB1453-NMB1454	-0,16	-2,55	-2,79	-2,70
R	NMB1453	1501758	1502374	3'	126		0,02	0,61	1,00	1,13
F	NMB1458	1506585	1508067	3'	93		0,16	3,46	3,59	3,19
R	NMB1488	1535378	1536994	5'	189		-0,05	-1,27	-0,96	-1,00
F	NMB1537	1587848	1589688	5'	76		-0,11	-0,48	-1,14	-1,07
F	NMB1547	1603145	1603508	3'	60		0,10	0,73	1,48	1,48
R	NMB1562	1622131	1623116	5'	60		0,06	-0,43	-0,71	-0,63
R	NMB1590	1652378	1652788	5'	72		-0,10	-1,52	-0,73	-0,73
F	NMB1615	1678777	1679156	3'	93		0,16	-0,79	-1,37	-1,38
R	NMB1647	1713234	1715531	3'	791	NMB1646	0,02	2,23	2,53	2,39
F	NMB1710	1786070	1787743	3'	345	NMB1711	0,07	2,31	2,12	2,07
F	NMB1712	1788748	1789214	3'	168		0,08	2,73	3,42	3,26
F	NMB1717	1796823	1797545	3'	93		0,06	-0,37	-1,00	-1,34
F	NMB1727	1810577	1811072	3'	60		-0,08	0,15	0,93	1,05
F	NMB1753	1834489	1835121	5'	200		-0,09	-0,29	1,53	1,61
F	NMB1840	1941540	1942748	3'	701	NMB1841	-0,07	1,01	2,24	2,46
R	NMB1845	1944037	1944835	5'/3'	138/157		-0,03	-1,64	-1,91	-1,77
F	NMB1846	1945073	1946232	3'	79		-0,01	0,35	-0,37	-1,07
F	NMB1853	1955218	1955735	5'	246		-0,08	-0,09	-0,91	-0,67
R	NMB1946	2041082	2042015	5'	60		-0,05	1,18	1,35	1,28
F	NMB1951	2046446	2048003	3'	982	NMB1952-NMB1953	-0,08	1,31	1,46	1,45
R	NMB1952	2046459	2047583	3'	728	NMB1951	0,12	1,30	0,58	0,44
F	NMB1975	2072771	2074566	5'/3'	124/138		-0,10	0,92	1,54	1,48
R	NMB1985	2084859	2089358	5'	139		-0,08	-0,95	-1,25	-1,28
F	NMB1988	2092580	2094796	5'	65		-0,08	2,12	2,17	1,96
F	NMB2103	2220722	2221619	5'/3'	100/78		0,18	1,19	-0,08	-0,18
F	NMB2136	2249509	2251175	3'	208		0,12	0,64	0,66	0,63
F	NMB2137	2251472	2251786	3'	78		0,25	0,70	0,75	0,70

Table S4. Operons identified in this study.

strand	genes	start	end	length (nt)	M value (log2 cy5/cy3) t0	t30	t60	t90	UTR
F	NMB0034-NMB0035	32447	34537	2090	0,27	2,09	2,32	1,88	3' UTR of 60 nt
R	NMB0037-NMB0038	36050	37824	1774	0,10	1,02	0,68	0,53	
R	NMB0053-NMB0054	57706	59117	1411	0,15	0,43	0,84	0,73	5'UTR of 306 nt overlapping to NMB0055
F	NMB0071-NMB0072-NMB0073	80382	83532	3150	0,20	0,83	0,84	0,71	
F	NMB0086-NMB0087	98128	99352	1224	-0,02	0,65	1,34	1,09	
F	NMB0091-NMB0092-NMB0093	104402	105107	705	0,26	0,67	0,97	1,40	
F	NMB0094-NMB0095	105233	105583	350	0,20	0,67	0,62	0,52	
F	NMB0113-NMB0114-NMB0115-NMB0116	120884	126125	5241	-0,05	-0,98	-1,13	-0,94	
R	NMB0119-NMB0120	129053	130472	1419	0,16	0,19	0,67	0,67	
F	NMB0130-NMB0131	135921	136850	929	-0,43	-0,36	-0,88	-0,61	
F	NMB0132-NMB0133	137034	145550	8516	-0,18	0,06	-0,60	-0,77	
F	NMB0134-NMB0135	145842	146245	403	-0,08	1,28	0,45	0,34	
F	NMB0152-NMB0153-NMB0154-NMB0155	156596	158047	1451	0,34	-0,39	-0,82	-1,03	
R	NMB0176-NMB0177	172346	175072	2726	0,05	0,78	2,42	2,32	
R	NMB0203-NMB0204	204405	205601	1196	0,17	0,89	0,68	0,66	
F	NMB0213-NMB0214	216743	219853	3110	0,15	0,49	1,02	0,86	
R	NMB0227-NMB0228-NMB0229-NMB0230	235461	239203	3742	-0,18	0,27	1,30	1,29	
R	NMB0235-NMB0236	242881	243255	374	0,19	0,12	1,01	1,37	
F	NMB0241-NMB0242-NMB0243-NMB0244-NMB0245	246614	249768	3154	0,41	-0,28	0,46	0,76	
F	NMB0253-NMB0254-NMB0255	257407	258989	1582	0,05	-0,76	-0,38	0,15	
R	NMB0261-NMB0262	265087	266235	1148	-0,04	0,38	0,73	0,64	
F	NMB0291-NMB0292	300379	301524	1145	-0,14	0,75	0,85	0,53	
R	NMB0316-NMB0317	327694	329178	1484	-0,06	-0,30	-0,83	-0,94	3' UTR of 247 nt
F	NMB0318-NMB0319	329613	332405	2792	0,29	1,04	2,09	2,26	3' UTR of 82 nt
R	NMB0330-NMB0331-NMB0332	339089	340854	1765	-0,16	-1,16	-1,28	-1,34	3' UTR of 60 nt
R	NMB0357-NMB0358	364163	365742	1579	0,24	0,57	0,81	0,78	
F	NMB0364-NMB0365	369877	371340	1463	0,16	-0,28	0,81	0,91	5' UTR of 223 nt; 3' UTR of 180 nt overlapping to NMB0366
R	NMB0370-NMB0371	373725	374673	948	0,23	1,22	1,04	1,23	3' UTR of 136 nt
R	NMB0374-NMB0375	375924	378269	2345	0,11	1,61	1,79	1,67	
R	NMB0392-NMB0393-NMB0394	395691	399575	3884	-0,03	1,10	1,31	0,92	3' UTR of 683 nt overlapping to NMB0391
F	NMB0398-NMB0399	402157	403425	1268	-0,10	-1,20	-1,24	-1,48	3' UTR of 117 nt
R	NMB0401-NMB0402	405841	411225	5384	0,04	1,12	1,50	1,06	
F	NMB0410-NMB0411-NMB0412	418069	419819	1750	-0,21	-0,85	-0,83	-0,36	
F	NMB0414-NMB0415-NMB0416-NMB0417	421599	426484	4885	0,14	-0,85	-0,83	-0,93	3' UTR of 60 nt
F	NMB0419-NMB0420	427758	429957	2199	-0,10	-0,41	-0,83	-0,16	5' UTR of 109 nt; 3'UTR of 60 nt
F	NMB0429-NMB0430-NMB0431	440168	442618	2450	-0,04	1,81	3,32	3,57	3' UTR of 75 nt
F	NMB0432-NMB0433	442691	446522	3831	0,16	0,71	1,46	1,28	3' UTR of 399 nt
F	NMB0434-NMB0435	446786	449972	3186	-0,29	0,69	0,96	1,64	5' UTR of 183 nt; 3'UTR of 234 nt
F	NMB0460-NMB0461	475581	480553	4972	0,07	1,08	2,37	2,47	
F	NMB0509-NMB0510	536372	537436	1064	0,16	0,59	0,68	0,89	
F	NMB0512-NMB0513-NMB0514-NMB0515-NMB0516	539472	542027	2555	0,12	0,34	0,82	0,96	
F	NMB0528-NMB0529	548098	549333	1235	-0,14	-0,09	-1,11	-0,49	5' UTR of 79 nt; 3'UTR of 150 nt
F	NMB0548-NMB0549	572492	575686	3194	0,00	0,33	-0,54	-1,37	
F	NMB0556-NMB0557	585156	586325	1169	0,09	-0,34	0,60	0,86	
F	NMB0574-NMB0575	602078	603801	1723	0,17	0,34	0,70	0,57	
R	NMB0587-NMB0588	619290	621075	1785	0,28	2,80	1,65	1,32	5' UTR of 135 nt
F	NMB0611-NMB0612-NMB0613-NMB0614	641554	644827	3273	-0,23	-0,39	-0,84	-0,80	
R	NMB0628-NMB0629-NMB0630	660840	662417	1577	0,12	0,71	0,71	0,42	
F	NMB0649-NMB0650-NMB0651	680999	682124	1125	-0,02	0,27	0,87	1,11	
F	NMB0652-NMB0653-NMB0654	682237	684777	2540	0,16	1,70	1,96	1,90	
R	NMB0667-NMB0668	695186	697133	1947	0,34	0,02	0,72	0,70	3' UTR of 126 nt
R	NMB0683-NMB0684-NMB0685	709662	711155	1493	0,00	-0,13	-0,51	-0,81	3' UTR of 154 nt
F	NMB0686-NMB0687	711318	713035	1717	0,07	-0,86	-1,18	-1,49	
R	NMB0688-NMB0689-NMB0690	714853	717683	2830	0,13	2,01	1,81	1,34	
R	NMB0713-NMB0714	744473	746803	2330	-0,17	-0,30	-1,04	-1,52	
F	NMB0722-NMB0723	753522	754222	700	0,08	-0,61	-0,62	-0,81	5' UTR of 121 nt
F	NMB0742-NMB0743	775722	776876	1154	0,14	-0,59	-1,08	-1,11	
R	NMB0748-NMB0749	779232	780644	1412	0,02	0,30	0,74	0,67	
R	NMB0765-NMB0766	793147	796171	3024	-0,21	-0,38	-0,91	-0,61	5' UTR of 60 nt
F	NMB0769-NMB0770-NMB0771-NMB0772-NMB0773	798278	801060	2782	0,02	-0,74	-0,77	-0,72	
F	NMB0787-NMB0788-NMB0789	815688	818417	2729	0,13	-2,09	-2,57	-2,78	3' UTR of 432 nt
F	NMB0803-NMB0804	829644	831192	1548	-0,13	0,91	0,91	0,63	
F	NMB0824-NMB0825-NMB0826-NMB0827	847097	851280	4183	-0,15	-0,93	-0,78	-0,36	
R	NMB0856-NMB0857-NMB0858-NMB0859-NMB0860-NMB0861-NMB0862-NMB0863	881777	884607	2830	-0,08	0,93	1,59	2,17	5' UTR of 162 nt
R	NMB0864-NMB0865-NMB0866	884624	886410	1786	0,12	2,15	3,15	2,17	
F	NMB0872-NMB0873	891453	894026	2573	0,07	0,17	0,69	0,69	
F	NMB0875-NMB0876	895292	896713	1421	0,22	-0,42	-0,75	-0,91	
R	NMB0879-NMB0880-NMB0881	899943	902973	3030	0,12	-2,08	-1,97	-2,82	

R	NMB0901-NMB0902-NMB0903-NMB0904-NMB0905-NMB0906-NMB0907-NMB0908	920380	923550	3170	-0,04	0,84	1,51	1,22	3'UTR of 240 nt overlapping to NMB0900
R	NMB0913-NMB0914	927243	927835	592	-0,13	0,30	0,92	0,70	
R	NMB0941-NMB0942	955642	956075	433	0,04	2,84	2,49	2,81	
F	NMB0948-NMB0949-NMB0950-NMB0951	962499	965828	3329	-0,10	0,70	1,15	1,32	
F	NMB0953-NMB0954	966063	967466	1403	0,03	1,46	2,05	2,37	
F	NMB0959-NMB0960	974079	976257	2178	-0,09	1,12	1,06	0,64	
F	NMB0985-NMB0986	1001562	1002484	922	0,02	1,54	0,90	0,89	
R	NMB0994-NMB0995	1010148	1012060	1912	0,16	-2,78	-2,65	-2,78	
R	NMB1002-NMB1003-NMB1004-NMB1005	1023227	1025225	1998	0,18	0,37	1,30	1,15	3' UTR of 306 nt
R	NMB1019-NMB1020	1034243	1035925	1682	-0,18	0,88	0,55	0,40	
R	NMB1034-NMB1035	1048979	1050092	1113	-0,28	1,14	1,08	1,10	5' UTR of 72 nt; 3'UTR of 85 nt
F	NMB1063-NMB1064	1081704	1082628	924	0,24	1,00	1,82	1,67	
R	NMB1068-NMB1069	1087643	1090093	2450	0,04	1,96	2,49	2,11	
R	NMB1072-NMB1073	1092903	1094961	2058	0,04	0,68	0,83	0,64	
F	NMB1081-NMB1082-NMB1083	1101146	1104699	3553	0,07	0,22	1,27	1,15	
F	NMB1101-NMB1102-NMB1103	1117312	1118574	1262	0,25	-1,13	-0,81	-0,90	
R	NMB1117-NMB1118	1132224	1132798	574	-0,07	0,19	1,19	1,28	
F	NMB1119-NMB1120-NMB1121	1132877	1133996	1119	0,19	0,44	0,64	0,73	
R	NMB1151-NMB1152-NMB1153	1157347	1162248	4901	0,06	-2,08	-1,65	-2,18	
R	NMB1154-NMB1155-NMB1156	1162290	1165529	3239	-0,15	-3,03	-2,65	-2,18	
R	NMB1189-NMB1190-NMB1191	1189392	1194327	4935	0,04	-2,06	-1,67	-2,18	
R	NMB1192-NMB1193-NMB1194	1194306	1197546	3240	-0,14	-2,92	-2,45	-2,84	
R	NMB1206-NMB1207	1210546	1211659	1113	-0,02	-2,78	-2,32	-2,38	5' UTR of 79 nt; 3'UTR of 60 nt
R	NMB1211-NMB1212-NMB1213-NMB1214	1212589	1220531	7942	-0,09	2,18	1,20	1,59	3' UTR of 184 nt
R	NMB1220-NMB1221	1224279	1225751	1472	0,00	0,44	1,12	0,99	
F	NMB1228-NMB1229	1233124	1234943	1819	0,26	0,77	0,60	0,28	
R	NMB1246-NMB1247-NMB1248	1252070	1254772	2702	0,14	0,88	0,81	0,65	
F	NMB1249-NMB1250	1254937	1257504	2567	0,00	-1,49	-1,20	-0,94	3' UTR of 132 nt
F	NMB1253-NMB1254	1260709	1262044	1335	-0,03	-0,25	-0,24	-0,87	
R	NMB1260-NMB1261	1268650	1273702	5052	0,24	-0,48	-1,03	-1,06	
F	NMB1284-NMB1285-NMB1286	1300715	1302818	2103	-0,17	-0,29	-0,69	-0,94	
R	NMB1320-NMB1321-NMB1322-NMB1323	1338126	1339508	1382	0,08	-0,69	-1,12	-1,30	
R	NMB1330-NMB1331	1347952	1350585	2633	0,40	1,57	0,63	0,80	5' UTR of 139 nt
R	NMB1362-NMB1363	1385450	1388663	3213	0,15	2,58	1,61	1,63	
F	NMB1393-NMB1394	1421511	1424374	2863	-0,04	-0,56	-2,14	-2,51	
F	NMB1406-NMB1407-NMB1408	1436108	1438492	2384	0,15	0,84	0,85	1,03	5' UTR of 331 nt
R	NMB1455-NMB1456	1503928	1504436	508	0,08	0,43	0,73	0,66	
F	NMB1493-NMB1494	1538749	1541208	2459	0,12	1,83	1,67	2,03	5' UTR of 183 nt overlapping to NMB1492
R	NMB1565-NMB1566	1625000	1626332	1332	-0,24	0,42	-0,69	-1,17	
R	NMB1574-NMB1575-NMB1576-NMB1577	1635918	1639732	3814	-0,17	0,68	0,53	0,39	5' UTR of 129 nt
F	NMB1578-NMB1579-NMB1580-NMB1581-NMB1582	1640713	1645550	4837	-0,18	-0,90	-0,26	-0,22	
R	NMB1632-NMB1633	1696386	1697106	720	0,12	0,67	1,44	1,37	3' UTR of 204 nt
R	NMB1639-NMB1640	1703630	1705069	1439	0,15	0,33	1,28	1,36	
F	NMB1641-NMB1642-NMB1643	1705411	1710427	5016	0,15	-0,80	-0,88	-0,89	
R	NMB1644-NMB1645	1710450	1713217	2767	0,02	0,34	0,53	1,16	
R	NMB1652-NMB1653	1719661	1721306	1645	0,19	1,01	1,14	1,08	
R	NMB1696-NMB1697	1775550	1776103	553	0,06	1,17	1,12	1,21	
R	NMB1698-NMB1699	1776107	1777611	1504	-0,05	0,68	0,88	1,21	5' UTR of 390 nt overlapping to NMB1717
R	NMB1714-NMB1715-NMB1716	1790503	1796434	5931	0,11	-1,67	-1,17	-1,55	
R	NMB1728-NMB1729-NMB1730	1811686	1813705	2019	0,19	2,00	2,19	2,18	
F	NMB1739-NMB1740	1824196	1825093	897	-0,03	0,51	1,79	1,98	
F	NMB1756-NMB175-7NMB1758	1835992	1837258	1266	-0,03	-0,79	-0,29	0,13	
F	NMB1759-NMB1760-NMB1761	1837422	1841281	3859	0,00	0,59	0,67	0,94	3' UTR of 175 nt
R	NMB1764-NMB1765	1843876	1844507	631	0,07	0,24	0,45	0,80	
R	NMB1777-NMB1778	1860917	1861533	616	0,31	0,42	0,97	1,33	3' UTR of 238 nt
R	NMB1781-NMB1782	1869786	1870280	494	-0,11	-0,34	0,36	1,23	
R	NMB1783-NMB1784-NMB1785-NMB1786	1870616	1873685	3069	0,00	1,12	1,75	1,23	
R	NMB1792-NMB1793-NMB1794	1880893	1883846	2953	-0,02	1,05	0,87	1,00	
R	NMB1841-NMB1842	1941516	1943332	1816	0,23	-1,71	-1,47	-1,58	5' UTR of 570 nt overlapping to NMB1840
F	NMB1862-NMB1863	1965686	1967178	1492	0,03	-1,14	-1,53	-1,38	
F	NMB1881-NMB1882	1985722	1988348	2626	-0,28	0,32	0,69	0,57	
R	NMB1885-NMB1886	1989168	1990424	1256	0,19	0,93	0,97	0,71	
F	NMB1898-NMB1899	1998759	1999884	1125	0,18	0,32	1,05	1,12	5' UTR of 97 nt
F	NMB1996-NMB1997	2102035	2106881	4846	0,14	1,03	0,73	0,49	
R	NMB2012-NMB2013-NMB2014	2128208	2130455	2247	0,09	-0,03	0,79	0,94	5' UTR of 169 nt
R	NMB2018-NMB2019-NMB2020-NMB2021	2137789	2140224	2435	-0,12	1,03	0,84	0,64	
F	NMB2033-NMB2034	2151211	2152549	1338	0,07	-0,04	-0,87	-1,04	
F	NMB2041-NMB2042	2162135	2163970	1835	0,16	0,36	0,69	0,73	
R	NMB2051-NMB2052-NMB2053	2173683	2176447	2764	0,00	0,44	0,55	0,71	
R	NMB2063-NMB2064	2185781	2187459	1678	0,04	0,34	0,21	0,77	
R	NMB2096-NMB2097	2215045	2216783	1738	0,00	0,11	0,76	1,33	3' UTR of 136 nt
F	NMB2107-NMB2108-NMB2109-NMB2110	2224751	2226032	1281	-0,10	-1,28	-1,19	-1,14	
R	NMB2127-NMB2128	2224567	2226314	1747	0,08	0,35	1,06	0,96	
F	NMB2130-NMB2131	2237952	2238455	503	0,02	0,80	0,57	-0,08	
R	NMB2150-NMB2151	2260255	2262396	2141	0,00	-0,21	-1,15	-1,14	3' UTR of 219 nt

Table S5. Primers used in this study

Primer	Sequence 5'- 3'	Restriction sites[b]
Deletion mutants		
Up0035_Fw	- gctctagaGCAGCTTCAGGATTCTGTGC-	XbaI
Up0035_Rv	- tcccccgggTTCAGCTCCTCTTTACGGGT-	SmaI
Dn0035_Fw	tcccccgggGCCGCAAGCGTTCAGACGGT	SmaI
Dn0035_Rv	ccgctcgaGAAGGCTTTGCCCAAAATGC	XhoI
C0035_Fw	- GGAACGCGCTTCAGGACATT -	
C0035_Rv	- CCGAGATAACCTCCGATTGC -	
Upkat_Fw	- gctctagaGCGTATGGTCGAGGATGTCT -	XbaI
Upkat_Rv	-tcccccgggGGGGGTAAACGGCTTACAGT -	SmaI
Dnkat_Fw	-tcccccgggGTAAGGGGGCATTATGTGGA -	SmaI
Dnkat_Rv	- ccgctcgaATAGGCTTTCCCGTTTGCTT -	XhoI
Ckat_Fw	- ACTGTAAGCCGTTTACCCCC -	
Ckat_Rv	- TCCACATAATGCCCCCTTAC -	
UptbpB_Fw[1]	- gctctagaGGAATGACGCGAACAGAAAC -	XbaI
UptbpB_Rv	-tcccccgggAGCCTGATTCACCAATGGATT-	SmaI
DntbpB_Fw	- tcccccgggGCCAACAGCCTGTGCGATA -	SmaI
DntbpB_Rv[2]	- ccgctcgaTTCAACCGGCACCAGCCTGTT-	XhoI
CtbpB_Fw	- AATCCATTGGTGAATCAGGCT -	
CtbpB_Rv	- TATCGCACAGGCTGTTGGC -	
UplctP_Fw[1]	- gctctagaGCCGCATCATCACTATCCTT -	XbaI
UplctP_Rv	- tcccccgggCGTAAATCAGCACTGCGGTA -	SmaI
DnlctP_Fw	- tcccccgggCGACAATTCGATGGTGAAAA -	SmaI
DnlctP_Rv[2]	- ccgctcgaAAATCTGCCGCTGTATTGCT -	XhoI
ClctP_Fw	- TACCGCAGTGCTGATTTACG -	
ClctP_Rv	- TTTTCACCATCGAATTGTCG -	
Up0595_Fw	- gctctagaCCATGCAAGACATTGCAAAA -	XbaI
Up0595_Rv	- tcccccgggATTTTGGGCATCATGGAATC -	SmaI
Dn0595_Fw	- tcccccgggAAAATTCGACCGCAGTATCG -	SmaI
Dn0595_Rv	-ccgctcgaGAGATGGGACAATTCGTCGTC -	XhoI
C0595_Fw	- GATTCCATGATGCCCAAAAT -	
C0595_Rv	- CGATACTGCGGTCGAATTTT -	
Up*nspA*_Fw[1]	- gctctagaTGTGAAGTGGGAAAGTGTTG -	XbaI
Up*nspA*_Rv	- tcccccgggTGCGCCTTATTCTGCAAACC -	SmaI
Dn*nspA*_Fw	-tcccccgggGGTTCCTTTATGGTCAGTTAG -	SmaI
Dn*nspA*_Rv[2]	- ccgctcgaGAACGCGTCCGGAAAATATG -	XhoI
C_*nspA*_Fw	- GGTTTGCAGAATAAGGCGCA -	
C_*nspA*_Rv	- CTAACTGACCATAAAGGAACC -	
Up*opc*_Fw	- gctctagaCGATGATGTTGTAGCGGA -	XbaI
Up*opc*_Rv	- tcccccgggGTCACTTTAAATGCCAAACC -	SmaI
Dn*opc*_Fw	- tcccccgggTGGATTGTAGTCGGATATG -	SmaI
Dn*opc*_Rv	- ccgctcgaCTATCGGAAATAACCGAAACC -	XhoI
C*opc*_Fw	- GGTTTGGCATTTAAAGTGAC -	
C*opc*_Rv	- CATATCCGACTACAATCCA -	
Up1064_Fw	- gctctagaATAAACCGAGCGGTTCTTGA -	XbaI
Up1064_Rv	- tcccccgggTCGCCGCCTAATTTTACTTC -	SmaI
Dn1064_Fw	- tcccccgggCGGTTTGCAATACTGGTTGA -	SmaI
Dn1064_Rv	- ccgctcgagCTGCTGCTGATTACCGGTTT -	XhoI
C1064_Fw	- GAAGTAAAATTAGGCGGCGA -	
C1064_Rv	- TCAACCAGTATTGCAAACCG -	
Up1483_Fw[1]	- gctctagaCGTTACAGCGGCAATTATTGC -	XbaI
Up1483_Rv	-tcccccgggCGCAGACAGTACAGATAGTAC-	SmaI
Dn1483_Fw	- tcccccgggATGTTCCGATATATAGCCTG -	SmaI
Dn1483_Rv[2]	- ccgctcgaCCCCTATTTTGTGGAACATC -	XhoI
C1483_Fw	- CCATCCGTTTCCATTGCAAAC -	
C1483_Rv	- TGCGGACTGACCGTTTCATC -	
Up1786_Fw	- gctctagaATGTCGCATTGTTCCAAACC -	XbaI
Up1786_Rv	-tcccccgggGGATGCTCATTACTTCCCCTTA-	SmaI
Dn1786_Fw	- tcccccgggTGGAAATTTTGTGAGGGATTC-	SmaI
Dn1786_Rv	- ccgctcgagCTTTACCCGTCAGGCTGGTT -	XhoI
C1786_Fw	- TAAGGGGAAGTAATGAGCATCC -	
C1786_Rv	- GAATCCCTCACAAAATTTCCA -	
Up1840_Fw	- gctctagaAACTGGCGGTCGTTCATATC -	XbaI
Up1840_Rv	- tcccccgggCTGCCCATGTTTTCTCCTTG -	SmaI
Dn1840_Fw	- tcccccgggGCTTGAGCCTCTTTCAGACG -	SmaI
Dn1840_Rv	- ccgctcgagAGGCTCGACGAAATCAAAAA -	XhoI
C1840_Fw	- CAAGGAGAAAACATGGGCAG -	
C1840_Rv	- CGTCTGAAAGAGGCTCAAGC -	
Up1946_Fw	- gctctagaGATGATGGTACGGCGTTTG -	XbaI
Up1946_Rv	- tcccccgggGGCAGTCGTATAAAATGATG -	SmaI
Dn1946_Fw	- tcccccgggCATTTTCTCCTGATGTTGTG -	SmaI
Dn1946_Rv	- ccgctcgagCTTCGTCATCCTGATGATTG -	XhoI

C1946_Fw	-CATCATTTTATACGACTGCC -	
C1946_Rv	- CCACAACATCAGGAGAAAAT -	
Complementing strains		
NspAcmpF	-gggaattccatATGAAAAAGCACTTGCCACAC-	NdeI
NspAcmpR	-ccaatgcatTCAGAATTTGACGCGCACAC-	NsiI
1483cmpF	-gggaattccatATGTTGAAACAAACGACAC-	NdeI
1483cmpR	-ccaatgcatTCAGAACGCGATATAGCTGTT-	NsiI
1567cmpF	-gggaattccatATGAACACCATTTTCAAAATC-	NdeI
1567cmpR	-ccaatgcatTTAATTTACTTTTTTGATGTCGAC-	NsiI
Sequencing of deletion mutants		
Up*fHbp*_Fw[1]	-CCAGCCAGGCGCATAC-	
Dn*fHbp*_Rv[2]	-CAGCGTATCGAACCATGC-	
Upmip_Fw[1]	-TCGGACGGCTTCAGGA-	
Dnmip_Rv[2]	-GACACGGTTTCCCTCGA-	
Up*fur*_Fw[1]	-GAGCGGTGTCATGTGTGTTCC-	
Dn*fur*_Rv[2]	-GAATGCGCGTACCCCATTTCG-	
Up*nalP*_Fw[1]	-CATATGCGAACGACCCCAACCTTCC-	
Dn*nalP*_Rv[2]	-TGCATGCATTCAGAACCGGTAGCCTACG-	
SeqKan Rv[3]	-CGCTTCATAGAGTAATTCTG-	
SeqKan Fw[4]	-GACTTACTGGGGATCAAGC-	
SeqEry Rv[3]	-CATGACGAATCCCTCCTTC-	
SeqEry Fw[4]	-CGTTACTAAAGGGAATGGAG-	
Southern blot analysis		
SB_Ery Fw	-GAAGGAGGGATTCGTCATG-	
SB_Ery Rv	-CTCCATTCCCTTTAGTAACG-	
SB_Kan Fw	-CTATAGAATGGGCAAAGCAT-	
SB_Kan Rv	-GCTTGATCCCCAGTAAGTC-	
5'-3' RACE for small intergenic RNAs		
NrrF_F	ccttttatatatcagatactc	
NrrF_R	GAATGTATGTCTCGTATATGC	
Bns1_F	aggcagatatattcgggagg	
Bns1_R	GCTGTTTCCTCTTTATTCAG	
Bns2_F	tggtcgaataacagggaatag	
Bns2_R	ACACATTACGGGGAAAACGT	
Bns3a_F	tggtcgaataacagggaatag	
Bns3a_R	ACTTCCGCGTAACTGCCGAT	
Bns3b_F	GACCAACCCAAATAAAAAAAGC	
Bns3b_R	GTCTGGTTTCTTTGAGTTC	
Bns4_F	aatgcggaaaatttcgtgaac	
Bns4_R	AACGATACGCTGAAAATGCGC	
Bns5_F	CCGCTCATATAAAGAACGGG	
Bns5_R	CAGGCATCCTCATAAAAGAAG	
Bns6_F	GATTGCCGGAAATGCGGAC	
Bns6_R	AACACTGCCGACGGTTGCC	
Bns7_F	TATCATAGCAACAAACCGCC	
Bns7_R	CGGTGATTCCAATATACAAGG	
RT-PCR for antisense RNAs		
a0752_F1	TCGGTTGCGCATTGTGCGC	
a0752_F2	TTTTCATCCACATCGACCACTT	
a0752_RT	TTTGAGAACACACGGAGCAC	
a0756_RT	ATTTGCCGTCAATGCTTCCG	
a0756_F	CAAGGCTTTTTGCCAGTCTG	
a0954_RT	AAGGCTTGCTTTATTATCGCG	
a0954_F	GGATCGCTAATCATCTCGTG	
a1650_F1	CCTCTGTGCGTGATGTTGTT	
a1650_F2	TTGCCCGATTTGGATTGC	
a1650_RT	GATCCTTCAACAGAATGCCC	
a1923_F	TGCGACAGGTTTCAGATATTTG	
a1923_RT	TATACATCATCGCTACTACCGTT	
a0176_F	TTCGTAGCCCGACAATTCC	
a0176_RT	ACTGAAAACCTATACAAATTGTG	
a0177_F	GCGCGTTTCATTGACGATG	
a0177_RT	GTCAGGCCTTGGTTTCTATG	
a0756_F	CAGCATCGTGCGGATAAAG	
a0756_RT	GACATTACCGATGCCGATG	
a0825_F	ATCGGTTCGCCTTCGCTGA	
a0825_RT	CGCGCAACATCGCTTCGTT	
a0884_Fe	CTACCCGAAATGATATAGCG	
a0884_RT	CAGCAACACTGCCAAAATAC	
a1686_F	AACACAAAACTCAATCGCCCA	
a1686_RT	GACAAAAACATCTTCATCGAAATAC	

a1704_F	GACGGACATAATCCAACCC
a1704_RT	GAAATCTCAAAAATTGTCCAAACC
a1729_F	ATACTGTTGCGGATTTGAATGA
a1729_RT	GGTGTGTTTGTGTTGATGATG
a1786_F	CTCATCTACGCTTATCTTCATC
a1786_RT	TTGCTGCCATGATTGCCGAC
a1985_F	TATCAGACAATGGAGCAGGCA
a1985_RT	ATCAGCGGCAATGTCGATCTT
a1995_F	TCTATCCGGCCGTCAGACT
a1995_RT	GTTCAAACTCGACGACGTG
a0211_F1	CATTTTCGTTTCTGTCCATCC
a0211_RT1	TGCACTATTTCCGCAAGTTC
a0211_F2	GATTTCGGCTTCGCCGCAT
a0211_RT2	TTTGCGGCAGGTTTGGATG
a0212_F	TGCTGATCATATTTTGCTCCG
a0212_RT	GAGGGTGCCAAGCTTTACA
a1840_F	TCAACGCCAGCACCAACAC
a1840_RT	GTTATCCGCACCAAACCCG
RT-PCR for 5' and 3' UTRs	
0615_Fi	ACTGGTGGAAGCCTTATTC
0615_Fu	GCCTAAGGATAAATCCTCC
0615_RT	CTTTTACCTGTATCCACAACT
0983_F	GCCCAAACCCTGCACAAAC
0983_RTi	CAATCACGTCCACGCCGTC
0983_RTu	ACTCATCATAAACCTGCCTT
1070_Fi	GCTATGACCAAAGAGGAAAAA
1070_Fu	GAAGCGTTGAAACAGCACGA
1070_RT	GCTCAAAGCGGAAAGGTAG
1452_Fi	GAACGATTGCCAGTGTGGAT
1452_Fu	AGGCTGCGTTCCGGAATAG
1452_RT1	GGCGTTAGTTATCATTGCC
1452_RT2	CGACGCAGTTTGTGTTTTACG
1646_Fi	GTAACCGTACACGCTGACAA
1646_RT	TTCACAGTGTAGGCAAAGAGT
1647_F	CTTTATCGCAGTTTCAGGCG
1710_F	CGTTCCATCAGGCGGTTGA
1710_RTi	TGACGAAACCGGCAATGTTC
1710_RTu	GTATGAGGCAATATCAAACCG
1840_Fo	CATTGGCATCGGCAGGCTT
1840_Fu	GCTTGAGCCTCTTTCAGAC
1840_RT	GAAGCCGCTGCTCGATGTG
RT-PCR for operon transcripts	
0429_Fo	CCAATTCAGATGTTTTCCCCTT
0430_Fi	GAACTATCATGCCTTCGAGC
0430_Ri	GGATTCGATTCTTTCACGGC
0431_Ri	GATAGCTCAAATCGTTGCCG
0431_Ro	CCTGTGTAGTTTGCGCTCG
0787_Fo	GGTATTGCCGCATTGGTTTTG
0789_RT	TGAGCGGACACATCTTCTTC
1362_Fo	TATCCAACCTGACCCGTGC
1362_Fi2	GTGCGCGTAAGCAAAGAACA
1363_Ri2	GTACGAGCCAACGGTTGAAAC
1363_RT2	GACAAAGACCATCACCACGC
Sequencing of TOPO-TA clones	
M13_F	GTAAAACGACGGCCAG
M13_R	CAGGAAACAGCTATGAC
Northern Blot probes	
NrrF_p	GAGTATCTGATATATAAAAAGGGAATGTATGTCTCGTATATGC

[a] Capital letters correspond to nucleotides of the meningococcal sequence and small letters correspond to nucleotides added for cloning reasons.

[b] Enzymes for which the restriction sites are present in the sequence of the primer, added for cloning reasons.

[1] and [2] indicates the pair of primers used to generate the PCR fragments for sequencing.

[3] and [4] indicates the primers used to sequence the flanking regions of the recombination site of the deletion mutants and to determine the antibiotic resistance cassette orientation (see Figure 10A).

Table S6. Plasmids used in this study.

Plasmid	Relevant characteristics	Reference or source
Deletion mutants		
pBluescript (pBS)	Cloning vector, Amp^r	Stratagene
pBS-UD*0035*_Ery	Construct for generating DELETION MUTANT of the *nmb0035* gene, Amp^rEry^r	This study
pBS-UD*kat*_Ery	Construct for generating DELETION MUTANT of the *kat (NMB0216)* gene, Amp^rEry^r	This study
pBS-UD*tbpB*_Ery	Construct for generating DELETION MUTANT of the *tbpB* (*NMB0460*) gene, Amp^rEry^r	This study
pBS-UD*lctP*_Ery	Construct for generating DELETION MUTANT of the *lctP* (*NMB0543*) gene, Amp^rEry^r	This study
pBS-UD*0595*_Ery	Construct for generating DELETION MUTANT of the *lctP* (*NMB0595*) gene, Amp^rEry^r	This study
pBS-UD*nspA*_Ery	Construct for generating DELETION MUTANT of the *nspA* (*NMB0663*) gene, Amp^rEry^r	This study
pBS-UD*opc*_Ery	Construct for generating DELETION MUTANT of the *opc (NMB1053)* gene, Amp^rEry^r	This study
pBS-UD*1064*_Ery	Construct for generating DELETION MUTANT of the *NMB1064* gene, Amp^rEry^r	This study
pBS-UD*1483*_Ery	Construct for generating DELETION MUTANT of the *NMB1483* gene, Amp^rEry^r	This study
pBS-UD*mip*_Ery	Construct for generating DELETION MUTANT of the *mip* (*NMB1567*) gene, Amp^rEry^r	Leuzzi *et al.,* 2005
pBS-UD*1786*_Ery	Construct for generating DELETION MUTANT of the *NMB1786* gene, Amp^rEry^r	This study
pBS-UD*1840*_Ery	Construct for generating DELETION MUTANT of the *NMB1840* gene, Amp^rEry^r	This study
pBS-UD*fHbp*_Ery	Construct for generating DELETION MUTANT of the *fHbp (NMB1870)* gene, Amp^rEry^r	Seib *et al.,* 2009
pBS-UD*1946*_Ery	Construct for generating DELETION MUTANT of the *NMB1946* gene, Amp^rEry^r	This study
pBS-UD*nalP*_Kan	Construct for generating DELETION MUTANT of the *nalP (NMB1969)* gene, Amp^rKan^r	This study
Complementing strains		
pCompRBS	Derivative of pSLcomCmr with tac promoter and downstream ribosome binding site. Cm^rAmp^r	Ieva *et al.,* 2005
pComppRBS-*nspA*	Construct to generate complementing strain for *nspA* gene (*NMB0663*) in 95N477 strain, Cm^rAmp^r	This study
pCompRBS-*1483*	Construct to generate complementing strain for the gene *NMB1483* in MC58, Cm^rAmp^r	This study
pCompRBS-*mip*	Construct to generate complementing strain for *mip* gene (*NMB1567*) in MC58, Cm^rAmp^r	This study

Amp^r = ampicillin resistance cassette
Cm^r= chloramphenicol resistance cassette
Ery^r = erythromycin resistance cassette
Kan^r=kanamycin resistance cassette

Table S7. Nm wild-type, deletion mutants and complementing strains used in this study.

Name	Relevant characteristics	Reference or source
Neisseria meningitidis		
MC58	Clinical isolate, B:15:P1.7,16b, cpx 32, ST 74	Tettelin *et al*., 2000
MCΔ*fur*	*fur* (*NMB0205*) deletion mutant of MC58, Ery^r	Delany *et al*., 2006
MCΔ*kat*	*kat (NMB0216)* deletion mutant of MC58, Ery^r	This study
MCΔt*bpB*	*tbpB* (*NMB0460*) deletion mutant of MC58, Ery^r	This study
MCΔ*lctP*	*lctP* (*NMB0543*) deletion mutant of MC58, Ery^r	This study
MCΔ*nspA*	*nspA* (*NMB0663*) deletion mutant of MC58, Ery^r	This study
MCΔ*opc*	*opc (NMB1053*) deletion mutant of MC58, Ery^r	This study
MCΔ1*483*	*NMB1483* deletion mutant of MC58, Ery^r	This study
MCΔ*mip*	*mip* (*NMB1567*) deletion mutant of MC58, Ery^r	This study
MCΔ*fHhp*	*fHbp* (*NMB1870*) deletion mutant of MC58, Ery^r	Seib *et al*., 2009
MCΔ*nalP*	*nalP* (*NMB1969*) deletion mutant of MC58, Kan^r	Serruto *et al.,* 2010
MCΔ*0035*	*NMB0035* deletion mutant of MC58, Ery^r	This study
MCΔ*0595*	*NMB0595* deletion mutant of MC58, Ery^r	This study
MCΔ*1064*	*NMB1064* deletion mutant of MC58, Ery^r	This study
MCΔ*1786*	*NMB1786* deletion mutant of MC58, Ery^r	This study
MCΔ*1840*	*NMB1840* deletion mutant of MC58, Ery^r	This study
MCΔ*1946*	*NMB1946* deletion mutant of MC58, Ery^r	This study
MCΔ−*Cfur*	MCΔ*fur* complemented with *fur,* Kan^{r}Cm^r	Delany *et al.*, 2006
MCΔ−*C1483*	MCΔ1*483* complemented with *1483,* Ery^{r}Cm^r	This study
MCΔ−*Cmip*	MCΔ*mip* complemented with *mip,* Ery^{r}Cm^r	This study

Cm^r= chloramphenicol resistance cassette
Ery^r = erythromycin resistance cassette
Kan^r=kanamycin resistance cassette